

N O T I C E

THIS DOCUMENT HAS BEEN REPRODUCED FROM
MICROFICHE. ALTHOUGH IT IS RECOGNIZED THAT
CERTAIN PORTIONS ARE ILLEGIBLE, IT IS BEING RELEASED
IN THE INTEREST OF MAKING AVAILABLE AS MUCH
INFORMATION AS POSSIBLE

DOE/NASA/0116-80/1
NASA CR-159845

(NASA-CR-159845) DESIGN STUDY OF STEEL
V-BELT CVT FOR ELECTRIC VEHICLES Final
Report (Battelle Columbus Labs., Ohio.)
131 p HC A07/MF A01

N80-32299

CSCD 13F

Unclass

G3/85 28613

DESIGN STUDY OF STEEL V-BELT CVT FOR ELECTRIC VEHICLES

J. C. Swain, T. A. Klausning, and J. P. Wilcox
Battelle Columbus Laboratories

June 1980

Prepared for
NATIONAL AERONAUTICS AND SPACE ADMINISTRATION
Lewis Research Center
Under Contract DEN 3-116

for

U.S. DEPARTMENT OF ENERGY
Electric and Hybrid Vehicle Division
Office of Transportation Programs

DOE/NASA/O116-80/1
NASA CR-159845

DESIGN STUDY OF STEEL V-BELT CVT FOR
ELECTRIC VEHICLES

J. C. Swain, T. A. Klausning, and J. P. Wilcox
Battelle Columbus Laboratories
505 King Avenue
Columbus, Ohio 43201

June 1980

Prepared for
NATIONAL AERONAUTICS AND SPACE ADMINISTRATION
Lewis Research Center
Cleveland, Ohio 44135
Under Contract DEN 3-116

for
U.S. DEPARTMENT OF ENERGY
Electric and Hybrid Vehicle Division
Office of Transportation Programs
Washington, D.C. 20545
Under Interagency Agreement EC-77-A-31-1044

TABLE OF CONTENTS

	<u>Page</u>
EXECUTIVE SUMMARY	1
INTRODUCTION	5
PROGRAM SCOPE	6
OBJECTIVES.	9
SUMMARY	10
RECOMMENDATIONS	14
TECHNICAL DISCUSSION	15
Steel V-Belt Background	15
CVT Operational Requirements.	25
Overall Transmission Configuration.	26
Introduction to Operating Modes and Control	28
Steel Belt Design Features.	30
Steel Belt Performance.	45
Belt Lubrication.	57
Discussion of Transmission Design	61
Hydraulic System Components	75
Transmission Control System	80
Efficiency Estimates.	92
Maximum Transient Power Output.	99
Reliability and Maintainability	99
Noise and Critical Speeds	110
Weight Estimates.	111
CVT Cost Estimate	112
Identification of Required Technical Advancements	112
Suitability of a Steel V-Belt CVT for Electric Vehicle Powered by Electric Motor Only	113
Suitability of a Steel V-Belt CVT for IC Engine/Battery Hybrid Vehicles	115
Scalability of Steel Belt CVT	116
APPENDIX A. Strut-Strut and Strut-Pulley Lubrication Process	118
REFERENCES.	122

LIST OF FIGURES

	<u>Page</u>
Figure 1. CVT Drivetrain Schematic.	2
Figure 2. CVT Longitudinal Cross Section.	3
Figure 3. CVT Plan View	11
Figure 4. CVT Transverse Cross Section.	12
Figure 5. Hydraulic Control System Schematic.	13
Figure 6. Metal Compression V-Belt.	17
Figure 7. Single Band Compression Belt Efficiency Versus Tension Ratio.	19
Figure 8. Multiband Compression Belt.	20
Figure 9. Multiband Compression Belt Test Setup	21
Figure 10. Stretch Rolling Setup for Nested Bands.	22
Figure 11. Strut -- Low-Speed Belt	32
Figure 12. Strut -- High-Speed Belt.	33
Figure 13. Design Tension Ratios	47
Figure 14. Steady-State Axial Pulley Forces.	49
Figure 15. Desired Steady-State Response in Terms of Variables Measured by Control System.	51
Figure 16. Effect of Viscosity on Strut-Strut or Strut-Pulley Lubricant Film Thickness at 38 C (100 F).	60
Figure 17. CVT Longitudinal Cross Section.	62
Figure 18. CVT Plan View	63
Figure 19. CVT Transverse Cross Section.	64
Figure 20. Monsa Model of Low-Speed Pulley Half.	67
Figure 21. Approximate Force Distribution on the Large Low-Speed Pulley at Normal Operating Condition of 16.4 kW (22 hp).	68

LIST OF FIGURES (Cont.)

	<u>Page</u>
Figure 22. Pulley Displacement Versus θ at 16.4 kW (22 Hp) Operation (Monsa Results)	69
Figure 23. Hydraulic Control System Schematic.	70
Figure 24. Block Diagram of Transmission Control System.	84
Figure 25. Block Diagram of TCS Analog Output Subsystem.	85
Figure 26. Block Diagram of TCS Main Process Schedule.	86
Figure 27. Block Diagram of TCS Start-Up Sequence.	87
Figure 28. Block Diagram of TCS Normal Control Sequence.	88
Figure 29. Block Diagram of TCS Shutdown Sequence.	89
Figure 30. Block Diagram of TCS Failure Mode	90
Figure 31. Block Diagram of TCS Interrupt Routing to Service I/O . . .	91
Figure 32. Full Torque Losses in Low-Speed Belt.	93
Figure 33. Calculated Losses in High-Speed Belt at Full Power.	94
Figure 34. Total Losses in CVT at 28,000 rpm of Flywheel (Power from Flywheel)	101
Figure 35. Total Losses in CVT at 28,000 rpm of Flywheel (Power to Flywheel)	102
Figure 36. Total Losses in CVT at 21,000 rpm of Flywheel (Power from Flywheel)	103
Figure 37. Total Losses in CVT at 21,000 rpm of Flywheel (Power to Flywheel)	104
Figure 38. Total Losses in CVT at 14,000 rpm of Flywheel (Power from Flywheel)	105
Figure 39. Total Losses in CVT at 14,000 rpm of Flywheel (Power to Flywheel)	106
Figure 40. Overall CVT Efficiency at 28,000 rpm of Flywheel.	107
Figure 41. Overall CVT Efficiency at 21,000 rpm of Flywheel.	108

LIST OF FIGURES (Cont.)

	<u>Page</u>
Figure 42. Overall CVT Efficiency at 14,000 rpm of Flywheel	109
Figure A-1. Coordinate System for Strut-Pulley Lubricant Analysis.	120

LIST OF TABLES

	<u>Page</u>
Table 1. Efficiency Summary of Tests of Six Steel V-Belts	24
Table 2. Summary of Steel Belt Design Parameters.	31
Table 3. Band Stresses.	38
Table 4. Gap Closing Capability at Full Torque.	44
Table 5. Typical Full Load Band Tension and Strut Compression for Various Operating Conditions	48
Table 6. Consequences of Chordal Action	52
Table 7. Band Material Comparative Rating	55
Table 8. Hydraulic Control System Power	97
Table 9. Belt Losses - Percent of Power to or from the Flywheel	100
Table 10. Steel V-Belt CVT Weight Estimate	111
Table 11. Manufacturing Cost Estimates for Steel V-Belt CVT.	112

DESIGN AND TECHNOLOGY
ASSESSMENT REPORT

on

DESIGN STUDY OF STEEL V-BELT CVT
FOR ELECTRIC VEHICLES

Contract DEN3-116

to

NATIONAL AERONAUTICS AND SPACE
ADMINISTRATION
Lewis Research Center

from

BATTELLE
Columbus Laboratories

June, 1980

EXECUTIVE SUMMARY

The scope of this contract was to conduct an engineering design study and perform the necessary analysis to determine the optimum arrangement of a steel V-belt continuously variable transmission (CVT) to couple the high-speed output shaft of an energy storage flywheel to the drivetrain of an electric vehicle as shown in Figure 1. The CVT included the variable speed elements along with the necessary clutches and gear sets. Based on the results of the study, a specific arrangement was recommended and a design layout was prepared. Technology advancements necessary to develop the CVT to satisfy the design criteria were identified. In addition, the scalability of the CVT to larger 10,000 kg (22,000 lb) and smaller 790 kg (1750 lb) vehicles was briefly studied. Evaluation of the steel V-belt CVT for use on straight electric vehicles or on internal combustion engine/battery hybrid vehicles was also considered.

The CVT arrangement which was chosen is shown in Figure 2. It weighed 70 kg (155 lb) including the slipping clutch. Its size was approximately 53 by 25 by 36 cm (21 by 10 by 14 inches). Overall potential efficiency of 94 to 95 percent was projected for the average power condition of 16 kW (22 hp). The maximum torque requirement was 450 N-m (330 lb-ft) at the driveline, and the maximum power transient was 75 kW (100 hp) for 5 seconds. An oil wetted modulated clutch at the driveline input to the CVT served the dual purpose of starting the vehicle and protecting the remainder

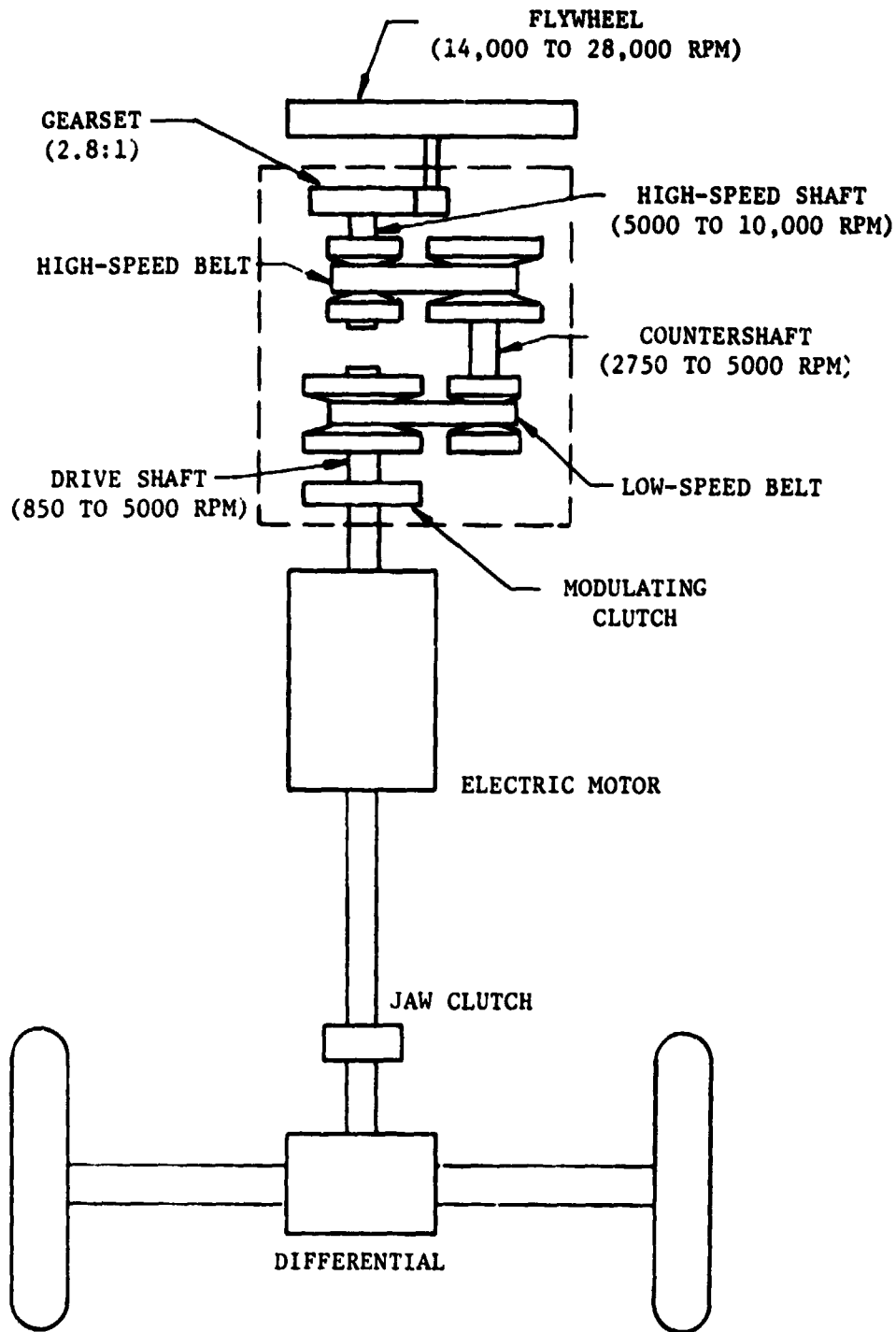


FIGURE 1. CVT DRIVETRAIN SCHEMATIC

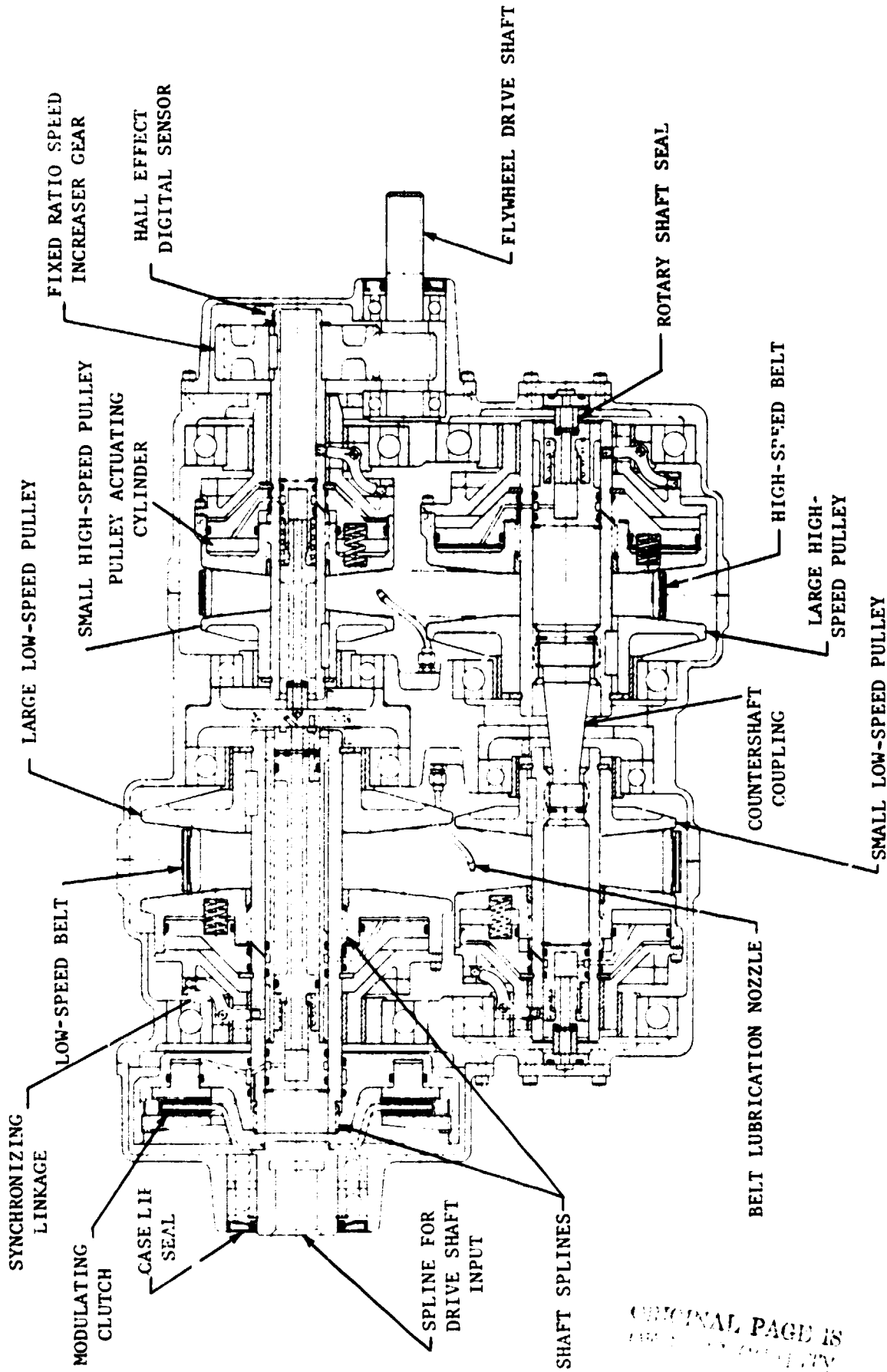


FIGURE 2. CVT LONGITUDINAL CROSS SECTION

ORIGINAL PAGE IS UNCLASSIFIED

of the CVT against excessive driveline shocks. A low-speed steel V-belt immediately in series with the clutch served to vary the driveshaft speed from 1550 rpm to 5000 rpm. A high-speed steel V-belt in series with the low-speed belt varied the driveline speed from 950 rpm to 1550 rpm and also accommodated the flywheel speed variation of 14,000 rpm to 28,000 rpm. A spur gear of 2.8/1 ratio stepped the flywheel speed down to that of the high-speed belt.

An electrohydraulic control system interfaced with an overall vehicle control microcomputer and with speed, torque, and ratio sensors in the CVT. The output of this electrohydraulic control system was the appropriate pressures for each of the V-belt pulleys and for the modulating clutch.

The study concluded that a steel V-belt CVT of this general type could be scaled by classical means to larger or smaller vehicles by an appropriate choice of a gear set between the CVT and flywheel and in some cases, between the CVT and the vehicle driveline.

With regard to the application of the steel V-belt CVT in the driveline of straight battery powered vehicles, the study concluded that the functional requirements could be easily met by a single belt version which was substantially simpler, smaller, and less costly than that required for flywheel-assisted vehicles. An alternative was suggested for the overall approach to vehicle motor control which might conceivably make a CVT more attractive on straight battery vehicles.

The application of a steel V-belt CVT in the driveline of a battery-assisted internal combustion engine hybrid vehicle was judged to be feasible. The CVT for this application utilized one steel V-belt and the overall size, weight, and cost were substantially lower than those required for the flywheel-assisted vehicle. The study noted that the requirements for such a CVT are essentially identical to those of small front wheel drive, 4 cylinder engine passenger cars. The steel V-belt transmissions now in advanced stages of commercial development for those cars could be adapted for prototype use on battery-assisted internal combustion engine hybrids.

INTRODUCTION

Modern flywheels offer the potential for high specific energy storage and high specific power acceptance or delivery. Because of this, they appear attractive for augmenting the performance of battery electric vehicles, for increasing the vehicle range, and for increasing battery life. However, there are no proven transmissions available for effectively coupling the flywheel to the electric vehicle driveline. An efficient, lightweight, compact, quiet, reliable, and low-cost transmission, able to perform the required functions, does not exist. It is, therefore, necessary to develop new technology and hardware if the potential of the flywheel is to be realized.

Battelle Columbus Laboratories (BCL) was in the desirable position of having developed (for an industrial sponsor) a technology on steel variable ratio V-belts. The industrial sponsor granted BCL permission to utilize information from that development in this continuously variable transmission (CVT) program.

Steel variable ratio V-belts were proposed for NASA-Lewis consideration because they offered the best potential for efficiency and quiet operation at the required speed ratio range, power, and torque. They were free of the limitations of Hertzian stress and lubricant sensitivity which plague conventional "traction drives". There were, of course, design and development problems to be overcome on steel V-belts, but they were considered to be capable of solution.

BCL proposed a configuration with two steel variable ratio V-belts in series in order to cover the required large speed ratio spread. A modulated clutch between the CVT and the vehicle driveline served as the vehicle starting clutch. A 2.8/1 speed decrease was provided by fixed gearing between the flywheel and the CVT.

The effort of this program, reported herein, consisted of analysis, design, and engineering feasibility investigations. No hardware or laboratory evaluations were included. The work was conducted from May 7, 1979, to March 7, 1980, as part of the Electric and Hybrid Vehicle Program of the U.S. Department of Energy. It was performed under Contract DEN 3-116 and managed by the Bearing, Gearing, and Transmission Section of the NASA, Lewis Research Center.

PROGRAM SCOPE

The scope of this program included the following three main tasks:

- Task I - Design Study of a Steel V-Belt CVT for Flywheel Application
- Task II - Identification of Required Technology Advancements
- Task III - Determination of the Suitability of a Steel V-Belt CVT for Alternate Electric and Hybrid Vehicle Applications.

Various reporting and administrative tasks were included within the scope but are not discussed in this report.

BCL applied most of the total program effort to Task I and the reporting thereof. The approach to it consisted essentially of the following sequential steps:

- (1) Determination of the required axial pulley forces
- (2) Conceptualization, analysis, and choice of the pulley loading means
- (3) Design and analysis of the steel V-belt assemblies
- (4) Investigation and choice of steel V-belt band materials and processing methods
- (5) Lubrication investigation and choice
- (6) Conceptualization and choice of the basic pulley arrangement
- (7) Overall transmission configuration and layout. (This iterative process continued throughout the program.)
- (8) Investigation of sensors
- (9) Conceptualization and preliminary electrical control system design
- (10) Hydraulic system conceptualization, analysis, and design
- (11) Bearing calculations
- (12) Critical shaft speed analysis
- (13) Pulley structural analysis
- (14) Efficiency calculations and projections

- (15) Weight estimates
- (16) Manufacturing cost estimates.

The design criteria for the CVT were based on a representative vehicle having a curb weight of 1700 kg (3750 lb.). The CVT was to couple a flywheel with a maximum usable energy of 0.5 kWh to this vehicle over the following range of conditions:

- (1) High speed (flywheel) shaft speed of 14,000 to 28,000 rpm
- (2) Low speed (differential input) shaft speed of 0 to 5000 rpm
- (3) Maximum transient power output of 75 kW (100 hp) for 5-second duration
- (4) Maximum transient torque output, at wheel slip, of 450 N-m (330 lb-ft)
- (5) Maximum shift time (from maximum to minimum reduction ratio and vice versa) of 2 seconds
- (6) Weighted average output power of 16 kW (22 hp)
- (7) Average output (drive shaft) speed of 3000 rpm
- (8) Average input (flywheel) speed of 21,000 rpm
- (9) 10 percent life of 2600 hr.

The CVT was to be capable of bi-directional power flow at the above condition but it did not have to provide for reverse operation of the vehicle. A variable speed clutch element could be incorporated to regulate the drive shaft output speed between 850 and 0 rpm. Provisions to disengage the flywheel from the drive shaft were required. The CVT system was required to withstand the sudden shock load and torque conditions expected in typical automotive applications.

In addition, the steel V-belt CVT was to be designed based on the following qualitative criteria (in decreasing order of importance):

- (1) Efficiency - The transmission was to have high efficiency over its entire operating spectrum. Special attention was to be given to maximizing transmission efficiency under those operating conditions in which the transmission spends most of its operating time.
- (2) Cost - Future production costs of the transmission on a large-scale basis (100,000 units per year) was to be an early consideration.
- (3) Size and Weight - The overall size and weight of the CVT, including suitable controls and all ancillary mechanical

components, were not to be significantly greater than present automotive transmissions of equal horsepower.

- (4) Reliability - The transmission, including all support systems (i.e., cooling and controls), was to be designed to operate a minimum of 2600 hr at the average conditions at an estimated 90 percent reliability.
- (5) Noise - Was to be an important consideration in the early stages of design
- (6) Controls - The control system used to operate the transmission drive system was to be stable, reliable, and responsive. The system was to provide driver "feel" response similar to that of a standard automatic transmission equipped, internal combustion engine passenger vehicle. The control system was to be an integral part of the transmission design. The control system selected was to closely simulate the full-scale system required for actual vehicle application.
- (7) Maintainability - The transmission was to be designed with maintainability equal to or better than the maintainability of present-day automotive automatic transmissions. All internal components which require normal maintenance and/or occasional replacement were to be made readily accessible.

BCL applied only a modest effort to Task II, the Identification of Required Technology Advancements, because the only such area identified was the need for lower cost electrohydraulic pressure control valves.

Task III was also a modest effort and included no design work or analysis per se. It consisted of parametric scaling, qualitative assessments, a brief literature review on hybrid vehicle systems, and a telephone investigation of electric motor characteristics with principals in the electric and hybrid vehicle programs.

OBJECTIVES

The primary objective of this project was to develop a steel V-belt concept into a preliminary design of a functional model of an efficient, low cost, reliable, continuously variable transmission (CVT) that could couple the high-speed output shaft of an energy storage flywheel to the drivetrain of an electric vehicle. A functional model is a full-scale, self-contained working unit which incorporates all of the essential operating characteristics of a proposed design approach, while not necessarily resembling the anticipated production model. Areas of technology advancement required to fully develop the CVT were to be determined.

A secondary objective was to determine the applicability of the proposed CVT concept to two other potential applications: (1) matching of an electric motor to the drivetrain of an electric vehicle for better system efficiency, lower cost, or other advantages; and (2) similar matching of a heat engine to an electric hybrid vehicle drivetrain. The scalability of CVTs based on steel V-belts to higher and lower torques and powers for larger and smaller vehicles was also to be briefly examined.

SUMMARY

A design was completed with encouraging results as regards weight, size, and efficiency. Potential long-term manufacturing cost was difficult to quantify at this stage, but an estimate of \$312 (1980 dollars) was made. The CVT housing package, Figures 3 and 4, was 52.3 cm long by 24.9 cm high by 35 cm wide (20.6 in. long, 9.8 in. high, and 13.8 in. wide). The estimated weight was 70 kg (155 lb). The efficiency was somewhat a function of the speed ratio and the direction and amount of power being transmitted. Overall efficiency as high as 94 to 95 percent at the average rated conditions was projected based on calculations.

An electrohydraulic valve was used to generate a varying hydraulic pressure for each of four sets of pulleys, Figure 5. The necessary torque and speeds were sensed within the CVT and communicated to a vehicle microprocessor control along with operator commands and other vehicle system signals. Output signals for the electrohydraulic valves were generated by the microprocessor and modified by closed-loop torque feedback.

An electric motor was chosen to drive the hydraulic control system pump and the lubrication pump. The electric motor adds weight and cost but provides a control pressure under all foreseeable conditions whereas a mechanically driven pump or pumps would not. Parasitic hydraulic losses were minimized by using a pressure-compensated variable-displacement pump and further by modulating the working pressure setting of this pump to match the demands of the belt pulleys at various operating conditions.

A modulated clutch was located on the input (vehicle driveline) side of the transmission. This clutch served as a complete disconnect for the CVT/flywheel for straight electric operation. It also served as the vehicle start-up clutch with slippage occurring up to 850 rpm of the driveline. During flywheel mode operation, this clutch was modulated to slip before either belt within the CVT to protect against severe driveline shocks.

The overall speed ratio spread of approximately 11.9/1 was accomplished with a high-speed belt and a low-speed belt in series. The design of these belts was completed.

A modest effort was applied to the questions of steel V-belt CVT scalability, applicability to straight electric vehicles, and the applicability to IC engine/battery hybrid vehicles. They can be scaled effectively to higher or lower powers. Their overall effectiveness on a straight electric vehicle with a series motor appeared questionable; however, they may be defensible with other motors and control schemes as a means of eliminating high-power solid-state power-conditioning devices. Their cost effectiveness on IC engine/battery hybrids could not be determined within the scope of this study. Functionally, the design of a unit for that application was felt to be not difficult compared to the current flywheel program.

The primary area of new technology required was found to be low cost, simple, electrohydraulic pressure control valves.

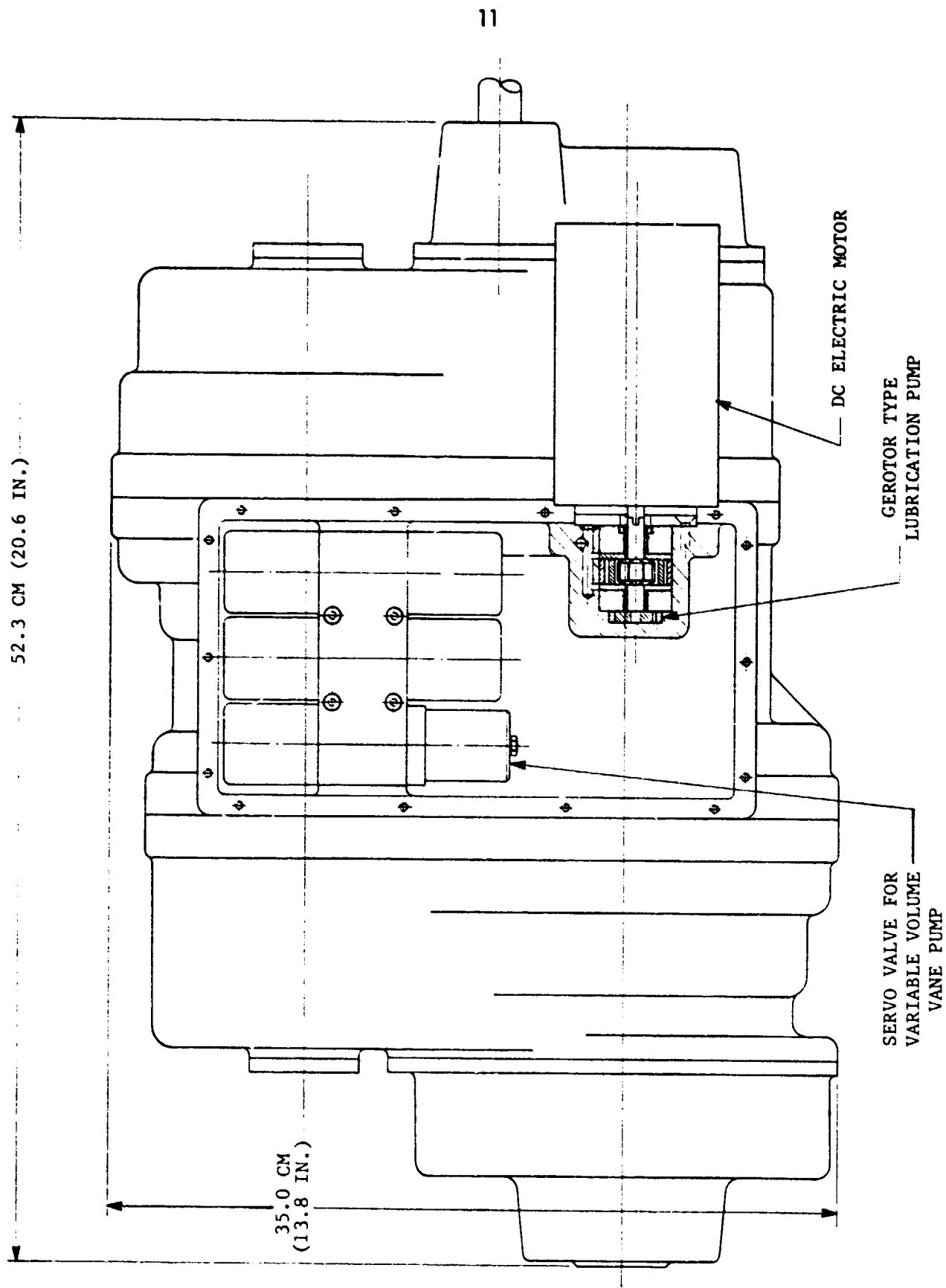


FIGURE 3. CVT PLAN VIEW

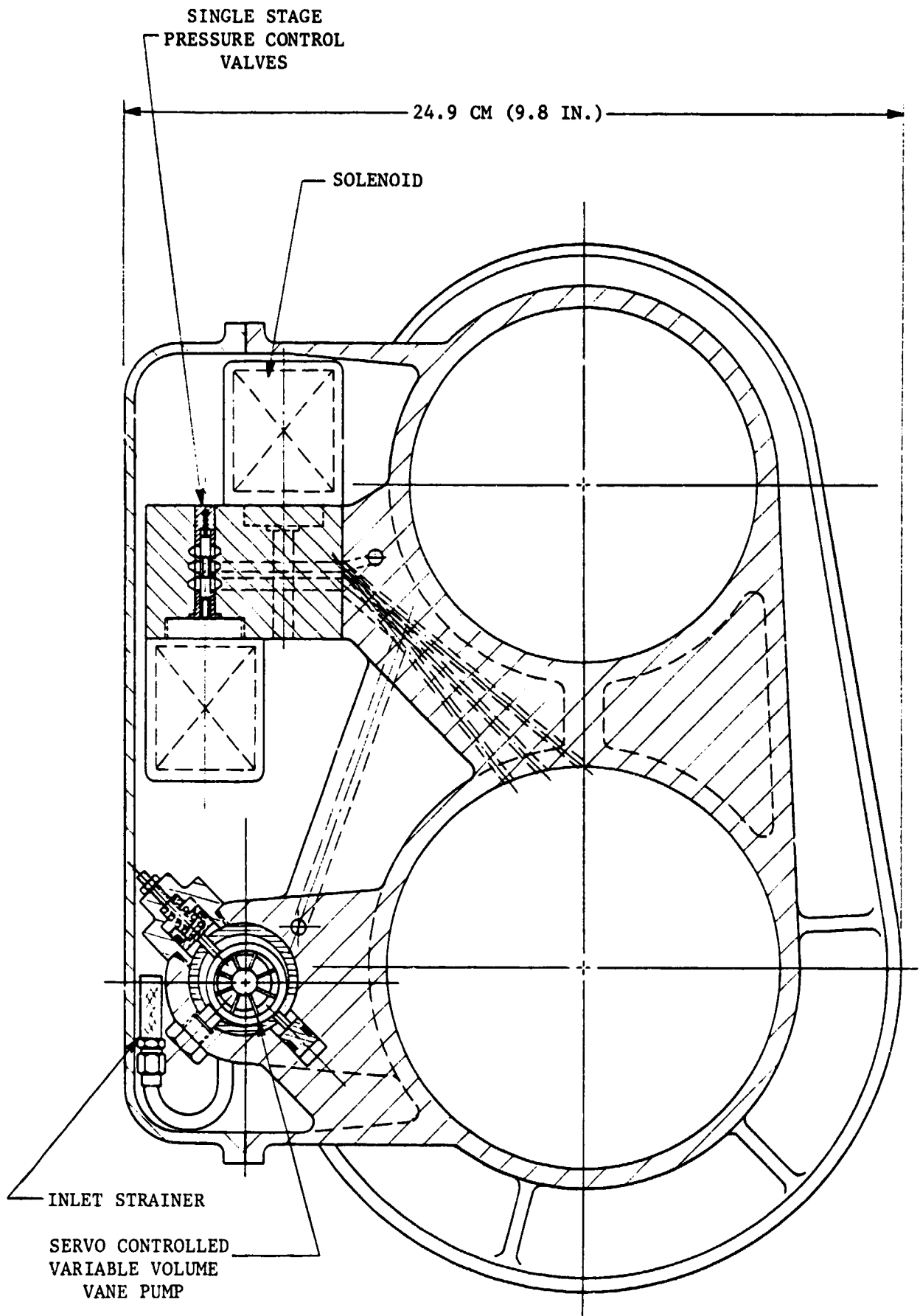


FIGURE 4. CVT TRANSVERSE CROSS SECTION

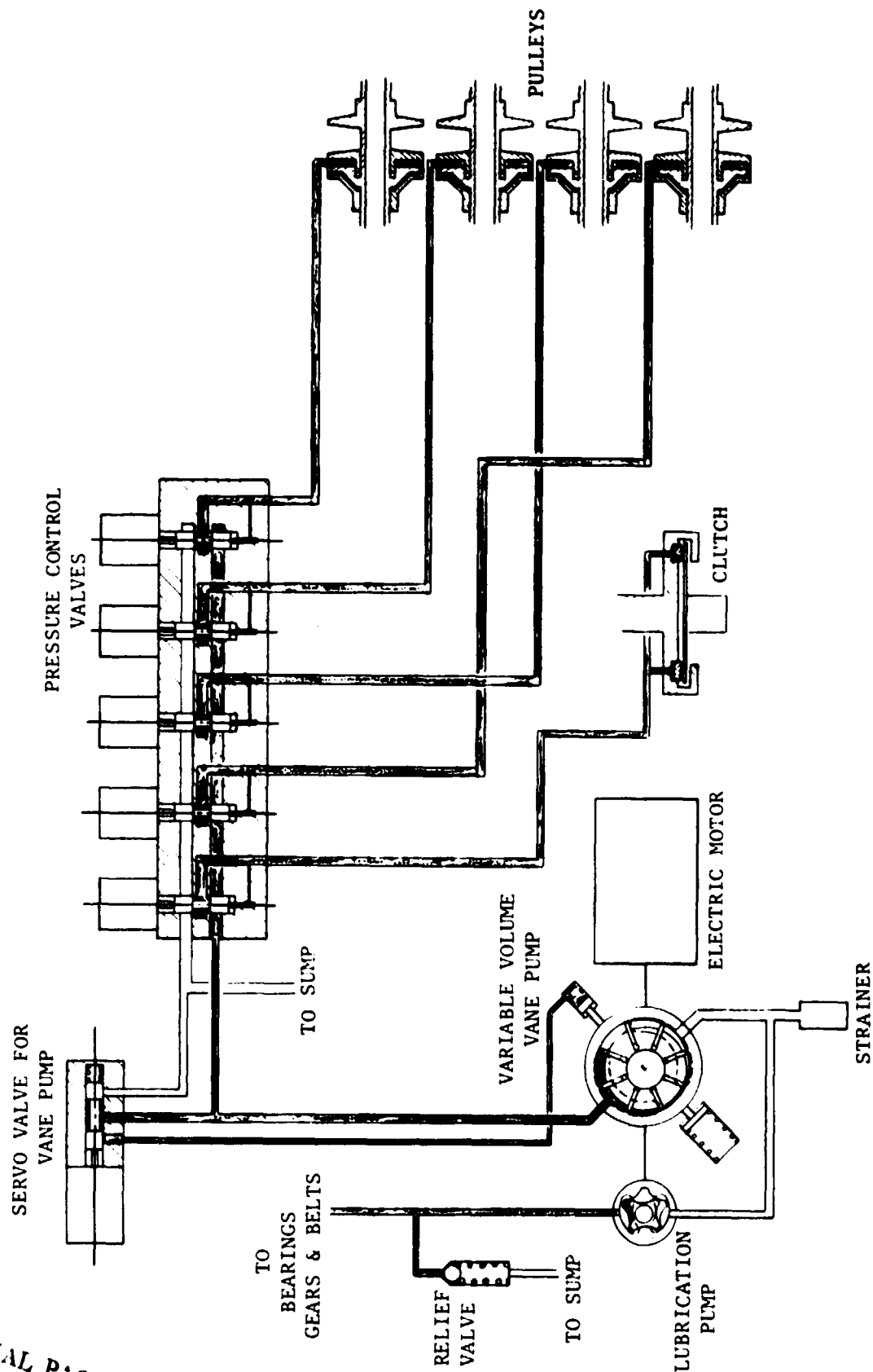


FIGURE 5. HYDRAULIC CONTROL SYSTEM SCHEMATIC

ORIGINAL PAGE IS
OF POOR QUALITY

RECOMMENDATIONS

It is recommended that NASA/Lewis proceed without delay into the detail design, hardware fabrication, and laboratory test phase of a steel V-belt CVT. Steps should be taken to assure, if possible, continued incorporation of the compression-type steel V-belt proprietary technology in the design.

TECHNICAL DISCUSSION

Steel V-Belt Background

The potential advantages of metal variable-speed V-belt drives have fascinated power transmission engineers for many years. These advantages are:

- High efficiency
- High power density
- Stepless speed ratio variation
- Quiet operation.

Earlier developments included one arrangement with a wire-wound tensile carrying band and solid cross struts attached thereto. This arrangement achieved high efficiency, but was limited in power capacity because of low tension ratios and because the wire could be only one layer deep and the diameter of the wire was limited by bending stress. The tension ratio is the ratio of tight-side tension (T_1) to slack-side tension (T_2). The power transmitted by a given belt is proportional to $T_1 - T_2$. Therefore, for a given T_1 (tensile member maximum load) the transmission of high power requires a low value of T_2 , or expressed differently, a high T_1/T_2 ratio. The maximum theoretical tension ratio is approximately

$$\frac{T_1}{T_2} = e^{\frac{f_\alpha}{\sin \frac{\Theta}{2}}} \quad (1)$$

where:

- f = coefficient of friction between struts and pulleys
- α = angle of the belt wrap around the pulley
- Θ = included pulley cone angle
- e = base of natural logarithms.

Attempting to increase specific power by increasing tension ratio by decreasing the angle Θ was tried but led to low angles in which the struts tended to lock and not leave the pulleys cleanly.

A private inventor conceived an approach to this problem which allowed the struts to exit smoothly without locking. A low-power version of this belt was built and tested at BCL for the inventor. High tension ratios were achieved and very encouraging efficiency obtained. There were, however, serious reservations regarding the mechanical competence of this belt. In addition, the specific power of this arrangement, while improved, remained limited by the tensile capacity of the single-layer, wire arrangement.

In a later transmission development program for over-the-highway trucks, Battelle carried forward the analytical and experimental evaluations

of several steel V-belt concepts. The emphasis of that program was on improving the belt tensile capacity so that high power could be transmitted with a solid strut design and without low locking angles on the pulleys. The first compelling results of that program were:

- That multiple nested bands could carry many times more tension than wires or single bands.
- That a new concept, the compression belt, made it possible to use nested bands and was superior to the earlier tension belt designs.

The remaining effort on that transmission program (which was extensive) was focused on the compression belt.

The compression belt is illustrated in Figure 6. It consists of a series of struts strung upon flexible metallic bands in such a manner as to allow them to slide freely along them. In addition to contacting the pulleys, the struts contact each other and are provided with rolling surfaces which transmit compressive forces from strut to strut along the length of the belt. It is by means of these forces that power is transmitted from pulley to pulley. The driver pulley actually pushes the driven pulley through a stack of struts. The bands carry a tensile force which is essentially unvarying throughout the length of the belt and is somewhat greater than the maximum compressive force being transmitted. It serves to press the struts into the grooves of the pulleys and to keep the compressed stack of struts from buckling.

The first versions allowed the struts to separate slightly from each other while passing from the driven pulley to the driver. In order to obtain proper kinematic action, therefore, it was necessary to provide some mechanism for closing the gaps between the struts before they entered the driver. This was done by locating the bands on the outer side of the struts so that they round the pulleys beyond the pitch radius. In the straight portions of the belt, the bands travel faster than the struts and tend to drag them forward, bringing them into contact with each other before they enter the driver.

An alternative approach to preventing the struts from separating while passing from the driven pulley to the driver is to preload the strut stack by means of initial preload tension in the bands. This was not considered a viable approach initially because of concern over loss of preload from strut wear. However, it may be a candidate for future designs.

When viewed externally to the belt, the mechanical action and force relationships of the compression belt are the same as those exhibited by conventional belts which transmit power by tensile forces. At any point along its length, the compression belt may be considered to have a net tension which is equal to the band tension minus the strut compression. It is this net tension which acts to pull the belt into the grooves of the pulleys and to pull the pulleys toward each other. Since the band tension is essentially constant throughout the length of the belt, any variation in net tension along the length corresponds to an equal but opposite variation in compression. The net tension is analogous to the tension of a conventional belt, and may be used to define a tension ratio that has the conventional meaning.

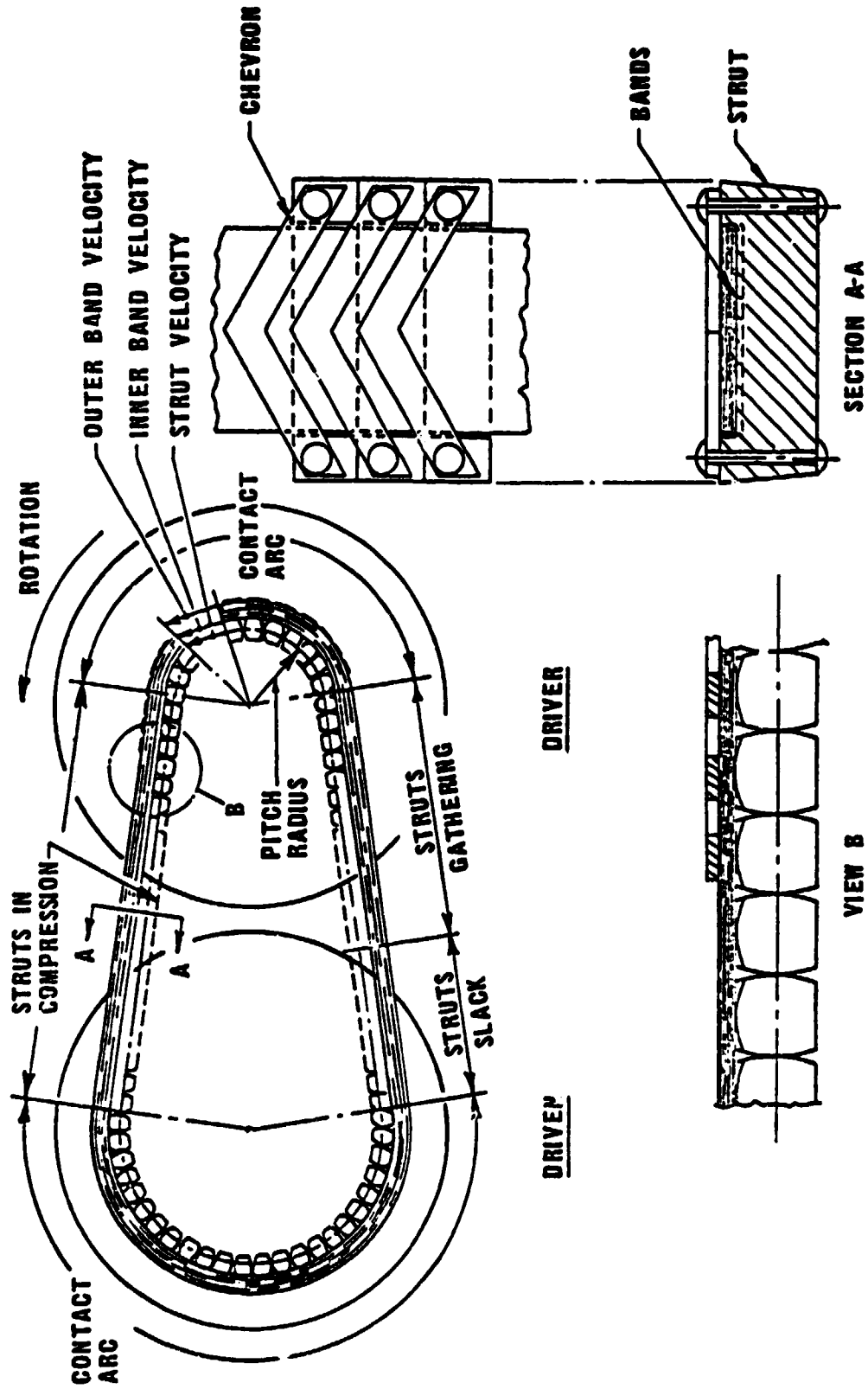


FIGURE 6. METAL COMPRESSION V-BELT

When first conceived, the compression belt seemed completely novel and advantageous. It is interesting to note that the European van Doorne development (Reference 1)* has now appeared to go down a very similar path.

The primary advantages of the compression belt are:

- (1) It completely eliminates the need for any transfer of tension forces from the struts to the bands. Thus the need for attachment to the bands with resulting stress concentrations is eliminated.
- (2) It permits the use of nested multiple-band construction. Thus high tension strength and high-power CVT's can be obtained within a reasonable package size. (A multiple band tensile belt would be very difficult to design. The bands must migrate with respect to each other which makes the transfer of strut-to-band tensile force through an attachment difficult.)

A single-band, low-horsepower version of the compression belt was fabricated first and very encouraging efficiency results were obtained. Figure 7 shows the efficiency results at 3.7 kW (5 hp) and 2500 rpm input speed. The actual efficiency for the belt itself is higher than indicated because parasitic test stand drag losses of about 45N-cm (4 lb-in.) on both the input and output side were charged against the belt.

A multiband belt employing three nested bands was then fabricated, Figure 8. Figure 9 shows this belt in a test stand. This belt ran successfully at 15 kW (20 hp) with input speeds of 2500 and 3000 rpm. Its efficiency at 15 kW (20 hp) and 2500 rpm was 94.7 percent and at 3000 rpm was 93.25 percent. Shift time from 1.5:1 downdrive to 1:1.5 updrive at 1200 rpm input was as low as two seconds, even though only moderate pulley pressures corresponding to 15 kW (20 hp) operation were applied.

A substantial effort was applied to the choice of material for the steel bands and to the methods of fabrication of them. The bands utilized in the majority of the belts tested in this earlier transmission development program were Type 17-7 PH stainless steel. Certain logistic considerations and availability of pertinent and consistent reversed bending fatigue data influenced that choice. While adequate bands were produced in 17-7 PH, it may not be the optimum material when all design requirements are considered. Battelle's current position on band materials and band fabrication is included later in this report.

A novel method of sizing the bands (for length) was developed during the program. Final sizing was accomplished by nesting the set of multiple bands on a fixture on a tensile fatigue tester, Figure 10. The nest of bands was then subjected to yielding tensile loads while rolling uniformly around

*Numbers in parentheses refer to references which appear at the end of this report.

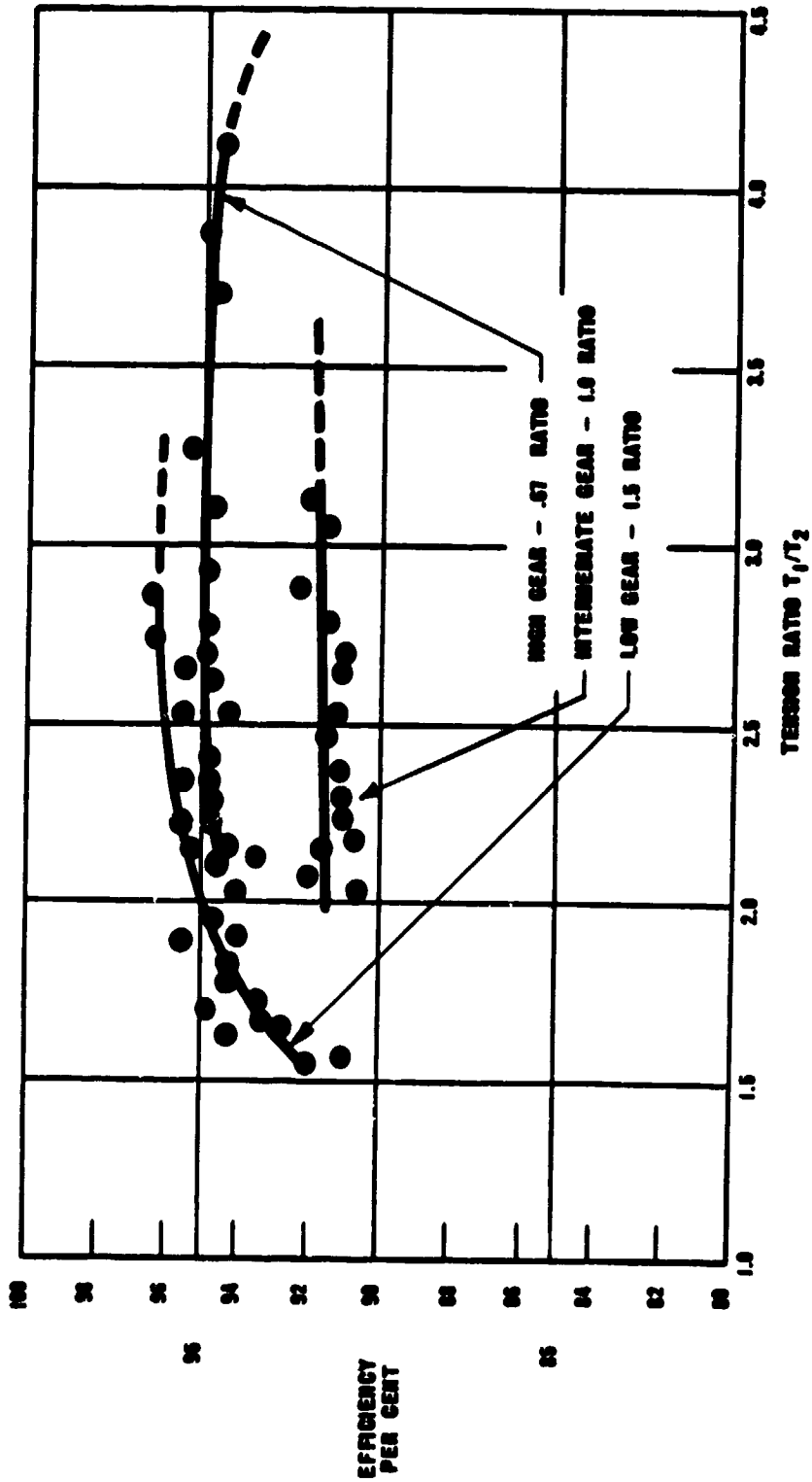


FIGURE 7. SINGLE BAND COMPRESSION BELT EFFICIENCY VERSUS TENSION RATIO
At 3.7 kW and 2500 rpm input speed

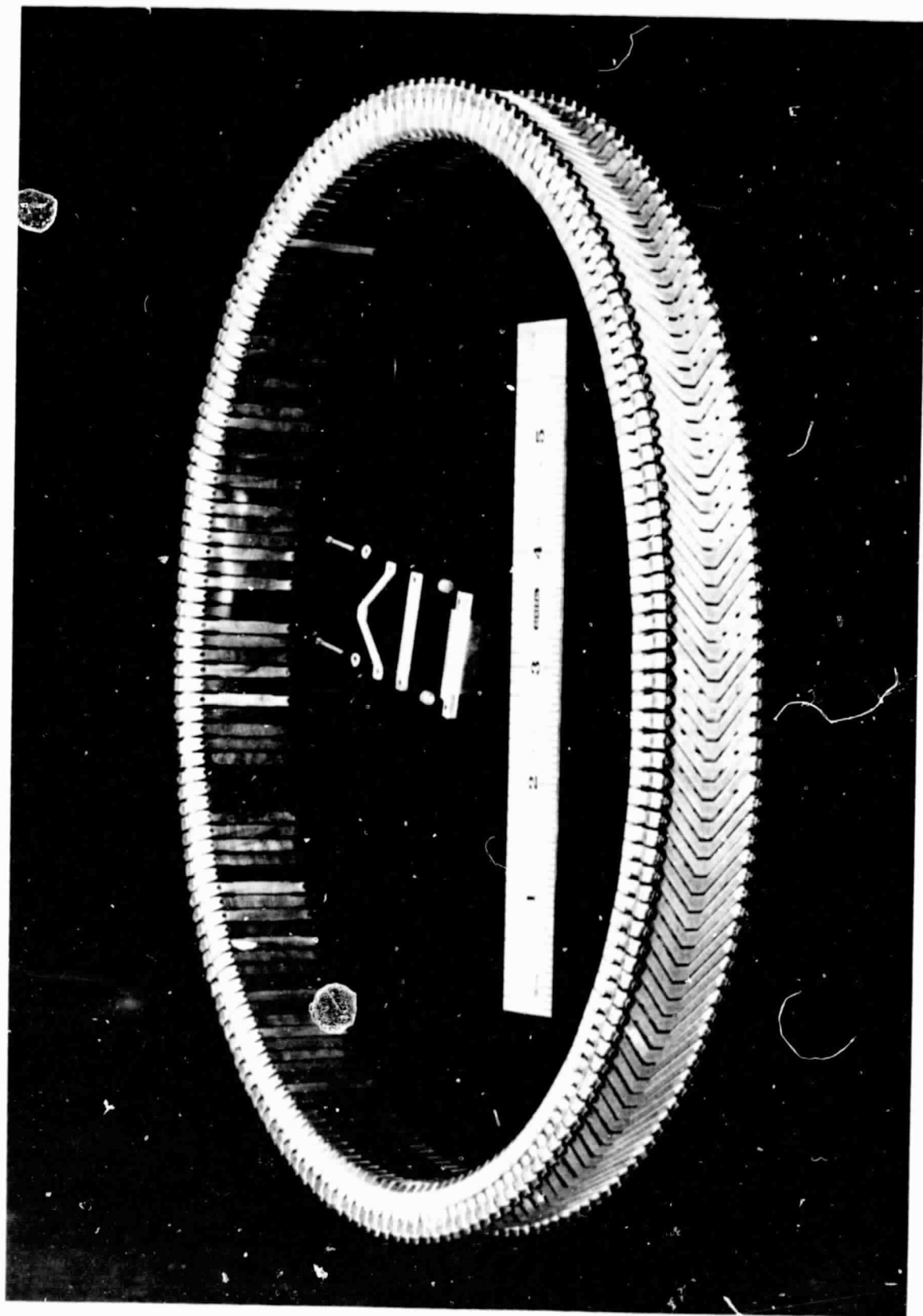


FIGURE 8. MULTIBAND COMPRESSION BELT

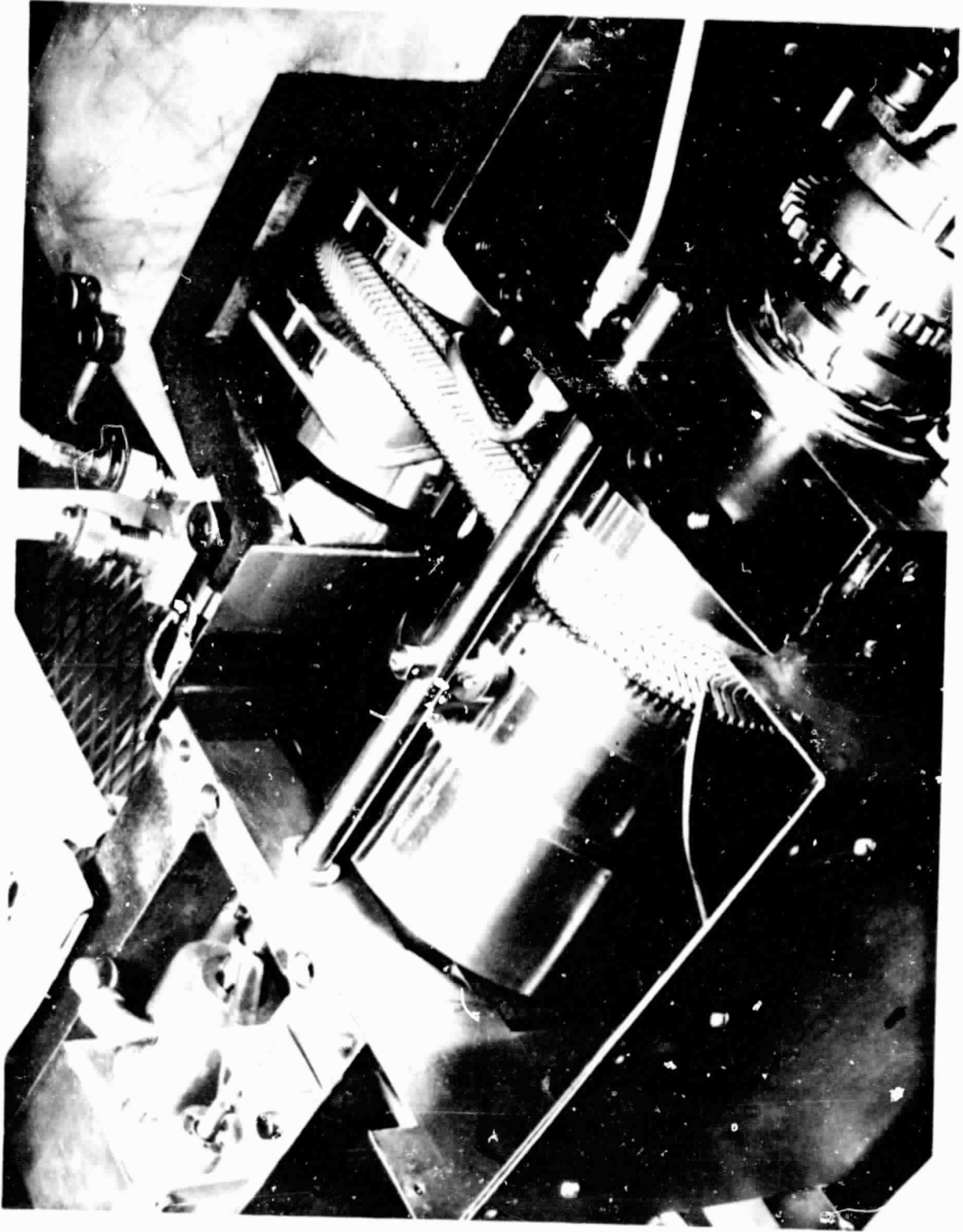


FIGURE 9. MULTIBAND COMPRESSION BELT TEST SETUP

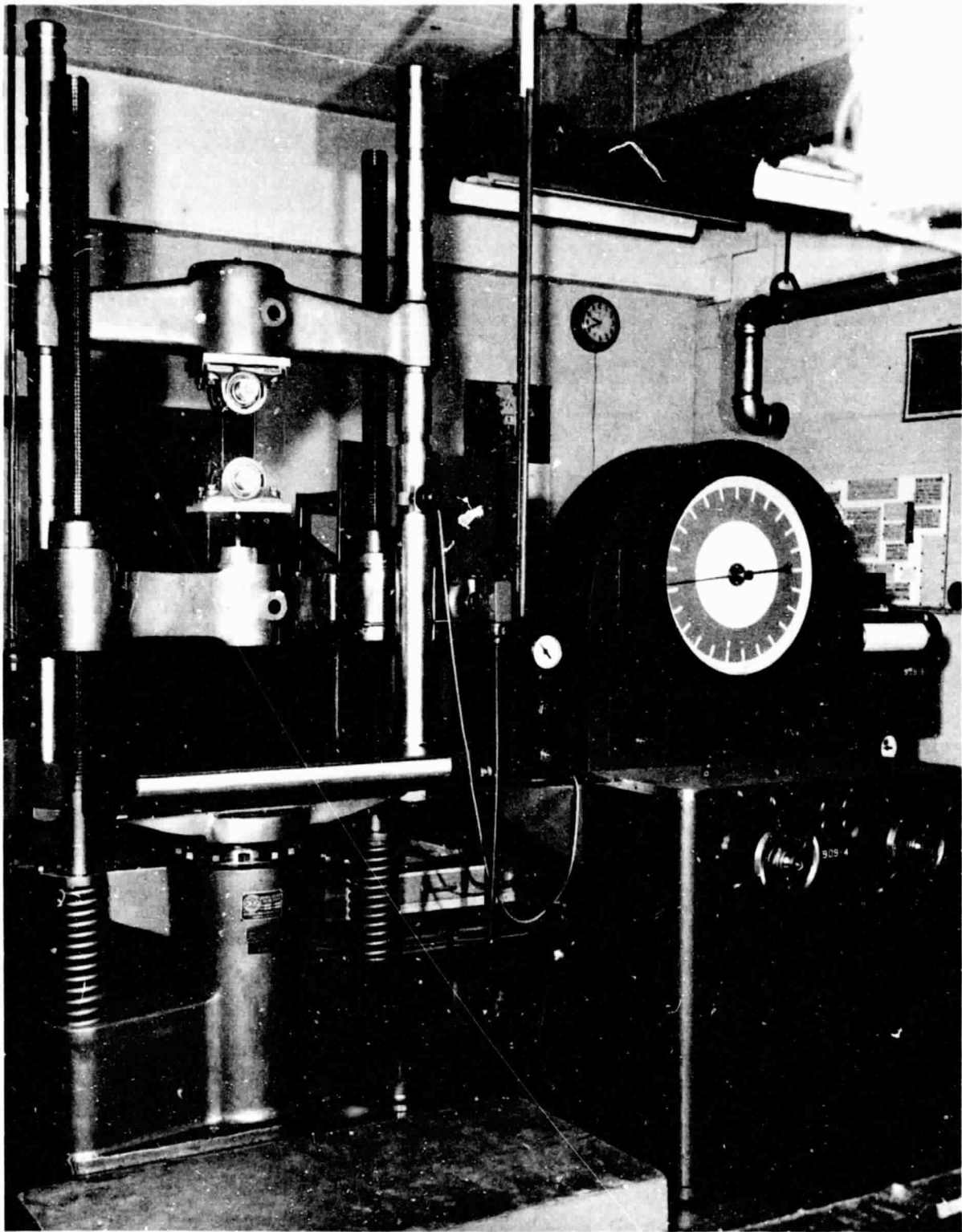


FIGURE 10. STRETCH ROLLING SETUP FOR NESTED BANDS

flat cylindrical pulley surfaces. This technique produced sets of bands containing eight individual bands with the set possessing the required accuracy.

A series of additional design modifications and belt tests was carried forward. This series included tests of six different compression belt configurations, some of which contained 8 nested bands. It included tests of a 30 kW (40 hp) belt which had been parametrically scaled to simulate a 225 kW (300 hp) application in over-the-highway truck transmissions. Throughout this series of six steel V-belt tests they continued to show the potential for high efficiency. Review of approximately 190 efficiency test data points is summarized in Table 1. The efficiency over a range of belt designs and operating conditions spanned from 90.5 to 99.0 percent. Both of these extremes may contain small experimental measurement errors. The important fact is that the average value was 95.0. Although not as high as had been expected (hopes had been for 96 to 98 percent), these results still indicate a very favorable long-term efficiency potential for steel V-belts. The most logical explanation for the failure to achieve the 96 to 98 percent efficiency was a modest speed loss attributed to "pulley-to-pulley" vibrations in the test rig. These vibrations are expected to be much reduced in a CVT design which will have a more rigid pulley mounting arrangement. They will also be reduced by locating the bands closer to the strut pitch radius.

Some other general conclusions from this test series on the six belts were:

- Nested bands can be made to track and perform effectively.
- The pulley included angle for belts with solid struts should not be reduced below about 12 to 13 degrees. Belts F, G, and H were designed with 13, 11, and 9 degrees, respectively, and the average efficiency for their test runs was 96.3, 94.6, and 93.0, respectively.
- The tension ratios achieved were acceptable for a CVT design but were not as high as expected. This was attributed to the aforementioned "pulley-to-pulley" vibrations excited by the struts leaving the pulleys. It is expected that the CVT design will result in higher tension ratios.
- The most demanding durability problem was wear of the inner surface of the inner band caused by its contact with the strut tops. This problem is believed to be amenable to solution by changes in materials and processing of the inner band and by a belt design in which the bands are located radially closer to the pitch line of the struts. This will improve efficiency, tension ratio, and inner band durability. This approach could be supplemented by a return to a design which uses band preload to prevent separation of the struts on the slack side. (It is felt that the strut-to-strut side wear may be made low enough to make this approach viable.)

At the end of the above steel V-belt transmission development program, it was concluded that the metal compression V-belt was functionally

TABLE 1. EFFICIENCY SUMMARY OF TESTS OF
SIX STEEL V-BELTS *

Belt	Efficiency, percent									
	90	91	92	93	94	95	96	97	98	99
C					94.0	x	95.5	97.0		
D					94.0	x	95.5	97.0		
E			92.0			x	94.9	96.0		
F			92.1					x	96.3	99.0
G			92.0			x	94.6	96.0		
H	90.5			x	93.0	94.2				

x = Average for each belt (95.0% average for all tests).

* Based on 190 test data points.

feasible and had the greatest potential of any known V-belt configuration for continuously variable vehicle transmissions.

CVT Operational Requirements

Operating Range Requirements

The design requirements are based on a representative vehicle having a curb weight of 1700 kg (3750 lb). The CVT is to couple a flywheel with a maximum useable energy of 1.8 MJ (0.5 kWh) to this vehicle over the following range of conditions (as specified by NASA/Lewis).

1. High-speed (flywheel) shaft speed of 14,000 to 28,000 rpm
2. Low-speed (differential input) shaft speed of 0 to 5000 rpm
3. Maximum transient power output of 75kW (100 hp) (5-second duration)
4. Maximum transient torque output, at wheel slip, of 450 N-m (330 lb-ft)
5. Maximum shift time (from maximum to minimum reduction ratio and vice versa) of 2 seconds
6. Weighted average output power of 16 kW (22 hp)
7. Average output (drive shaft) speed of 3000 rpm
8. Average input (flywheel) speed of 21,000 rpm
9. 10 percent life of 2600 hr.

The CVT must be capable of bi-directional power flow at the above conditions but the CVT does not have to provide for reverse operation of the vehicle. If required, a variable speed clutch element may be incorporated to regulate the drive shaft output speed between 850 and zero rpm. Provisions must be made to disengage the flywheel from the drive shaft when required. The CVT system must withstand the sudden shock load and torque conditions that may be expected in typical automotive applications.

Control Requirements

The transmission control system is to provide flywheel system operation that is stable, reliable, and responsive. The transmission is to provide driver "feel" similar to that of a standard automotive transmission equipped, internal combustion engine passenger vehicle.

Overall Transmission Configuration

The transmission configuration selected is illustrated in Figure 2. The total ratio spread is achieved by the use of a two-stage, steel V-belt system of the compression type. A 2.8/1 spur gear reducer is used between the flywheel and the high-speed belt. A hydraulically actuated modulating clutch is used between the drive shaft and the low-speed belt.

The transmission system illustrated accomplishes the stated objectives. It provides a continuously variable ratio spread of 11.76:1, sufficient to couple the flywheel in its operating range (14,000 to 28,000 rpm) with the driveshaft at speeds from 850 rpm to 5000 rpm. The modulating clutch is used at driveshaft speeds below 850 rpm, and to bring the flywheel up to its 14,000 rpm minimum operating speed (if the flywheel is accelerated with the vehicle in operation). It also functions as a torque limiter to prevent belt slippage or other damage resulting from transient loads.

The transmission is controlled by an electrohydraulic control system. The axial clamping force of the pulleys (required to prevent belt slippage and accomplish ratio changes) is provided by hydraulic pressure applied in a chamber behind one face of each pulley set. Individually controlled hydraulic pressures are applied to each of the four pulleys and also to the hydraulically actuated modulating clutch. These control pressures are obtained from electrically controlled pressure regulating valves, one for each pulley and the clutch. The pressures required at each location are computed by a vehicle microprocessor and are based upon the amount and direction of torque desired and on the instantaneous transmission ratios. Further details of the control logic are given in the Transmission Control System section of this report. Shifting is accomplished by increasing or decreasing the axial force on the appropriate pulleys.

The hydraulic pressures applied to the pulleys are calculated to provide sufficient axial clamping force on the belts to prevent gross belt slippage, with a modest factor of safety. Excessive overpressures must be avoided to minimize power losses and prevent belt overloading. Details of the axial force requirements are discussed in later sections.

It should be mentioned that in the early phases of this program, other methods of pulley control and axial loading were considered. Several of these systems were of the type in which the axial force was generated by mechanical or hydraulic loading that was directly related to the instantaneous torque being transmitted and to the pulley ratios. They were arranged so that torque could not be developed without a corresponding axial load for each pulley. Thus, these systems were intended to provide all the intelligence needed to operate the belts effectively and protect them from transient loads.

Since pulley control and axial loading are major factors in the design of a steel V-belt transmission, the alternate approaches were considered in some depth. It was ultimately decided to use the electrohydraulic approach. Factors influencing this choice included (1) the potential for a somewhat smaller package size, (2) the mechanical simplification of the transmission itself, (3) the reduction in the number of seals required, (4) the

ease of coupling the transmission controls with the microprocessor technology of the main vehicle control system, and (5) the fact that the alternate systems would still have required pressure control devices to accomplish the ratio selection.

In the selected configuration shown in Figure 2, both sheaves of each pulley are moved to accomplish ratio changes. Both sheaves of the pulleys are controlled so that as the ratios change, the belt remains in the theoretically correct alignment. Although this shifting arrangement is more complex than the usual belt drive configuration where only one sheave of each pulley is stroked, it was thought to be desirable to prevent even the relatively modest misalignment that results from the usual configuration. It is possible that later development programs might show that the simpler shifting arrangement is adequate, and the design could therefore be simplified at that time.

The shifting of both pulley sheaves is accomplished by permitting one pulley sheave to slide on the shaft. The shaft itself is free to shift and the other sheave is fixed to the shaft. The two sheaves are constrained by an axially grounded synchronizing link in such a way as to keep the belt centerline in a fixed position. The synchronizing link is not required to carry any of the major loads. It carries only secondary sliding friction loads.

The hydraulic control fluids are communicated to the control cylinders through face seals at the pulley support shaft ends and then through the shafts themselves. The shaft-end face seals were selected because of the relatively low sliding velocities at this location, low leakage, and the design simplicity. The seals consist of pressure balanced, carbon graphite elements running against hardened steel inserts.

A disc-type modulating clutch is used to couple the CVT to the drive-shaft. This clutch is of the single disc, hydraulic type. It accomplishes the start-up function as well as protecting the CVT from sudden torque transients. The control system sets the hydraulic pressure in the clutch at a level sufficient to prevent slippage under the desired steady-state conditions. Any sudden increases in torque will then result in clutch slippage rather than belt slippage or damage.

Hydraulic control pressures for each of the four pulleys and for the modulating clutch are regulated by a control valve package which is attached to the transmission case. This valve package contains five identical pressure control valves. The valves are single-stage spool type valves with solenoid actuation. The electrical transmission control system monitors the transmission condition and the vehicle control commands and provides an electrical input current to each of the valves that corresponds to the hydraulic pressure required from each valve. These pressures are regulated to provide the proper (efficient and safe) axial load on each pulley and on the modulating clutch based on the desired operating condition. Ratio shifting is accomplished by slight changes in these pressures. Torque transmitted through the transmission's countershaft is the primary controlled parameter.

The hydraulic supply system for the transmission consists of two hydraulic pumps driven by a common electric motor. The main pump is a

servo-controlled, variable volume vane pump. This unit supplies oil to the valve package at the required pressure and flow rate. Both the pressure and the flow rate are varied to meet the demand.

A second pump, of the fixed displacement Gerotor® type is used to supply low-pressure lubricant and cooling flow to the transmission bearings, belts, and gears.

A DC electric motor is used to drive the pumps. This is a high-speed (10,000 rpm) motor which draws its input power from the vehicle battery system.

The pump and motor system above was selected on the basis of efficiency and flexibility. The primary advantage of the electric motor driven system is that hydraulic pressure is available for transmission start-up.

Introduction to Operating Modes and Control

The transmission control system (TCS) for the vehicle must operate in conjunction with the overall vehicle control system (VCS) to select the division of power between the mechanical system (flywheel and CVT) and the electric motor drive system. For the purposes of this report, it is assumed that the VCS receives flywheel system status signals from the TCS and combines this information with overall vehicle status signals and driver input commands to select the desired division of power. This report will primarily be concerned with control of the transmission and flywheel rather than with overall vehicle control. The overall vehicle control system and the total range of operating modes have not been fully defined and therefore the CVT system is based on assumed vehicle control modes.

Operating Modes

The steel V-belt CVT design is compatible with the basic modes of operation of the vehicle. However, it should be noted that the basic philosophy in the design of the CVT and the CVT control system has been to design a system that will transmit torque to or from the flywheel at the level commanded by the overall vehicle control system. Therefore, the total range of operating modes is determined primarily by the overall vehicle design. The CVT system is capable of accommodating the assumed operating modes.

Start-Up. The flywheel can be started in various modes depending on the preference of the vehicle operator and the flexibility of the vehicle control system. In one potential mode, the flywheel can be brought up to operating speed by the drive motor while the vehicle is at rest. The modulating clutch is engaged while the drive motor is at very low speed, and then the motor and flywheel are gradually brought up to speed while the vehicle is stationary.

In another mode, the flywheel can be brought up to speed after the vehicle is in motion, by slipping the modulating clutch until the flywheel

speed is within the range that the belt ratios can accommodate. The driver could select a rate at which the flywheel would be charged.

Normal Operation. During normal driving involving relatively frequent vehicle starts, stops, and speed changes, the driver would control the torque transferred to or from the flywheel by his positioning of the "accelerator" pedal and the brake pedal. The vehicle control system will divide the load between the drive motor and the flywheel or between the vehicle's service brakes and the flywheel. The microprocessor would calculate the desired load division by comparing the vehicle's speed, the battery condition, and the flywheel status with the input commands from the drive.

Flywheel Setpoint Speed. It seems probable that the vehicle control system would provide the driver with some provision for inputting a nominal setpoint for the flywheel speed. This setpoint speed might be related to an "aggressiveness" factor as well as to the type of driving conditions the driver is anticipating. For example, in driving situations in which the driver anticipates the need for rather frequent applications of rapid acceleration, or substantial hill climbing capability, the flywheel setpoint speed could be toward the 28,000 rpm end of the range. This would ensure the availability of substantial flywheel energy when demanded, with the trade-off of higher parasitic power losses and the reduced ability to accept regenerative braking energy under prolonged or repeated brake applications.

Under more normal driving conditions the operator might select a midrange setpoint which would provide adequate flywheel energy for several rapid starts while still providing storage capacity for regenerative braking. In a situation where little usage of the flywheel is anticipated (such as prolonged cruising at a steady speed), the driver could choose a low speed setpoint, or disengage the flywheel system entirely.

The flywheel speed setpoint system would be incorporated into the TCS microprocessor. The system would try to bring the flywheel up to the setpoint speed by means of regenerative braking energy whenever possible. This braking energy would continue to be transferred to the flywheel as long as the flywheel was below its 28,000 rpm maximum speed limit. If the amount of braking energy available is insufficient to bring the flywheel up to the setpoint speed in a reasonable amount of time, energy from the main drive motor would gradually be transferred to the flywheel during periods of relatively low total vehicle power demand.

Shutdown. The vehicle operator can initiate the flywheel shutdown procedure at any time, or the shutdown mode will be automatically selected when the vehicle is switched off. In the shutdown mode, the modulating clutch is totally disengaged. The pulleys are then set to the 1:1 ratio to facilitate the next start-up mode. The hydraulic system then continues to run until the flywheel has stopped, so that pulley control and system lubrication are maintained. Since the drive ratios can't be shifted while the flywheel is stopped, it is advantageous to leave the system in the 1:1 ratio to assist in the eventual restart.

Steel Belt Design Features

The two belts recommended for this flywheel CVT are similar in design to those previously built and tested by Battelle, except that the band stack has been moved closer to the pitch radius of the struts. Though similar in proportion, the two belts are used differently by the CVT in that the low-speed belt carries constant torque on its small pulley throughout its ratio spread while the high-speed belt carries constant torque on its large pulley. Also, the high-speed belt uses a greater portion of its tensile capacity to withstand centrifugal tension. Consequently, the belts differ somewhat in their critical loads and efficiency projections.

The strength of the belts is adequate to allow for some error in the axial force control system. At extreme ratio, for instance, the low-speed belt should be run at a tension ratio of 2.63, but stresses and bearing loads are calculated for a tension ratio of 2.40. The belts are designed for a countershaft torque of 14.44 N-m (1278 lb in.) at 5128 rpm.

The basic dimensions and critical loadings of the two belts are summarized in Table 2. Details of the design are shown in Figures 11 and 12. Design philosophy and methods of calculation are discussed in the following paragraphs.

Band Stacking and Action on Struts

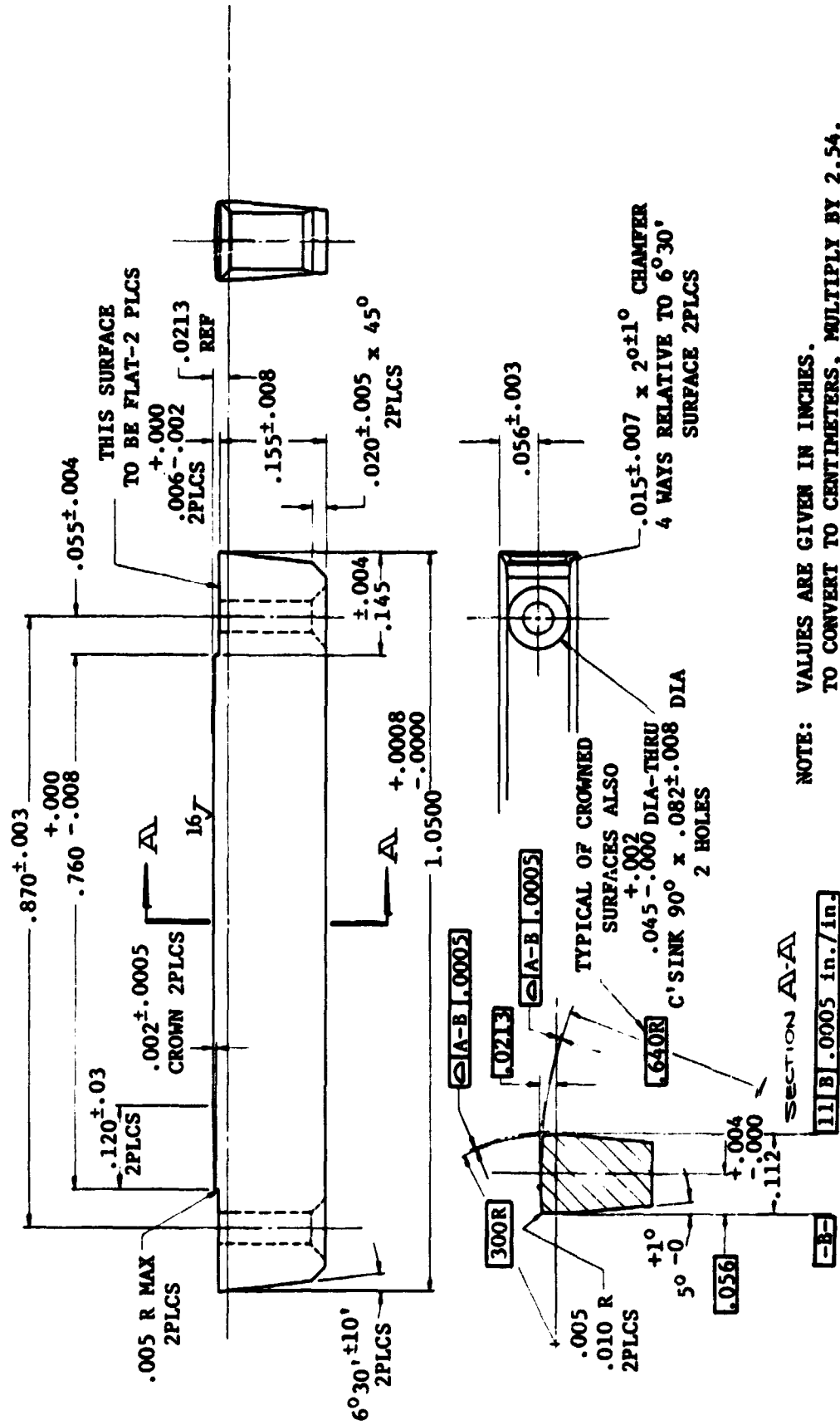
Bands are used as tensile members rather than other alternatives such as wire because they present smooth bearing surfaces that allow several bands to be stacked atop one another. There are small but continuous relative motions between adjacent bands and between the bands and struts which must be allowed if destructive stresses are to be avoided. The thickness of individual bands is limited by bending stress. The diameter of wire would be similarly limited, so that multiple layers of wire would also be needed to achieve adequate tensile capacity. No convenient construction is known whereby multiple layers of wire can move relative to one another as required. The compelling advantage of the compression belt is that it also allows the desired freedom of motion between the bands and the struts.

The number of bands that can be stacked may be limited by the degree to which they can be made to share the tensile load, by the ability to make them track in a centered position on the strut tops, or by the bearing pressure on the inner band resulting from the combined tensile contributions of all the bands stacked atop it. It is believed that the first two problems have been solved to such a degree that the third one is now the controlling factor. Battelle has run stacks of eight bands and van Doorne has run stacks of at least ten. Ten bands are recommended for each of the belts in the flywheel CVT.

Fabrication of accurately nested steel band stacks was achieved in the earlier Battelle truck transmission developed by stretching bands around two cylindrical drums which were rotated while the distance between their centers was slowly increased. Localized tensile yielding takes place each

TABLE 2. SUMMARY OF STEEL BELT DESIGN PARAMETERS

	Low-Speed Belt, Metric	High-Speed Belt, Metric	Low-Speed Belt (U.S.)	High-Speed Belt (U.S.)
Ratio spread (from 1:1)	3.305	3.939	3.305	3.939
Minimum pitch radius	2.540	2.540 cm	1.000	1.000 in.
Minimum center distance	14.92	13.34 cm	5.875	5.250 in.
Cone angle	6.5	6.5 degrees	6.5	6.5 degrees
Width at pitch radius	3.56	2.67 cm	1.40	1.05 in.
Pitch	.381	.284 cm	.150	.112 in.
Weight	.025	.016 kg/cm	.140	.088 lb/in.
Band width	2.29	1.63 cm	.90	.64 in.
Band thickness	.0135	.0102 cm	.0053	.0040 in.
Number of active bands	10	10	10	10
Maximum band stress	7.79×10^8	$7.79 \times 10^8 \text{ N/m}^2$	113,000	113,000 psi
Band bearing pressure, nominal	2.59×10^7	$2.59 \times 10^7 \text{ N/m}^2$	3750	3750 psi
Rolling contact radius	1.02	.762 cm	.400	.300 in.
Maximum rolling contact stress	1.25×10^9	$1.27 \times 10^9 \text{ N/m}^2$	182,000	184,000 psi
Maximum pulley contact stress	1.05×10^9	$9.45 \times 10^8 \text{ N/m}^2$	153,000	137,000 psi
Maximum strut body tensile stress	3.52×10^8	$2.21 \times 10^8 \text{ N/m}^2$	51,000	32,000 psi



NOTE: VALUES ARE GIVEN IN INCHES.
 TO CONVERT TO CENTIMETERS, MULTIPLY BY 2.54.

FIGURE 12. STRUT -- HIGH-SPEED BELT

time an increment of band wraps on or off one of the drums. In this way the yielding is evenly distributed around the length of the band, and the final length can be accurately adjusted. By proper choice of drum diameter, a residual stress pattern was left in the bands such that the surfaces are in compression and, if cut in two, the band naturally curls to a radius of curvature twice that of the minimum pulley on which it is to be run. This residual stress pattern significantly enhances the fatigue strength of the bands.

Very accurate nesting is essential to both load sharing and tracking. At Battelle, this was achieved by a final stretching on rotating drums of the entire assembled stack.

Tracking of the bands on one another and in the center of the struts is achieved by crowning the top of the struts in much the same way that pulleys for flat belts are crowned. It is essential that the bands never contact the sides of the channel in which they run, because this invariably results in upset edges from which fatigue cracks propagate across the bands. The crown should not be greater than necessary, since it causes parts of the band to run farther from the neutral axis and thereby increases the bending stress. A small crown is beneficial from a stress standpoint, however, because it counteracts the tendency of the band edges to curl outward on the pulleys (anti-clastic bending). In both belts of the CVT, the bands are allowed .152 cm (.060 in.) of freedom on each side before their edges will make contact. The crown consists of a bevel that extends under the band another .152 cm (.060 in.), while the center of the strut top is left uncrowned. This crown contour was selected as the result of a theoretical and experimental study of tracking done during the earlier project. It results in a maximum tracking effect for a given increase in bending stress. It is also necessary that the drive be accurately aligned; the shafts must be parallel and the pulleys not axially offset from one another.

Relative motion between the bands arises by virtue of their different mean radii on the pulleys. They tend to run without slipping on one another on the struts on the large pulley because this pulley has the greater angle of wrap. On the straight runs of the belt, the bands near the outside of the stack run faster than those near the inside, and the entire band stack runs faster than the struts. This relative motion is helpful in bringing the struts into contact before they enter the driver, and has no ill effects because the contact pressure is nil on the straights. On the small pulley, the increment of radius between adjacent bands is the same, but the angular velocity is higher. Hence this pulley tries to drive the outer bands faster yet, but as it is unable to do so, the outer bands slide backward on the inner ones and the whole band stack slides backward on the struts. This relative motion combines with the high unit loading due to the band tension acting around the small radius to create a bearing situation that limits the capacity of belts of the proposed design.

These small relative motions on the small pulley will also induce large tensile stresses in the inner band if the coefficients of friction on its inner and outer sides are much different. The friction characteristics of the strut-to-band contact may differ from those of the band-to-band contact

because the materials are different and the geometry is different. If one of the surfaces is roughened by rapid wear, the differences may be expected to increase.

In the experimental belts built by Battelle, the one durability problem that persisted to the end of the project was a scoring of the band-to-strut bearing surface. This was often accompanied by a gradual elongation of the inner band such that it no longer nested without compressing with the rest of the stack. This elongation was attributed to tension arising from differing coefficients of friction, which became more severe as the bearing failure progressed. The band-to-band bearing surfaces remained healthy unless contaminated by wear debris from the strut-to-band contact. In these belts, the band contact was purposely located at least .33 cm (.13 in.) outboard of the pitch surface in the struts to facilitate gap gathering. The strut-to-band relative velocity on the small pulley was thus several times the band-to-band velocity. Battelle proceeded on the theory that this explains the failure of the one surface while the other survived.

In the present belt designs, the band-to-strut contact has been placed as close to the pitch surface as possible without interrupting the rolling contact between the struts. This has resulted in an approximately five-fold reduction of sliding velocity at this critical contact. The bearing pressure is about the same as in the earlier belts. It is not possible to place the contact surface exactly on the pitch surface, because the pitch surface migrates radially in the struts by about two band thicknesses as the pulley radius varies. It was considered better, therefore, to leave the contact surface far enough out to generate a minimum velocity for oil film maintenance, to retain some gap gathering capability, and to leave the strut rolling surfaces intact.

Another design change worth considering is the inclusion of a dummy inner band that has been cut transversely to relieve it of power-carrying tensile stresses. This band might be of a better bearing material since it would not have to be welded and sized. It would be better able to withstand local tensions due to differing coefficients of friction on its inner and outer sides because power-carrying tension would not be superimposed. Cut inner bands have been run in some of the belts built at Battelle with good results as far as the bearing durability was concerned, but the cut bands did not track well except near unity ratio. This should be pursued farther, however, as it might be possible to key the ends of the band to one another well enough to maintain tracking. Space for a cut band has been provided in the belts of the flywheel CVT.

Computation of the bearing pressure actually felt by the bands is complicated by the effects of their stiffness and by tolerance variations. The strut tops are radiused such that if all the struts run at the same radius on the smallest pulley, and if the bands stretch to a straight line from strut top to strut top, then the bands will wrap around and contact 85 percent of the width of the strut top. A nominal bearing pressure may be calculated for this condition, and the belts of the CVT are designed for $2.59 \times 10^3 \text{ N/m}^2$ (3750 psi) at the maximum relative velocity of 45.5 cm (17.9 in.) per second.

In practice, however, infinite tension would be required to stretch a stiff band into a perfectly straight line. The bands actually arch in an exponential curve from strut top to strut top, and this curvature subtracts from the angle of wrap on the struts. Computations indicate that a load concentration factor of 1.9 would result on the smallest pulley at maximum tension. This load concentration can be reduced substantially only if the strut tops are formed to a noncircular contour. It was preferred to leave them radiused because this provides an allowance for tolerance variation in the strut length. If one strut of the low-speed belt is .0020 cm (.0008 in.) longer than its neighbors, it will run enough farther out in the pulley so that the 85 percent strut top contact will just be restored, and contact with the corners of the strut top will still be avoided. A tolerance range of .0015 cm (.0006 in.) is similarly allowable in the high-speed belt.

"Wearing-in" of the strut tops to only a very small extent would modify their shape such that bearing pressure would vary back toward the nominal value. A wear-in coating might permit this to take place without roughening of the surface.

Band Stress

It is desirable that the bands be as thick as the bending stress limit permits, because overly thin bands are delicate and hard to make and susceptible to stress concentrations from surface defects. Up to a point, thicker bands also have more tensile capacity, so that fewer are required. For the bands of this CVT a further increase in thickness would reduce the percentage of the allowable stress available for tension faster than the transverse area increases so that the tensile capacity would decrease.

The band material is assumed to have an ultimate strength of 1.55×10^9 N/m² (225,000 psi), a fully-reversed fatigue strength of 6.89×10^8 N/m² (100,000 psi), and a modulus of 20×10^{10} N/m² (29×10^6 psi). A maximum shear stress theory of failure is used because it yields lower safety factors in this case than the maximum tensile stress theory. Goodman's equation is used to calculate the effect of mean stress superimposed on fatigue stress.

Approximately 4.14×10^8 N/m² (60,000 psi) is allocated as tensile capacity for the belt. This is not considered to be a fatigue loading because it does not change substantially as the belt makes its circuit around the pulleys.

A beneficial residual stress pattern is left in the bands by stretching on rotating drums. If the drum radius is equal to the strut top radius, the outer half of the band's thickness will be at a uniform tensile stress when it is wrapped around a strut, and the inner half of the band's thickness will be at the same uniform tensile stress when the band is straightened. If the band is severed and allowed to assume its free radius, this will be twice the radius of the strut top and both surfaces will be in compression. In addition, for reasons not completely understood, the stretching operation leaves a residual stress in the transverse direction which is sometimes as large as that in the longitudinal direction. When the band is flattened by

assembly between a strut and crossbar, the outer surface is placed in transverse compression and the inner surface in transverse tension. By the maximum shear stress theory of failure, this transverse compression of the outer surface is equally as damaging as the same amount of longitudinal tension.

Bending stress is calculated on the basis of the band being wrapped around the strut top radius, regardless of what radius the strut may be at in the pulley. Plate bending theory is used for the center of the band and simple beam bending for its edges. The crowned contour of the strut top contributes an additional bending stress component since it causes parts of the band to be farther from the neutral axis. The band is assumed to be running centered on the crown. Bending stresses are a fatigue loading which should be below the endurance limit of the bands.

Table 3 summarizes stress components at the two points of highest loading in the band cross section. These values are typical of both belts. The low-speed belt has .0135 cm (.0053 in.) thick bands operating on 2.159 cm (.850 in.) radius struts and is most highly loaded at extreme ratio. The high-speed belt has .0101 cm (.0040 in.) thick bands operating on 1.626 cm (.640 in.) radius struts and is most highly loaded at unity ratio. The highest tensile and shear stresses occur at the outer center fibre, while the lowest safety factor on the fatigue component is found at the inner corner fibre.

Traction Contact Loads

The strut ends are configured with a flat pad in the middle for maximum stability of the strut attitude to the pulley face, and with a slight chamfer (2 degrees) around the edges to prevent high local stresses due to contact of the corners. Surface contact with the pulley will not extend more than halfway across the chamfers. The precise form of the strut end will not be a matter of great concern in production.

In order to calculate the normal load on the end of an individual strut as a function of net belt tension, it is assumed that the strut is sliding inward on the pulley face at an angle of 45 degrees from the radial with a coefficient of friction of .06. The largest strut end load seen by the low-speed belt is then 476 kg (1050 lb), and that seen by the high-speed belt is 165 kg (364 lb).

Contact stresses are calculated by a two-dimensional Hertzian analysis. The chamfered strut end is treated as a cylinder of equivalent radius with a flat, and the conical pulley face is treated as a second cylinder having the same local curvature. Contact stresses for this configuration may be found by the superposition of three simple solutions:

- (1) Two cylinders pressed together such that the contact width is greater than the flat, minus
- (2) Two cylinders pressed together such that the contact width is equal to the flat, plus

TABLE 3. BAND STRESSES

Values given are typical of both belts.

	N/m ²		psi	
	Outer center fibre, 10 ⁸	Inner corner fibre, 10 ⁸	Outer center fibre	Inner corner fibre
On pulley				
Load-carrying tension	4.16	4.16	60,400	60,400
Bending due to band thickness	3.40	-3.10	49,300	-44,900
Residual bending stress	-1.70	-1.70	-24,700	-24,700
Residual transverse stress	1.70	---	24,700	---
Bending due to crown	.255	-3.40	3,700	-49,300
Total	7.82	-40.3	113,400	-58,500
Off pulley				
Load-carrying tension	4.16	4.16	60,400	60,400
Bending due to band thickness	3.40	-3.10	49,300	44,900
Residual bending stress	-1.70	-1.70	-24,700	-24,700
Residual transverse stress	-1.70	---	24,700	---
Total	.765	5.56	11,100	80,600
Mean stress	4.29	.761	62,250	11,050
Allowable alternating stress	4.98	6.56	72,300	95,100
Actual alternating stress	3.53	4.80	51,150	69,550
Factor of safety on endurance limit	1.41	1.37	1.41	1.37

- (3) A cylinder and a plane pressed together such that the contact width is equal to the flat.

This solution is applied first to stress variations in the tangential direction, assuming the load to be evenly distributed radially. Then, using the calculated average pressure at the strut center, it is applied again in the radial direction to find the maximum stress and the stress at the center of the pad. The results for the low-speed belt are $1.05 \times 10^9 \text{ N/m}^2$ (153,000 psi) at top and bottom where the chamfer meets the flat, and $2.90 \times 10^8 \text{ N/m}^2$ (42,000 psi) at the center. Contact stresses in the high-speed belt are lower.

These Hertzian stresses are low compared to those commonly found in rolling contact traction drives and antifriction bearings, and are not particularly high compared to common practice in gearing. Consequently, the strut ends and pulley faces should not be subject to fatigue spalling or to rapid wear from the small relative motions encountered in ordinary service.

It has been Battelle's experience that gross slippage is unacceptable. If the pulley load is insufficient to transmit the instantaneous torque during a power surge, the traction surfaces will gall and the performance of the drive will be permanently impaired. The CVT control system protects against gross slip in the following manner. For any given operating condition each of the belt loading pulleys is pressurized to a level approximately 1/3 higher than that required to prevent belt slip. The modulating clutch is pressurized, for any given operating condition, to a level approximately 15 percent higher than that required to prevent its slippage. In the event of rapid torque transients, the clutch will slip to protect the belts. The control system is not required to respond rapidly to driveline shocks or torque transients.

Cone Angle

The cone angle is defined as the angle between an element of the pulley face and a radial line. Thus, as the cone angle approaches zero, the pulley approaches the shape of a disc, and as the cone angle approaches 90 degrees, the pulley approaches the shape of a cylinder. Steel belt drives are designed with much lower cone angles than rubber belt drives because of the lower coefficient of friction at the lubricated steel traction contacts. The proper choice of cone angle for the materials and lubricant used is important to the capacity, smoothness of operation, and efficiency of the drive.

For a belt of given dimensions and with a given coefficient of friction, the torque that can be transmitted without slipping is basically proportional to the total normal force between the strut ends and the pulley faces. This total normal force is related to the axial load on the pulleys by the cosine of the cone angle. Since the cosine remains near unity for the small angles under consideration, the axial force required to transmit a given torque is nearly independent of the cone angle.

On the other hand, belt tension induced by the axial force increases nearly linearly with cone angle, since radially outward force on the struts is generated via the tangent of this small angle. A drive designed with higher-than-necessary cone angle must therefore operate with excess tension on both the slack and tight belt runs, a condition that is commonly referred to as a low tension ratio. More bands are required in the stack, the bearing pressure between the bands and the strut tops is higher, and some important components of inefficiency associated with band sliding and recirculating power are increased. Since the strut-to-band contact is the most critically loaded bearing of the belt, the size of the drive required to transmit a given torque is directly affected and there is strong motivation to design for a small cone angle.

Also, a larger cone angle requires more axial stroke of the pulley faces, and hence longer pulley assemblies and a larger hydraulic supply.

Cone angle is limited on the low side by rough action as the struts are pulled out of the pulleys and by increase of the component of inefficiency due to radial scrubbing of the strut ends on the pulley faces.

Exiting roughness is noticed only at very low speed, where static friction conditions have time to develop between the strut ends and the pulleys, and the coefficient of friction can be as high as 0.3. As the drive attains a speed of a few hundred rpm, the coefficient of friction appears to drop to more nearly .06, and the struts exit freely. During start-up, however, the low cone angle is definitely a self-locking taper. The chevrons (Figures 6 and 8) used in the earlier Battelle steel belt design were very effective in reducing the force required to start the struts moving, and consequently they make feasible the use of lower cone angles than might otherwise be considered. Also, the flywheel CVT is a favorable application for steel belts because the start-up situation is not encountered every time the vehicle comes to rest. Start-up of the belts would be encountered anytime the flywheel is shut down or anytime the CVT is declutched from the flywheel and driveline to reduce parasitic losses. (A clutch may be added between the flywheel and CVT for this purpose.)

The effect of cone angle on efficiency was studied during the earlier program at Battelle. Angles of 6.5, 6.0, and 5.5 degrees were investigated with experimental belts. It was concluded that a significant increase in efficiency could be detected in going from 5.5 to 6.0 degrees, but that little further increase was to be expected, particularly above 6.5 degrees. These tests were conducted on hydraulically loaded laboratory pulleys of substantial thickness. In the flywheel CVT, pulley face rigidity will no doubt be sacrificed to some degree for weight reduction, which will tend to make the cone angle for maximum efficiency higher. This is not contradictory to the earlier statement (page 23) that the CVT would be more rigid than earlier laboratory set-ups. That comment referred to the transmission housing stiffness (which controls pulley-to-pulley centerline distance vibrations), not to pulley face stiffness.

A 6.5 degree cone angle was chosen for the flywheel CVT because it was consistent with past Battelle experience and it appeared to result in a

good compromise between size and efficiency. It is also consistent with the design of the German PIV drives, which used a belt of chain-link construction on 6.35 degree cones. It is not consistent with the van Doorne drive, which utilizes an 11-degree cone angle.

It is interesting to note that the cone angle of the V-belt drive constitutes a design variable not available in rolling contact drives. It can be used to compensate for the differing friction characteristics of various materials and lubricants. Rolling contact drives are typically limited in capacity by Hertzian stress at the traction contacts, so that the torque transmittable by a drive of given dimensions is proportional to the coefficient of friction. Consequently, material and lubricants for rolling contact drives are chosen with high coefficients of friction as an important objective. Steel V-belts, on the other hand, are not limited in capacity by stress on the traction contacts, because the area in contact is relatively large. A lower coefficient of friction can be accommodated in the design by increasing the axial pulley load and decreasing the cone angle. The band tension and the critical bearing loading between the struts and the bands remain unchanged, as do the exiting difficulties. It can be shown that the component of inefficiency due to radial rubbing of the struts on the pulley faces is somewhat higher with a low coefficient of friction and a correspondingly low cone angle. However, this loss is offset by reduced friction elsewhere, particularly in the band contacts. Consequently, steel belt materials and lubricants need not be chosen so much for high friction as for repeatable friction over the life of the drive and over the range of operating variables such as temperature. Conventional automatic transmission and engine oil are compounded for similar requirements.

Strut Body Stresses and Rotational Stability

From the standpoint of force alignment, it would be desirable for the pulley contact pads to be at the same height on the struts as the strut-to-strut rolling contacts. However, the rolling contacts define the pitch surface, and the bands must be close to the pitch surface, so the body of the strut must lie almost entirely below the rolling contact. If the axial pulley force is transmitted to the strut very far above the center of its body, a moment results in the strut that adds to that created by the radially inward band force to generate excessive bending stress.

A compromise was reached whereby the pulley contact pads were centered .18 cm (.07 in.) below the rolling surface centers in the low-speed belt. This results in strut body stresses of $3.52 \times 10^8 \text{ N/m}^2$ (51,000 psi) tension at the bottom in the center of the span and $8.69 \times 10^8 \text{ N/m}^2$ (126,000 psi) compression at the top. The misalignment of tractive effort forces causes a rolling moment on the strut that is opposed by a shifting of the line of action of the band contact force by .030 cm (.012 in.) away from the centerline of the strut.

The struts are also loaded in bending in the tangential direction as tractive forces are carried to the center of the belt. The resulting stresses are estimated as $3.24 \times 10^8 \text{ N/m}^2$ (47,000 psi) tension and

$6.69 \times 10^8 \text{ N/m}^2$ (97,000 psi) compression. The compressive stress at the rivet holes is $6.07 \times 10^8 \text{ N/m}^2$ (88,000 psi).

The struts of the high-speed belt are not so highly stressed because of the easier load schedule it sees in the CVT. The same proportions are used in this belt, however, because the lowered pulley contact pads also lead to a better strut configuration for production.

Preload and Gap Gathering

An unfortunate aspect of the compression belt concept is that the struts in the belt strand between the driven and driver pulleys tend not to be in intimate contact with one another. If a gap between struts is carried into and around the driver to the region where compression should be building up, a point will eventually be reached where there are too few struts under compression in contact with the driver pulley to maintain traction. The driver will then slip ahead, closing the original gap and tending to open a similar one at its entrance point. The resulting percent efficiency loss is greater than the total gap as a percentage of the belt length in the tight strand and the driver arc, and may be as high as the total gap as a percentage of part of the driver arc. The higher value is more probable at low speed.

To preload the belt sufficiently to avoid gaps when the bands are fully stretched by working tension and the struts are fully compressed would be to build forces near the maximum into the belt at all times. Several points of efficiency would be lost to band friction at lighter loads, and life would probably be poor as well. Also, the belt would be more difficult to assemble with this much preload.

Instead, a mechanism is provided for bringing the struts into contact with one another before they enter the driver. On the pulleys, the band stack runs outboard of the pitch point of the struts and hence has a greater velocity. On the straight runs, the bands migrate slowly ahead through the strut stack and, by friction, tend to carry the struts forward until they contact one another. This friction is enhanced by the transverse residual stress in the bands, which causes them to press against the top bars at their center and against the struts at their edges.

In Battelle's earlier belts, the band stack was far outboard of the pitch surface, and the gap gathering capability was great enough to allow for a gap of nearly one strut pitch at assembly, plus considerable wear on the strut rolling surfaces. In the designs now recommended, the band stack has been placed much nearer the pitch surface to reduce relative velocity at the strut-to-band bearing surface. Consequently, the gap gathering capability is adequate only if the belts are carefully assembled and if wear between the struts does not turn out to be a problem.

It is proposed to fill the belts by selective assembly, using an appropriate number of struts having .03 cm (.01) in. greater than normal pitch to fill out each belt. With the belts off the pulleys and in their natural circular configuration, the total gap remaining after the belts are filled

should be $.051 \pm .020$ cm ($.020 \pm .008$ in.) for the low-speed belt and $.025 \pm .018$ cm ($.010 \pm .007$ in.) for the high-speed belt. When the belts are deformed into their ovate running shapes, the pitch length of the strut stack increases slightly so that the remaining clearance is taken up and a light preload is developed. At extreme ratio and with the initial gap at the low end of the tolerance range, the maximum preload is 150 kg (330 lb) in the low-speed belt and 113 kg (250 lb) in the high-speed belt. These preloads are not high enough to cause much additional friction, and they will be relieved by band stretching and strut compression whenever the belts are carrying much power.

Table 4 summarizes the maximum gap formed versus the gap closing capability for several operating conditions.

Functions of Chevrons

The chevrons, Figures 6 and 8, reduce the radially outward force needed to break loose the struts from the pulleys, thereby promoting smoother action at low speed and helping to avoid disaster if one strut, under unusual circumstances, should assume an undue share of the axial pulley force. By making feasible a lower cone angle, the chevrons allow more capacity in a drive of given dimensions. They also provide a limit to the transverse misalignment of neighboring struts, assuring that the belt will enter a pulley without protruding struts catching on its rim.

The chevrons are V-shaped plates mounted above the top bars and fastened to the struts by the same two rivets. They point in the direction of the belt's travel, which is always the same in the flywheel CVT, and extent to a point above the middle of the top bar of the second strut ahead. Thus, if the belt is flexed beyond its normal straight configuration, the chevrons contact the top bars at their tips and apply rolling moments to the struts to which they are attached. This rolling moment starts the struts moving so that a static friction condition is replaced by a dynamic one. The radial force needed to loosen a strut via the chevron is about one-eighth the force that would have to be applied directly to the strut.

It is not expected that the struts would get out of transverse alignment when the drive is running, but they might do so from vibration while the drive is being transported, or they might end up misaligned after initial assembly. Since each strut can move sideways $.152$ cm ($.060$ in.) on the bands, struts may misalign with each other by as much as $.305$ cm ($.120$ in.) if constrained only by the bands. Chamfers totalling this much would then be needed on the pulley rim and the inner corner of the strut to insure against collision of a protruding strut with the outer diameter of the pulley.

The chevrons can easily be toleranced to limit the possible misalignment of adjacent struts to $.114$ cm ($.045$ in.). This alignment can be held even if standard chevrons are used on the $.025$ cm ($.010$ in.) thicker struts used for filling the belt. A total chamfer of $.127$ cm ($.050$ in.) on the strut corner and pulley rim is then adequate.

TABLE 4. GAP CLOSING CAPABILITY AT FULL TORQUE

BELT RATIO	1:1	3.30	3.30	1:1	2.00	3.94
PULLEY DRIVING	--	small	large	--	large	large
	Low-Speed Belt, mm			High-Speed Belt, mm		
Maximum gap as assembled	.457	.051	.051	.203	.013	-.051
Band elongation	.711	.991	1.24	1.07	.97	.81
Strut stack compression	.203	.203	.457	.41	.33	.25
Total gap under load	1.99	1.24	1.75	1.68	1.42	1.02
Gap that can be closed	2.36	1.45	1.45	1.78	1.30	1.04
Remaining unclosed gap	0	0	.030	0	0.13	0
	Low-Speed Belt, in.			High-Speed Belt, in.		
Maximum gap as assembled	.018	.002	.002	.008	.005	-.002
Band elongation	.028	.039	.049	.042	.038	.032
Strut stack compression	.008	.008	.018	.016	.013	.010
Total gap under load	.054	.049	.069	.066	.056	.040
Gap than can be closed	.093	.057	.057	.070	.051	.041
Remaining unclosed gap	0	0	.012	0	.005	0
Efficiency loss, %	0	0	.2	0	.1	0

Strut Materials and Manufacture

Selection of a strut material and method of fabrication has not been undertaken during this project. It is to be expected that most materials that lend themselves to inexpensive forming will not perform as well as the hardened and ground tool steel struts used in laboratory belts, and that new materials will require experimental qualification. In production, most strut contours will have to be formed by molding or coining operations to keep the cost down. The shape of the part is suitable for powder metallurgy, if adequate material properties can be obtained. One sintered material that would probably have adequate strength is Ferro-Tic[®], a mixture of titanium carbide grains in a heat-treatable steel matrix. It has excellent bearing properties against hardened steel, is less dense than steel, and can be machined by conventional means before the matrix is hardened. It is, however, expensive. It may be found that a sintered steel strut would also perform adequately.

The top bars and chevrons would be steel stampings with a minimum of additional finishing. It is anticipated that most of the belt manufacture can be automated.

Steel Belt Performance

Mechanism of Power Transmission

The interaction of the compression belt with its pulleys is exactly the same as that of any V-belt. The belt is pressed radially into the pulley by its net tension, which is the excess of band tension over strut compression. The tractive effort that can be imparted to the belt by the pulley depends upon the force with which the belt is pressed into the pulley, and hence upon the net tension of the belt. Consequently, over a given arc of contact, the net tension change that can be imparted is proportional to the average net tension of the arc. Put another way, the pulley is able to produce a ratio of input net tension to output net tension, commonly called the tension ratio. The tension ratio can be higher if the angle of wrap is greater, but it is not a function of pulley diameter. The tension ratio at which a drive can operate is dictated by the angle of wrap on the smaller pulley, which becomes substantially less than 180 degrees at the higher speed ratios.

In practice, drives are not run at the highest tension ratio that the pulleys can impart because creep losses would be too high for optimum efficiency, and because any power surge or error in the control system could cause traction to be lost. On the other hand, tension ratios that are too low result in less capacity, shorter life, and too much friction for optimum efficiency. The belts for the flywheel CVT are intended to run at a design tension ratio that is 75 percent of the tractive capability of the pulleys, as projected from test data on compression steel belts on pulleys of the same cone angle. Stresses and bearing loads are calculated for a lower tension ratio (68 percent of tractive capability) to allow for inaccuracy in the

control system. The variation of tension ratio with drive ratio is illustrated in Figure 13.

Although most of the net tension change on a pulley is accepted by the belt as a change in the strut compression, there is also some unavoidable change in band tension because of friction with the strut tops. As explained in the section on band stacking, the bands always have a slight backward motion with respect to the struts on the smaller pulley. Consequently, they operate with a tension ratio corresponding to the limit of tractive effort of a flat belt wrapped around the arc of the smaller pulley, and, acting as flat belts, the bands transmit power from the small pulley to the large pulley. If this is the desired direction of power flow, less compressive force is required on the struts. If not, however, a certain amount of power recirculates and the struts must carry more compression as a result. Therefore, compression belts are more efficient when the small pulley is the driver. The effect is more pronounced if the tension ratio is lower than necessary, if the cone angle is high, or if the friction at the band bearings is high.

Centrifugal tension is contained within the belt and does not affect the belt's action on the pulleys. It does increase the recirculating power within the belt, because the strut-to-band bearing pressure is increased. Centrifugal tension is proportional to the weight per unit length of the belt and to the square of its velocity. It reaches a maximum of 127 kg (280 lb) in the high-speed belt and 249 kg (550 lb) in the low-speed belt.

Table 5 summarizes the maximum tensions and compressions that will occur in the belts of the CVT at various ratios. These numbers are based on the lower tension ratios that were used for stress and bearing calculations.

Axial Force Requirements

The control system is required to modulate axial force on the two pulleys so as to control the tension ratio and the rate of speed ratio change. The pulley loads that will result in optimum tension ratio and steady state operation (no speed ratio change) are discussed below. In general, pulley load should be a function of the transmitted torque, the speed ratio, and whether the pulley is driver or driven. It will be shown, though, that a simplification may be possible if one pulley is always the largest.

Detailed analytical study of the action of the belt on the pulleys is not a reliable approach to the determination of axial force requirements because it is difficult to include important factors such as squeeze film performance of the lubricant and deflections of the pulley face support structure. As far as possible, reliance was placed on experimental data, which can be nondimensionalized in terms of total tension and angle of wrap as shown in Figure 14. Total tension is the sum of tight side net tension and slack side net tension. Considerable extrapolation was necessary because we have no data at speed ratios as great as those proposed for the flywheel CVT. The end points of the curve were calculated based on a coefficient of friction of .06.

The variables available for sensing by the control system are torque and pulley face position. Pulley face position relates directly to belt

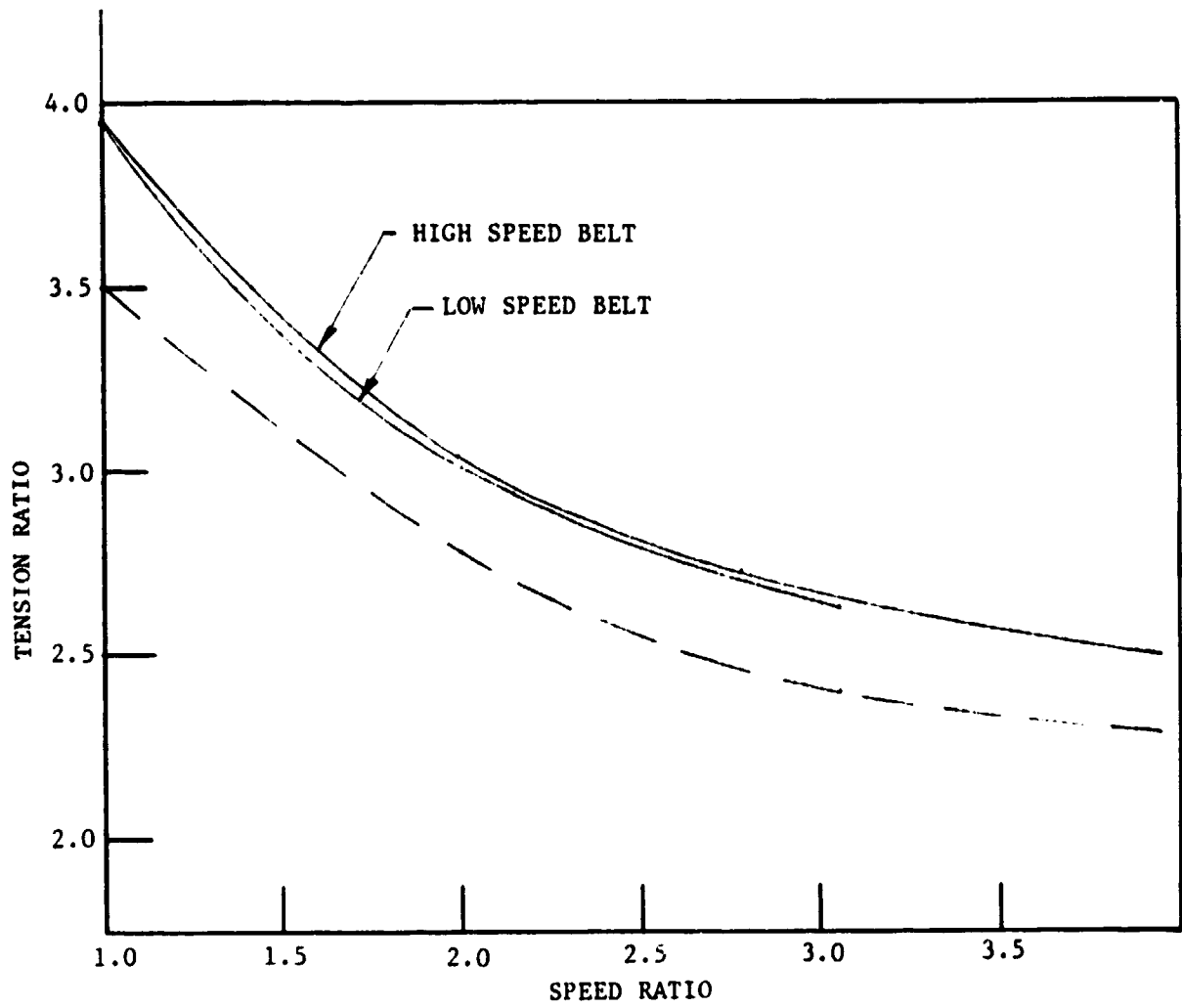


FIGURE 13. DESIGN TENSION RATIOS

— Optimum Running Values
- - - Values Used for Stress and
Bearing Calculations

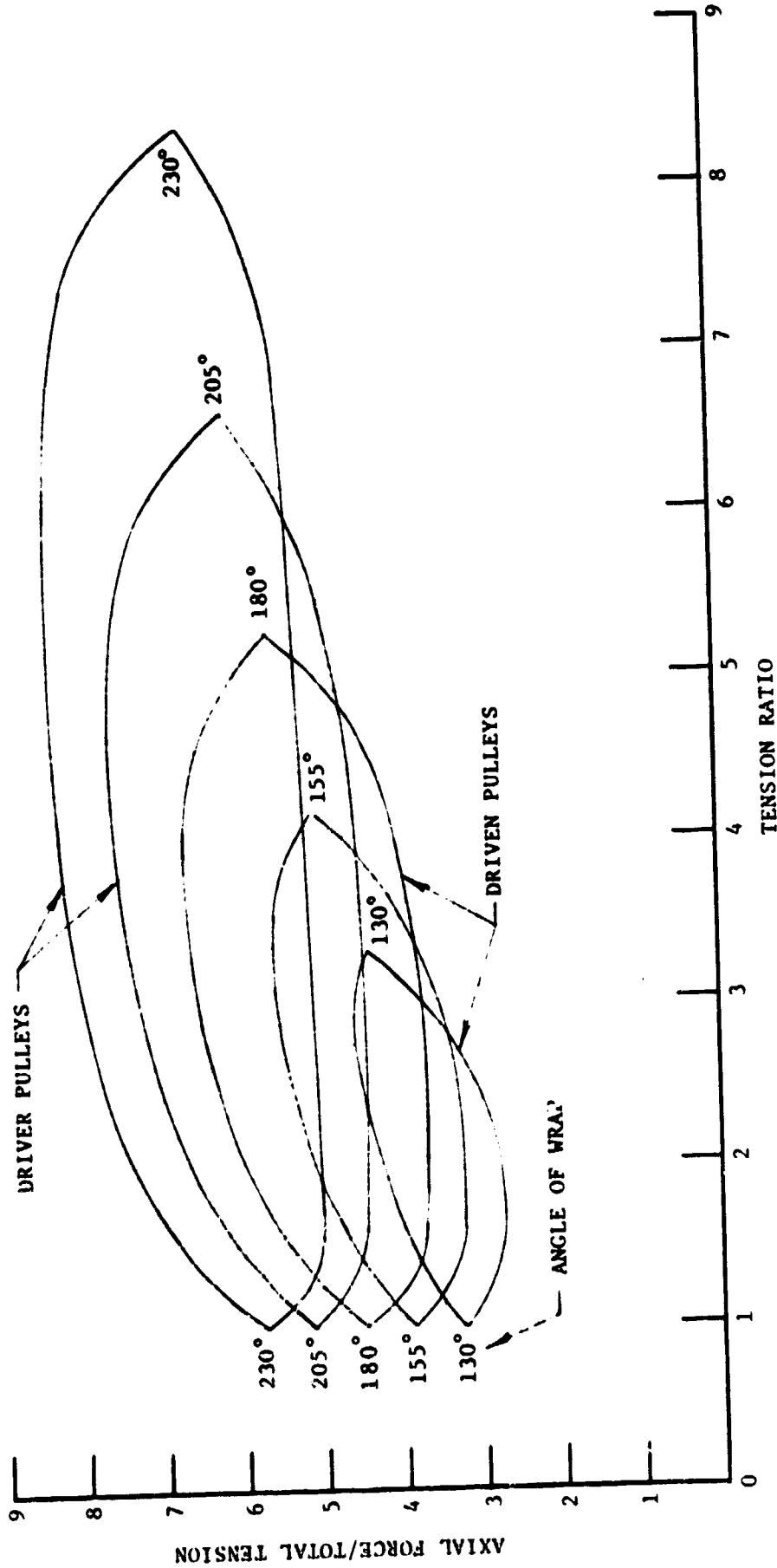


FIGURE 14. STEADY-STATE AXIAL PULLEY FORCES
 Cone Angle = 6.5° ; $\mu = .06$.

radius via the cone angle. Using design tension ratios from Figure 13, the data of Figure 14 may be translated into terms understood by the control system as shown in nondimension form in Figure 15. It can be seen that center distance significantly affects the performance of the large pulley but has only a negligible effect on the small one. This is because the effects of tension ratio and angle of wrap add on the large pulley and cancel on the small one.

Study of Figure 15 reveals that no great compromise is incurred if the control system for the larger pulleys does not comprehend pulley radius. The axial force provided for these larger pulleys can be simply a function of torque and direction of power flow. The small pulleys, on the other hand, will be severely compromised if their axial force is not modulated in response to pulley radius. A lesser but still serious compromise is incurred on both the large and small pulleys if the control systems do not comprehend the direction of power flow. The ratio control system will, of course, respond to over-pressurization of either pulley by over-pressurizing the other one as well.

Chordal Action

Like roller and silent chain, the compression belt is not strictly a constant speed drive. The effect is called chordal action in chain belts because of the way the chain links lie as chords to the sprocket circle. If one pulley is rotated slowly at constant angular velocity, the angular velocity of the other pulley will be observed to undergo a slight cyclical variation with the passage of each strut pitch. More realistically, if the drive is rotated fast enough so that both pulleys, acting as flywheels, turn at constant angular velocity, then cyclical displacements are generated at the ends of the strut stack which must be absorbed by its elastic deformation. A cyclical force is thus generated that may result in noise and vibration or may, in an extreme case, cause the drive to lose traction.

For the steel V-belt displacement from mean position generated at a point of wrap-on or wrap-off is approximately proportional to the rolling surface radius on the strut sides and the square of the strut pitch, and inversely proportional to the square of the pulley radius. Consequently, the greatest effect is generated by the small pulley at extreme ratio, so the phase relationship of events at the large pulley is not of much concern. Table 6 summarizes the displacements and forces generated by each belt of the flywheel CVT.

Although our past experience has been that the belts run quietly, it is evident from these calculations that resonances could be a problem in a light-walled automotive housing. It does not appear that the power-carrying capacity of the belt would be significantly impaired.

van Doorne⁽¹⁾ breaks up resonance in their drive by assembling the belt from a random mix of struts of different pitch. In this CVT design it is proposed to have struts of two different pitches to adjust the initial pre-load. It would be easy to intermix these randomly in the belts of the CVT if chordal action noise should become a problem.

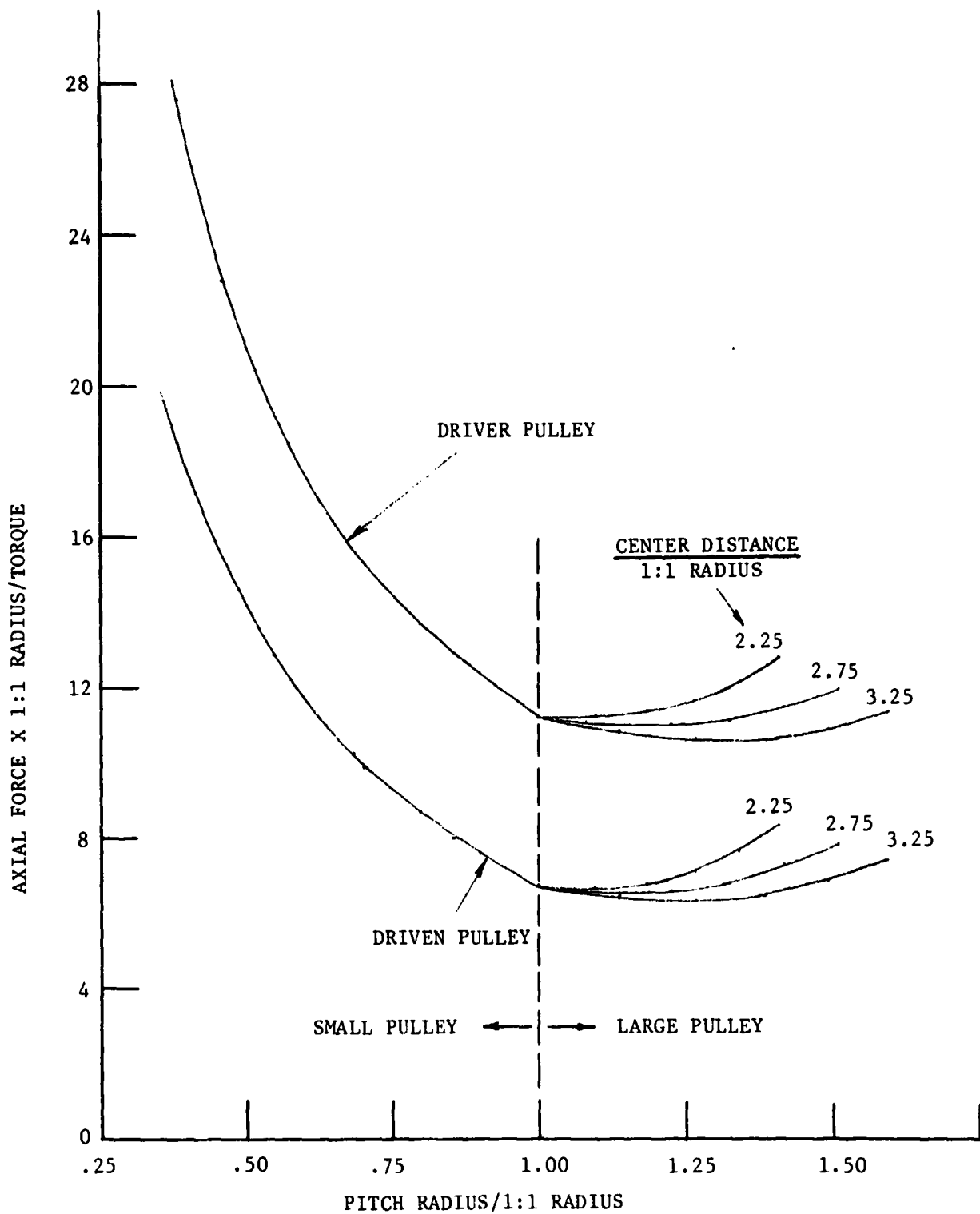


FIGURE 15. DESIRED STEADY-STATE RESPONSE IN TERMS OF VARIABLES MEASURED BY CONTROL SYSTEM

Factor of Safety on Tension Ratio = 1.33; Cone Angle = 6.5° ; $\mu = .06$.

TABLE 6. CONSEQUENCES OF CHORDAL ACTION

	LOW-SPEED BELT	HIGH-SPEED BELT
Velocity variation, maximum excursion from mean at extreme ratio, %	1.25	1.25
Displacement, total excursion, cm (Displacement, total excursion, in.)	.00120 (.00047)	.00086 (.00034)
Force variation, peak to peak, kg (Force variation, peak to peak, lb)	36 (80)	20 (43)
Variation in nominal full load compression, %	± 3.2	± 5.0

Band Material and Fabrication

Material Selection. The thin bands are subjected to a relatively high tensile loading, as well as a significant bending stress due to the small bending radius required by the overall transmission design. A multiplicity of thin bands are used in a nested configuration so that adequate tensile strength can be obtained without generating excessive bending stresses when the belt operates at a small pitch radius. The band material selected should, therefore, have a high tensile strength and a high fatigue limit. A low bending modulus would also help, since it is the ratio of the fatigue strength to the bending modulus that determines the minimum permissible bending radius.

Another area of importance is the band material's resistance to galling and wear when subjected to small relative motions between adjacent bands and between the inner band and the struts. In earlier experiments with this transmission concept, some tendency toward wear and galling was noted at the band/strut interface. It is anticipated that in the recommended transmission design the band/strut interface material requirements will be less severe, because the belts will be running at a position closer to the pitch radius of the struts, thus significantly reducing the relative motion involved. Galling and wear resistance was still considered to be a significant factor in the material selection, however.

Although it was recognized that the ultimate choice of band material would probably be a steel of some type, the investigations did include other metals. The materials considered included:

Precipitation Hardening Stainless Steels (i.e., 17-7 PH and Custom 455)

Maraging Steels (250 and 280 Grades)

Spring Steels (i.e., SAE 1095)

Alloy Steels (i.e., SAE 4340)

Titanium Alloys (i.e., Ti-6Al-4V)

Beryllium Copper (i.e., 1.9% Be, 0.20% Cu).

Precipitation hardening stainless steels, such as 17-7 PH and Custom 455, are good candidates for this application. Good cold forming characteristics, as well as low heat treat temperatures, combine with high yield and fatigue strengths to make them a reasonable choice. Welding can be used in fabricating these materials. The primary objection to them has been their relatively low resistance to galling when running against hardened steel parts.

Spring steels such as SAE 1095 are often used in similar applications involving the use of thin flexible bands wrapped around small radii. In hardened form, the high yield and endurance strengths of spring steels should prove satisfactory. The primary objections to the use of conventional spring steels are in the area of fabrication. High carbon steels are difficult to weld and are sensitive to oxidation and decarburization during heat treatment. They also lack toughness and ductility.

Alloy steels, such as 4340, offer characteristics similar to those of the spring steels except that alloy steels tend to have somewhat greater toughness and ductility at a given strength and hardness level. Their greater through-hardenability is not a significant factor with the thin sections involved in this application, but the lower carbon content improves weldability somewhat.

The high-nickel maraging steels offer good potential because they can be readily formed and welded. They can be aged at moderate temperatures to get extremely high tensile strengths, with little distortion or dimensional change. The primary question with regard to maraging steels appears to be their true fatigue strength relative to tensile strength.

Beryllium copper alloys offer a combination of good fatigue strength and excellent wear resistance against hardened steel combined with a relatively low modulus of elasticity, therefore making the material a good candidate. Beryllium copper is also capable of substantial cold working and of being solution heat treated, thereby aiding in the fabrication of the bands. High cost is the main drawback.

Titanium alloys such as Ti-6Al-4V have a very good ratio of bending fatigue strength to modulus. This is the result of the substantially lower modulus of the material, and results in the possibility of using slightly thicker belts without exceeding the bending stress limitations. Titanium belts could also be fabricated by welding. The principal objections to the use of titanium alloys are their poor resistance to galling, and their high material cost.

During the selection and evaluation of the candidate band materials described above, a number of other materials and fabrication possibilities were considered. Many of these concepts were aimed at the prevention of possible galling and/or wear problems at the band/strut interface and at band/band interfaces. Concepts considered included:

- The use of beryllium copper struts, or critical portions thereof.
- The use of galling resistant coatings on critical strut surfaces or on the inner band surface.
- The use of thin Mylar® (or similar) sheets installed between the bands.
- The use of a special inner band made of a highly gall-resistant material. The band could be made sufficiently thin to prevent excessive bending stresses and could have a modulus low enough to prevent excessive tensile loading. This band need not carry an appreciable share of the total loading.

It was not anticipated that measures of this type would be required in the suggested transmission design. They have been included here for purposes of completeness and to illustrate that a number of options are available in the event that they should be needed.

The seven basic material candidates were evaluated and rated to determine a relative ranking, although it is very difficult to assign objective numerical ratings to materials in an application of this complexity. Table 7 was prepared to aid in the selection process. This table shows comparative stress limitations [yield point stress (S_{yp}), fully reversed bending stress endurance limit (S_e), modulus of elasticity (E)], the ratio of the endurance limit to the modulus of elasticity (S_e/E), density (), and the Rockwell C hardness (R_c). In addition, the materials are rated for the more subjective qualities of weldability, workability and sizing, galling and wear resistance, and material cost.

The numbers in parentheses in Table 7 are the numerical ratings established for comparative purposes. Equal emphasis (a possible 10 points) was given to the (S_e/E) ratio, fabricability (5 points each for weldability and workability), and galling and wear resistance. Less emphasis (a possible 5 points) was given to material cost, since the raw material cost was assumed to be only a modest portion of the total cost of the manufactured belts.

The final choice of the leading candidate is complicated by the range of fatigue limit values published for the 280 grade maraging steel. It is suggested that additional fatigue life information be obtained, either experimentally or from other references, before the final decision on materials is made.

The two leading candidates are 280 grade maraging steel (assuming its fatigue limit is shown to be near the 6.89×10^8 N/m², or 100,000 psi value), and Custom 455 PH precipitation hardening stainless steel. Maraging

TABLE 7. BAND MATERIAL COMPARATIVE RATING

	4340 Steel (B.T. to R _c 51-53)	17-7 PH Stainless Steel (TM 1050 Condition)	102 H1 Maraging Steel (280 Grade)	1.92 Br. .202 Cu Beryllium Copper (H.T. Condition)	1095 Steel (Q&T Condition)	Custom 455 PH Stainless Steel (H-1000 Condition)	Ti-6Al-4V Titanium
S _{yp} x 10 ³ psi	215	150	270	160	200	185	145
S _e x 10 ³ psi	80	75	41-100 ***	40	65	100	55
E x 10 ⁶ psi	29	29	26.5	18.5	29	29	16
S _e x 10 ³ E x 10 ⁶	2.76 (8)*	2.59 (8)	1.55-3.77 (3-10)	2.16 (5)	2.24 (3)	3.44 (10)	3.44 (10)
σ lb/in. ³	.283	.276	.286	.298	.283	.276	.160
Hardness Rockwell C	51-53	38+	50+	40-45	50+	40+	-
Weldability	Somewhat tough in thin sections FAIR	GOOD	GOOD	GOOD	POOR	GOOD	GOOD
Workability Sizing	FAIR (2)	GOOD (4)	FAIR (3)	FAIR (3)	FAIR (2)	GOOD (4)	FAIR (3)
Galling and Wear Resistance	GOOD (7)	FAIR (4)	GOOD (7)	EXCEL.	GOOD (7)	FAIR (4)	POOR (2)
Material Cost	LOW (4)	MED (3)	MED (3)	MED-HIGH	LOW (5)	MED (3)	HIGH (1)
Comments	Care must be taken during welding and heat treatment (Oxidation & De- carburation)	-	Questionable fatigue strength compared to yield strength	Good wear and galling properties Good for strut material	Poor Weldability Prone to oxidation and decarburization	-	-
Total Score	23	23	20-27 ***	24	20	25	20

* Numbers in parentheses represent the numerical ratings.

** Against hardened steel struts.

*** Due to the range of fatigue values cited in several references.

steel is a good choice because of its high strength combined with good fabrication qualities and good resistance to galling and wear. Custom 455 PH stainless steel is also a good choice. It also has very high strength and good fabrication qualities. However, Custom 455 PH is not as good as maraging steel in the area of galling and wear resistance.

Next in the rankings is beryllium copper (1.9 percent Be, .20 percent Cu). This is an excellent material from the wear and galling resistance standpoint, and reasonable fabrication qualities. Its primary disadvantage compared to Custom 455 PH and maraging steel is its significantly lower (Se/E) ratio.

17-7 PH stainless steel (as used in much of Battelle's prior experimental steel V-belt work) is next in the rankings. However, since Custom 455 PH is a more recent stainless steel that has all of the basic characteristics of 17-7 PH, and is considerably stronger, there would seem to be little advantage in using 17-7 PH.

4340 alloy steel is next in the rankings. It combines an average (Se/E) ratio with good galling resistance and low material cost. The primary drawbacks are in the areas of weldability and fabricability. 4340 steel is somewhat difficult to weld and heat treat in such thin sections due to oxidation and decarburization, and distortion.

1095 spring steel is in last place primarily because of its poor fabricability. The high carbon content would result in brittleness and difficulty in welding, as well as difficulty in heat treating and sizing.

While both Custom 455 PH and maraging steel are considered to have an excellent chance of succeeding in this application, only prototype testing can confirm their acceptability. Should problems occur, there are several reasonable alternates that could be tested. Beryllium copper would be a good alternate if better galling and wear resistance is required. 4340 alloy steel would also be tested if appropriate fabrication methods are developed.

Fabrication Recommendations

The objective in the band fabrication is to produce a set of properly nested belts, of the proper thickness, and of uniform size and strength. The critical areas are:

- (1) Accurate sizing of the individual bands so that each band in a set carries its share of the load
- (2) Fabricating a belt that has uniform characteristics throughout its circumference
- (3) Achieving a good surface finish to promote a good fatigue life.

The fabrication technique that is suggested to produce a set of nested Custom 455 PH stainless steel bands is as follows:

- (1) Weld blanks straight across by melting down turned-up ends using argon-shielded arc. These blanks to be of correct dimensions to permit a 30 percent cold reduction and yet achieve band thickness and length. Also, blank width to be approximately 40 percent greater than design width to permit trimming.
- (2) Clean weld areas smooth.
- (3) Trim edges to remove weld end effects.
- (4) Cold reduce bands to approximate length required.
- (5) Completely anneal in vacuum at 829 C (1525 F).
- (6) Stretch bands individually to straighten and size as accurately as possible.
- (7) Heat treat at 829 C (1525 F) for 5 minutes and quench in water.
- (8) Age the belts at 538 C (1000 F) while on split ring mandrels.
- (9) Cool to room temperature.
- (10) Machine to the desired band width.
- (11) Stretch roll nested band sets for final sizing and mating.

This fabrication procedure should serve as a good starting point in the fabrication of a good set of nested Custom 455 PH stainless steel bands. Development work during the prototype testing may suggest useful revisions. A similar procedure could be used for the fabrication of maraging steel bands.

Belt Lubrication

The purpose of the lubrication evaluation was to develop a logical criteria for the selection of a lubricant for the steel V-belt. The recommended lubricant is automatic transmission fluid.

The belt lubricant must provide the dual functioning of minimizing friction-induced power losses and preventing wear and galling damage of the components. In addition, it is imperative that the friction coefficient between the strut ends and the pulley faces remain relatively constant so that belt slippage can be prevented.

Film Thickness Evaluations

During each contact period of a strut and pulley, some type of lubricant should be available to protect these interfaces. However, there are some critical questions as to how much lubricant and what type of lubricant is

optimum. A derivation of the film thickness between strut and pulley (ignoring end leakage) is given in Appendix A. In dimensionless form, this equation appears as

$$\frac{h}{a} = \sqrt{\frac{3\mu_0 \gamma}{t}} \quad (2)$$

where μ_0 = lubricant base viscosity
 γ = pressure viscosity constant
 a = half-width of strut-pulley contact
 t = residence time of contact
 h = film thickness.

From practical consideration, the lubrication process may (roughly) be divided into three regimes as follows:

- (a) $h/\sigma > 3$
- (b) $3 > h/\sigma > 1/3$
- (c) $1/3 > h/\sigma$,

where σ is the surface roughness.

Regime (a) is fully flooded conditions (elastohydrodynamic lubrication), (b) is a mixed lubricant condition, and (c) is a boundary lubricant condition. Boundary lubrication implies metal-to-metal contact in the presence of a reacted surface film.

In general, the thicker the film, the lower the traction, the higher the possibility for slip, but the longer the life. Conversely, the thinner the film, the higher the traction, but the shorter the fatigue life. A clear criteria for the traction belt is certainly not known. However, to optimize efficiency, it is reasonable that

$$\frac{h}{\sigma} < 1 \quad (3)$$

For such a condition, a good boundary lubricant is needed to yield acceptable performance life.

Effect of Viscosity on Film Thickness

Equation (3) can be used to estimate the thickness of the film between pulley and strut or strut and strut as a function of the contact time; the longer this time, the thinner the film. If a pulley is moving at 6000 rpm, the contact time might be on the order of .005 seconds (the time for one-half of a revolution for the strut-to-pulley contact) to as much as .02 seconds for the strut-to-strut contact. However, since some boundary contact is desirable, it is important that the lubricant be squeezed out as quickly as possible. For this reason, a reasonable characteristic time for the calculation might be on the order of 2×10^{-3} seconds.

A typical value for α for both strut-strut and strut-pulley is .10 cm (.04 in.) and γ is about 1.45 GPa^{-1} (10^{-4} psi^{-1}). Using these values in Equation (3), then it can be seen that

$$h = .15 \sqrt{\mu_c} \quad (\mu\text{m}) \quad , \quad (4)$$

where μ_c is the base viscosity in centipoise. Equation (4) is plotted as a function of viscosity in Figure 16.

In order to achieve boundary lubrication, a film on the order of the surface roughness is desired, hence a very low viscosity fluid is indicated. This implies a fluid such as automatic transmission fluid or a thin traction fluid (such as Santotrac 30). If either of these fluids are used, boundary contact may be achieved if the surface roughness is on the order of .4-.5 μm (15 $\mu\text{in.}$) which is reasonable for good surfaces.

Lubricant Selection

The lubricant selection process eventually comes to a choice between automatic transmission fluid, or a thin traction fluid such as Santotrac 30 or 50. Further consideration of the properties of the fluids resulted in the following comments.

- Santotrac 50 and 70 are the only Santotrac fluids formulated for boundary lubrication (antiscuffing, antiwear properties) effectiveness. Because a candidate fluid for practical use in a CVT should have such additives, these represent the only current commercial Santotrac fluids that should be considered good enough to lubricate sliding contact CVT's. Other traction fluids could be formulated for this application if there were sufficient commercial interest.
- ATF's have established good records on foaming characteristics whereas the foaming characteristic of Santotrac fluids is not as well documented. However, the performance of the antifoam additive in Santotrac fluids should be adequate for hydraulic fluid application being considered.
- Santotrac fluids should perform adequately in the clutch interfaces but probably will not represent a sufficient improvement over other fluids. If the heat generation does not form any undesirable films on the clutch faces or thermally punish any of the additives in the fluid, extended service in this application should be acceptable.

Based on the above comments, the recommended lubricant is automatic transmission fluid at least for the limited testing phases. This lubricant has a low viscosity to maintain a thin film condition, and good additive package for long life to the drive system as well as the lubricant. Of primary importance is availability of ATF and the compatibility of this fluid with the remainder of the hydraulic system in the transmission package.

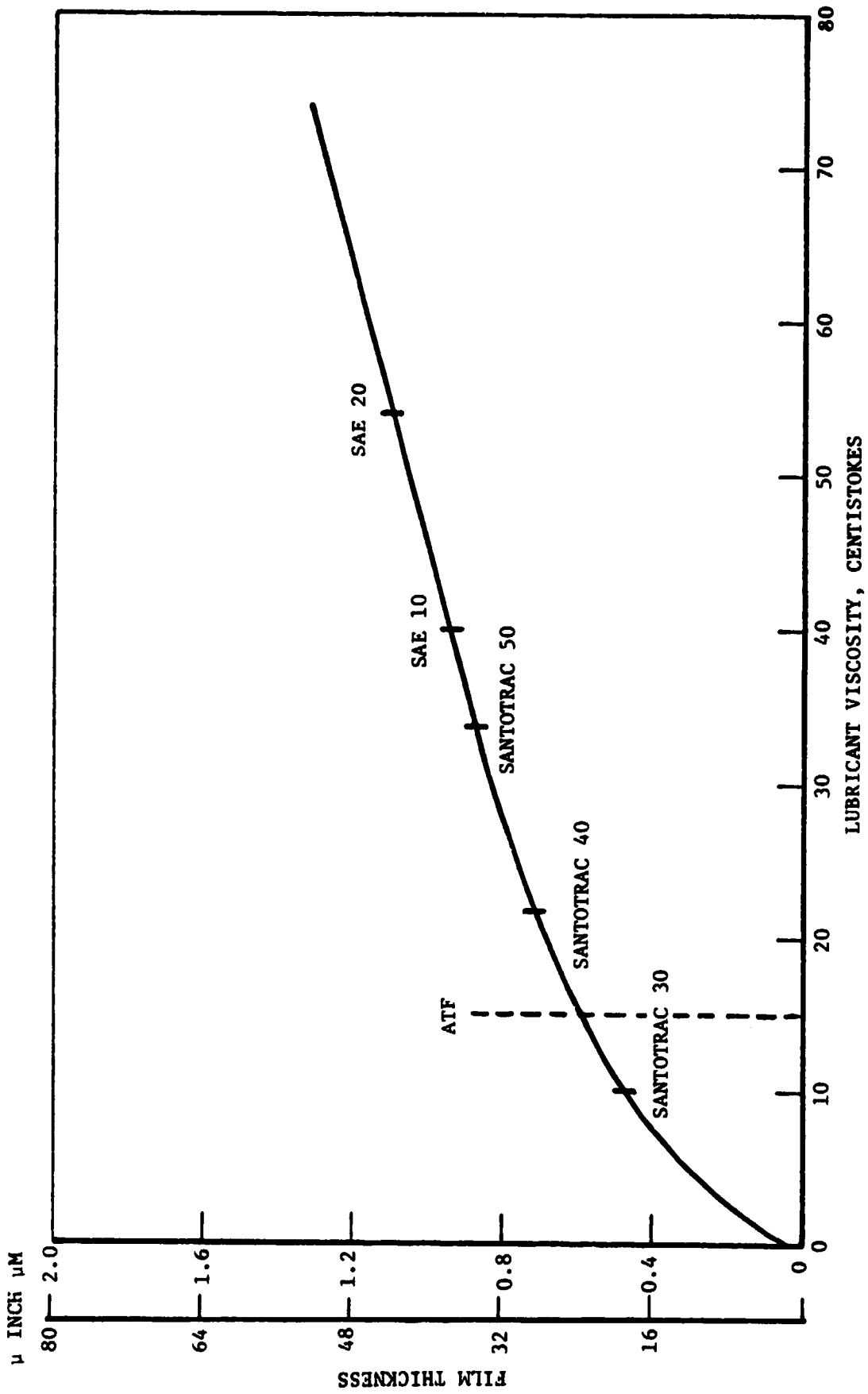


FIGURE 16. EFFECT OF VISCOSITY ON STRUT-STRUT OR STRUT-PULLEY LUBRICANT FILM THICKNESS AT 38 C (100 F)

Discussion of Transmission Design

The transmission is illustrated in Figures 17, 18, and 19. Details of the major components are discussed in the following sections.

Pulley Shifting

The four pulleys in the transmission are all shifted in the same manner. As illustrated in Figure 17, one-half of each pulley is connected to its support shaft by a splined joint so that it is free to slide axially along the shaft. The other half of each pulley is rigidly attached to its shaft by means of a press fit, a key, and a retaining snap ring. This pulley half moves axially along with the support shaft.

Shifting is accomplished by applying varying hydraulic pressures in the pulley actuating cylinders. This pressure acts to force the support shaft and the pulley half attached to it in one direction while forcing the sliding pulley half in the other direction. Since the support shaft is free to move axially with respect to the transmission case, the net effect is that the pulley halves move in opposite directions to each other and that both halves move relative to the transmission case. Small compression springs (three per pulley) are used to provide a modest preload on the pulleys at all times. The force provided by these springs (approximately 34 kg [75 lb.]) is negligible during normal operation.

The pulley halves are constrained to move in such a way that the axial position of belt centerline remains fixed. This constraint is provided by a synchronizing linkage that reacts the pulley motions to the transmission case in such a way that the pulley halves must always move in equal and opposite directions.

It should be noted that in most variable ratio belt drive systems, simpler shifting arrangements are employed. Typically, only one pulley half of each pulley is shifted. However, this typical type of shifting results in a small but significant belt misalignment, which was judged to be excessive for a steel V-belt of the type proposed. It is possible that prototype testing would show that this degree of misalignment is acceptable, and in this case the transmission design could be simplified accordingly.

Synchronizing Linkage

As discussed above, the shifting arrangement employed requires a synchronizing linkage to insure that the pulley centerline remains fixed. The linkage as shown in Figure 17 accomplishes this in a straightforward way. A link with two equal effective length arms is attached to the inner race of the bearing by a pivot joint. Thus, the linkage is effectively "grounded" in the axial direction in such a way that a motion of the sliding pulley half in one direction results in an equal and opposite motion of the support shaft and its fixed pulley half. The belt centerline is therefore fixed.

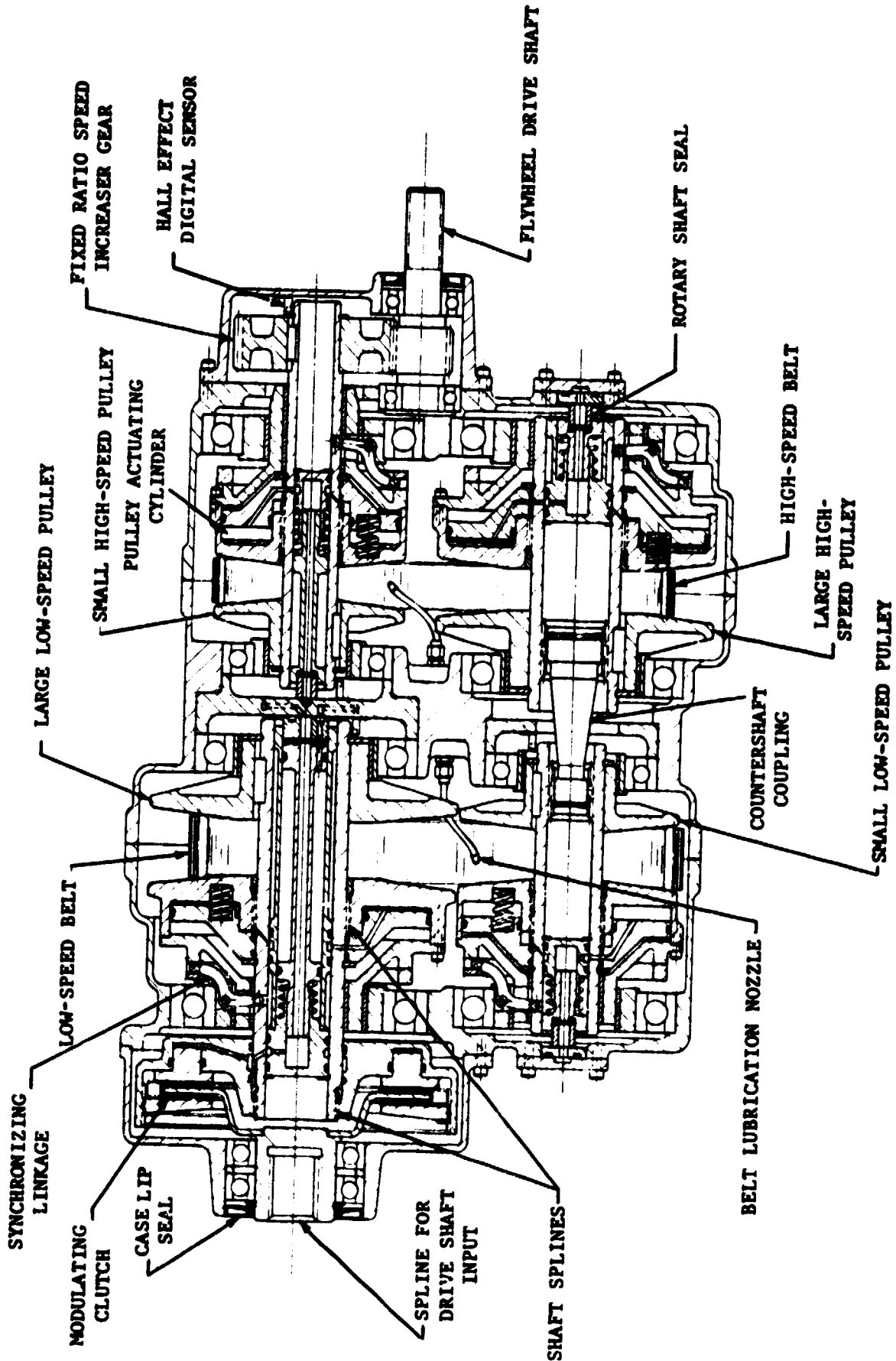


FIGURE 17. CVT LONGITUDINAL CROSS SECTION

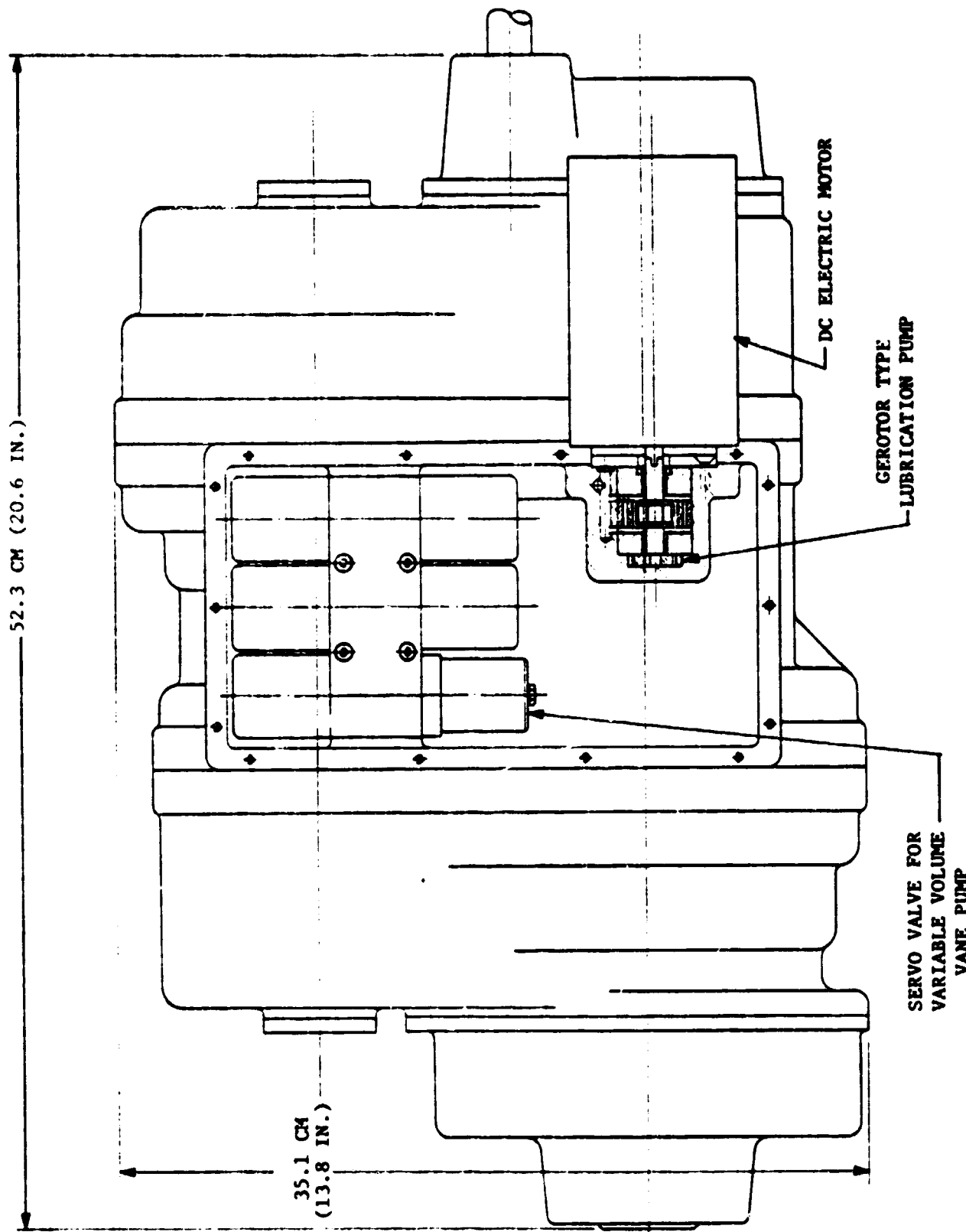


FIGURE 18. CVT PLAN VIEW

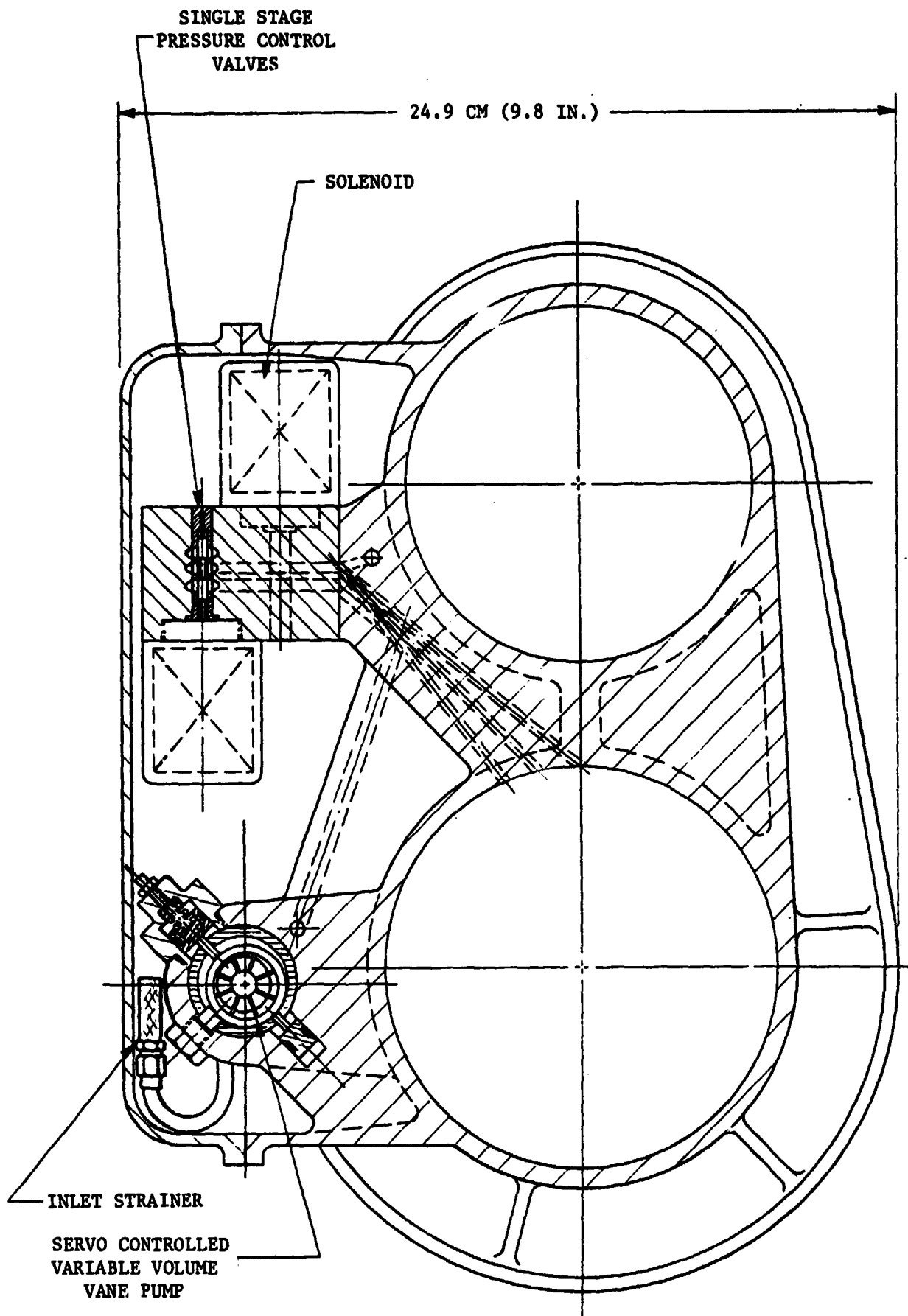


FIGURE 19. CVT TRANSVERSE CROSS SECTION

FIG. 18
PROPERTY

The synchronizing linkage is not required to transmit any large forces. The principal axial loads, the large axial clamping forces, are carried through the snap rings and the support shaft. A kinematic analysis based on free-body diagrams showed that the synchronizing linkage must provide only the force required to overcome sliding friction as one pulley half slides on the shaft and the shaft and its fixed pulley slide in their sleeve bearings. The magnitudes of these friction forces were estimated based on the transverse shaft loading and an assumed friction coefficient of .05. The results indicated that the "worst case" loading on the linkage ends is about 32 kg (70 lb.). Therefore, the linkage illustrated should be more than adequate to do the job.

Pulley Design

The pulleys are critical components in a steel V-belt transmission because of their interfacing with the metallic belt struts, and because of the high axial loading required to prevent belt slippage. Because of these requirements, it is recommended that the pulleys be made from heat-treated forged steel parts. The critical surfaces should be ground surfaces, of 8 to 16 microinch finish, carburized and heat treated to a suitable hardness. This combination should result in wear resistant, accurate parts with good overall ductility and toughness.

The pulley geometry shown in Figure 17 is suggested as the recommended starting point. The sliding pulley half is fabricated from two parts and is splined to the support shaft. The bearing sleeves are positioned to give a support length/diameter ratio of about 1.5. This should result in a smooth sliding motion even with the substantial cocking moments and torques applied to the pulley. Drilled passages feed lubricating oil directly to the spline area to reduce spline wear and friction.

The high axial loading applied requires that the pulleys be of substantial dimensions. Both strength and stiffness are required. Stiffness is very important in a steel V-belt design because the local pulley deflections due to the high loads must be kept small in order for the belt to operate efficiently. Uniform deflection around the entire pulley wrap angle is not a problem, since the pulley halves can shift to accommodate this type of deflection. Localized deflections which vary around the pulley circumference are the real concern, since this type of deflection can result in radial belt motion. This radial motion reduces efficiency and could result in severe belt and strut loads.

Calculation of the pulley stress and deflection levels is a difficult task. The pulley geometry and the support method is sufficiently complex to make precise hand calculations impractical. The calculations are complicated by the fact that the load distribution around the pulley circumference is a function of strut deflection, pulley deflection, and other belt-related factors. The complete analysis of this system would require extensive finite element work on a computer, and was judged to be beyond the scope of this preliminary design. However, a less extensive computer model was conducted, and these results were compared to those from hand calculation results for simplified models.

The computer solution was based on the "MONSA" program. MONSA (Multilayer Orthotropic Nonsymmetric Shell Analysis) is a computer program based on the multisegment numerical integration method for the analysis of boundary value problems. MONSA will determine displacements, forces, and stresses for a composite shell of revolution ("composite" here means a shell made up of parts having distinct shapes, e.g. cylinders, cones, etc.). For nonsymmetric loadings, the user must determine the Fourier harmonics of the loading and perform the appropriate number of calculations. In this analysis the large low-speed pulley was modeled as shown in Figure 20. This pulley was selected for study because it had the highest axial loading magnitude combined with the most severe location of the applied loads.

Figure 21 shows one load distribution used on the MONSA calculations. This loading is based on a total axial force of 1470 kg (3240 lb.), which corresponds to a 16.4 kW (22 hp) maximum reduction ratio condition. The distribution shape is estimated based on the known belt tension ratio and an assumed tension profile over the wrap angle. A 180 degree wrap angle was used in the approximation in order to simplify the calculations.

Pulley axial deflections are shown in Figure 22. A peak deflection of just over .005 cm (.002 in.) is calculated, and the curve shows that the deflection is localized in the sense that it varies substantially around the pulley circumference.

The computer results were checked by comparing the magnitude of the results with results from hand calculations based on plate methods found in Roark⁽²⁾. These calculations assumed average pulley dimensions and uniform loading around the pulley. The calculated deflections were of the same magnitude as those computed by the MONSA program.

The calculated approximate pulley deflections are large enough to be significant. It is for this reason that the pulleys shown in Figure 17 are substantially more rigid than those anticipated earlier in this CVT design program. The latest pulley dimensions are expected to be adequate for the application, since large deflections are indicated only under conditions of transient high torque operation where a modest loss in operating efficiency is acceptable. It is not deemed necessary to have pulley face stiffness as high as those of earlier Battelle laboratory evaluations.

Hydraulics and Seals

The hydraulic system is illustrated schematically in Figure 23. Two pumps, driven by a single electric motor, supply the hydraulic fluid to the transmission. A fixed displacement Gerotor® type pump supplies low pressure (about $1.4 \times 10^5 \text{ N/m}^2$ [20 psi]) lubrication and cooling flow to the bearings, gearing, belts, and clutch.

A variable volume vane pump is used to supply the high pressure portion of the system. This pump is servo-controlled to provide only the flow needed to maintain a system supply pressure at a level commanded by the TCS. Typically this pressure would be about $1.38 \times 10^6 \text{ N/m}^2$ (200 psi) above the highest working pressure in the transmission.

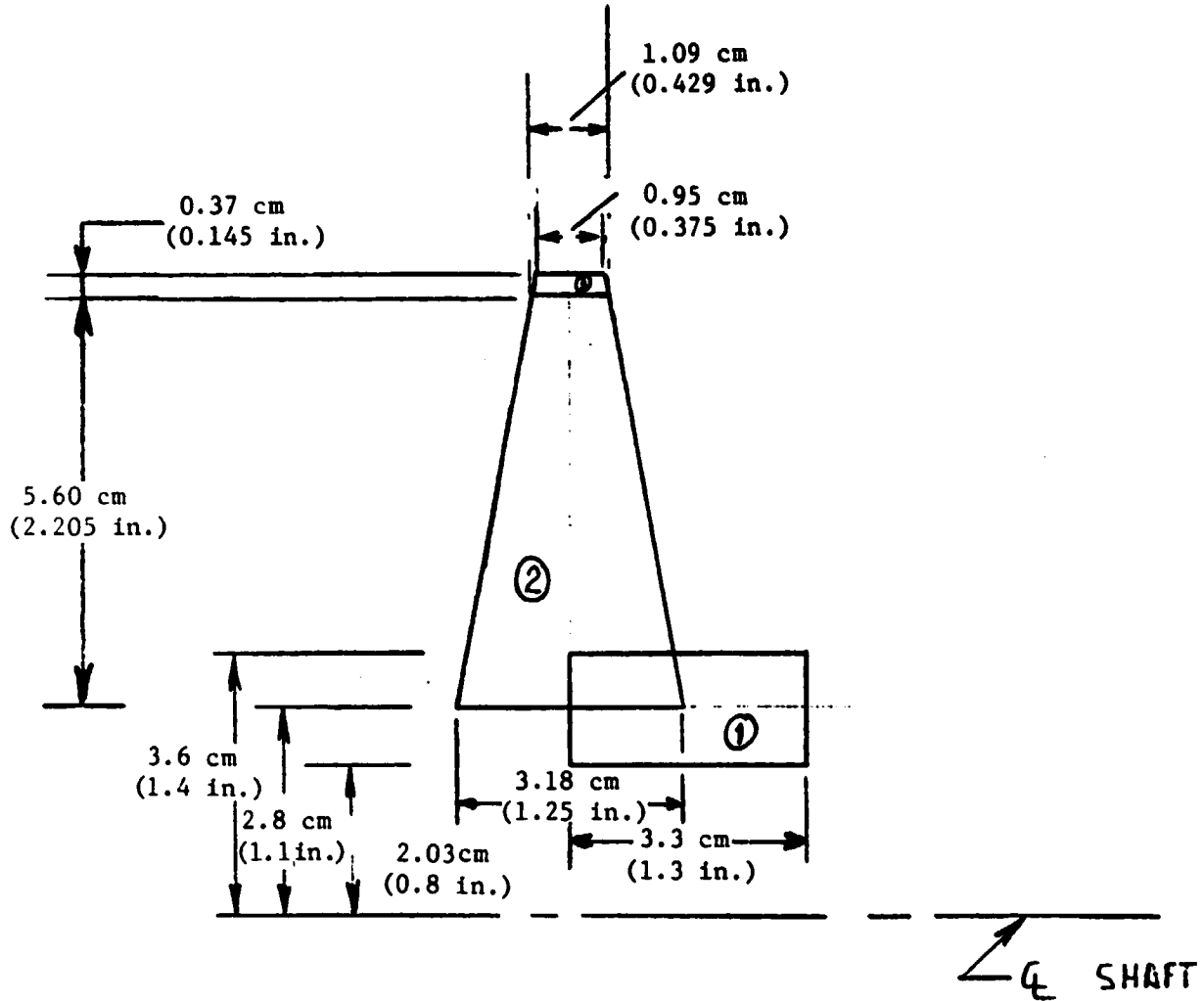


FIGURE 20. MONSA MODEL OF LOW-SPEED PULLEY HALF

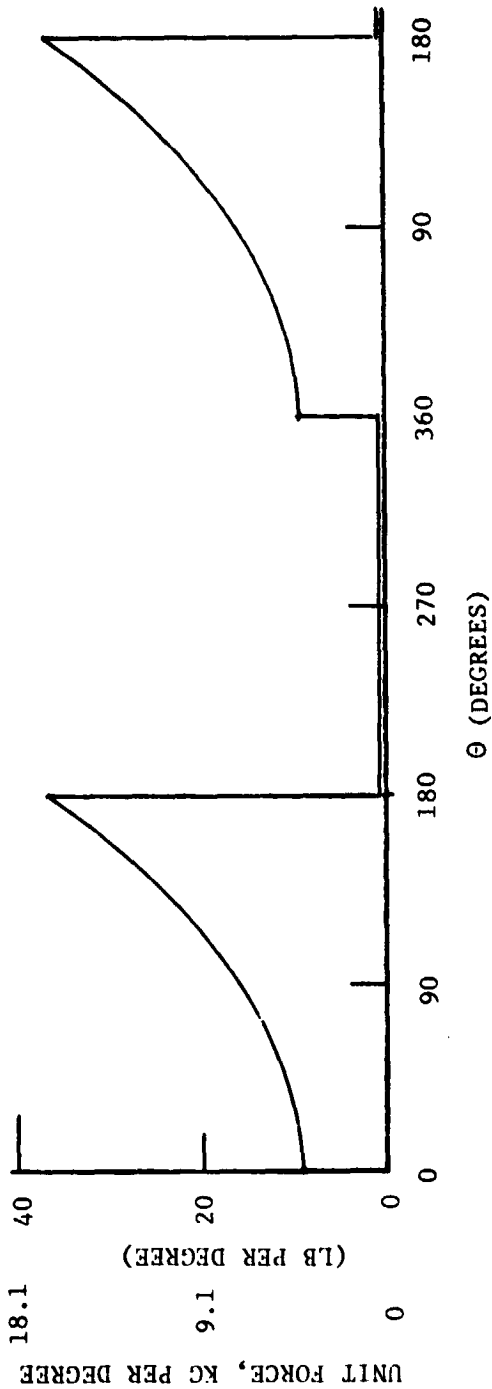
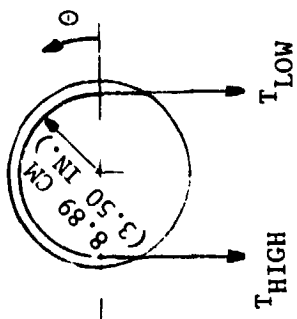


FIGURE 21. APPROXIMATE FORCE DISTRIBUTION ON THE LARGE LOW-SPEED PULLEY AT NORMAL OPERATING CONDITION OF 16.4 KW (22 HP)

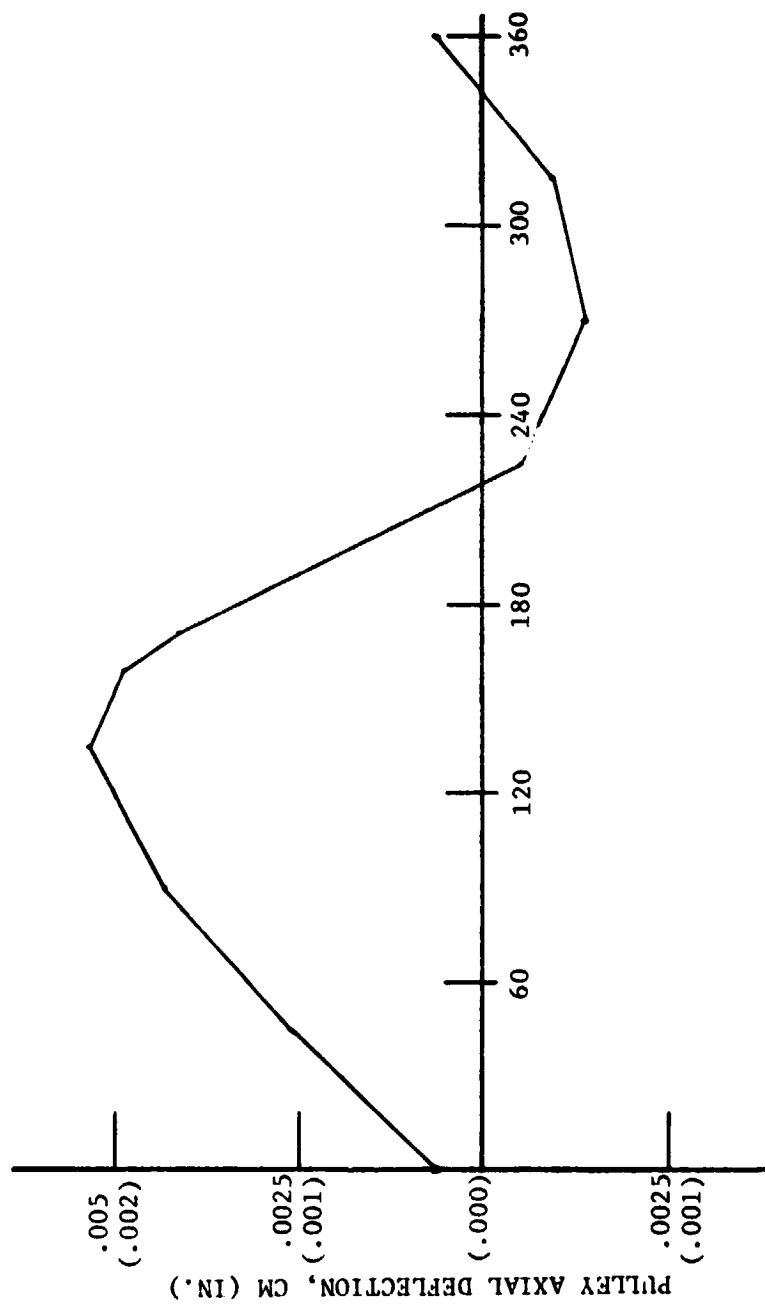


FIGURE 22. PULLEY DISPLACEMENT VERSUS θ AT 16.4 KW (22 HP) OPERATION
(MONSA Results)

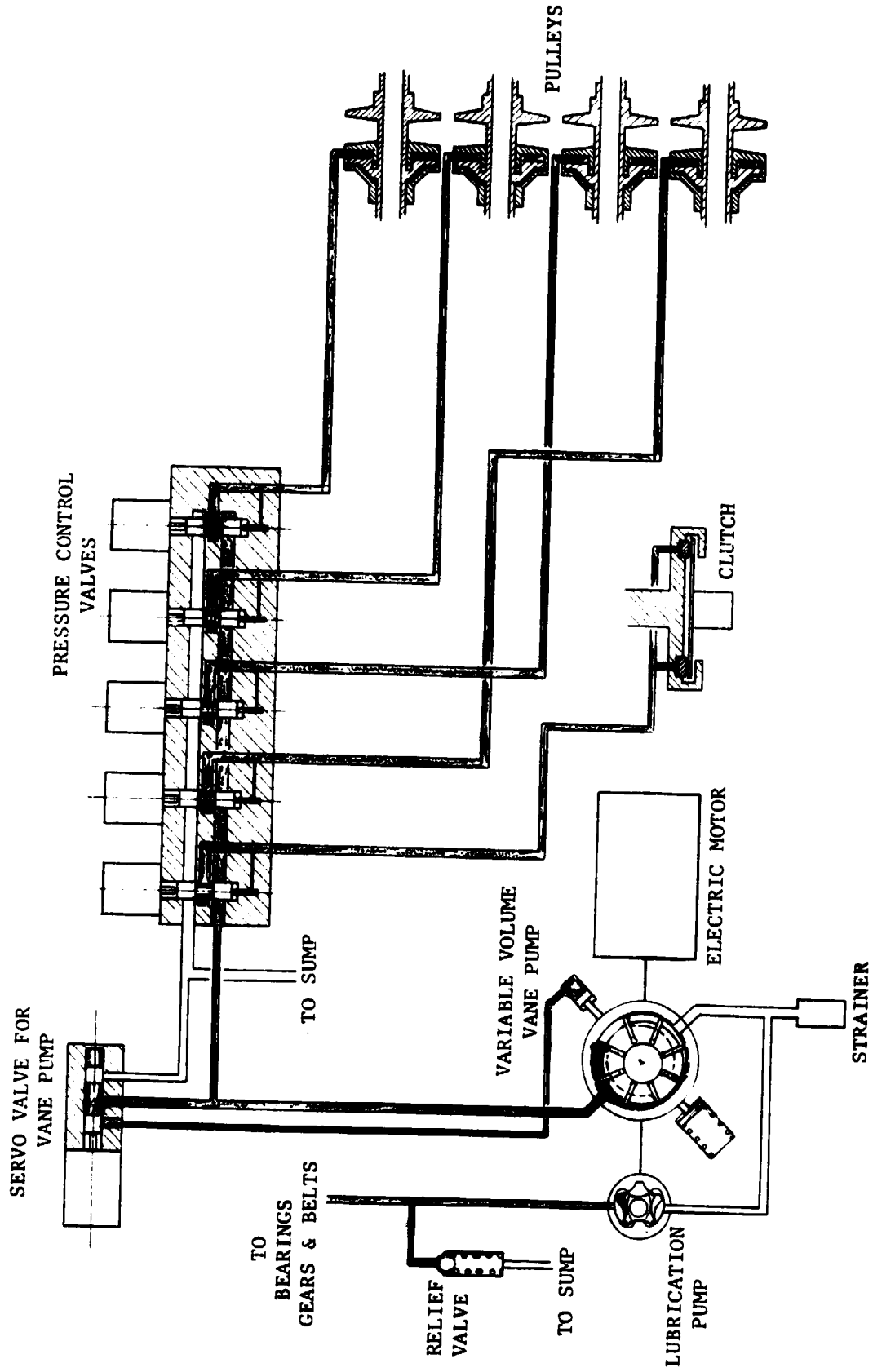


FIGURE 23. HYDRAULIC CONTROL SYSTEM SCHEMATIC

The high pressure supply is fed to the pressure control valve manifold where five identical pressure control valves regulate the separate working control pressures to each of the four pulleys and to the clutch. These control valves are of the single-stage solenoid actuated type, and receive their electrical input commands from the TCS. Each valve outputs a pressure proportional to its input current. Details of these components are discussed in a later section.

The control pressures are routed to the transmission components by both internal and external passages. The pressures for the large low-speed and small high-speed pulleys as well as for the modulating clutch are communicated internally through a manifold plate located between the shaft ends. The two pulleys on the countershaft are supplied via external case passages. In all cases, the pressures are brought into the shafts through dynamic seals at the shaft ends. This approach to the dynamic seals was taken to minimize the sealing problems and to improve seal efficiency by minimizing both the sealing path length and the relative sliding velocities.

The seals consist of carbon graphite inserts running against hardened steel wear plates. The carbon graphite inserts are supported by elastomeric elements that serve as static seals as well as provide for slight self-aligning motions so that the insert runs flush against the steel wear plate.

Since the shaft segments must be free to shift axially relative to the transmission housing, the seal construction includes sliding elements to accommodate this shifting. Clearance fits are used between those parts which have relative motion to minimize friction forces. A light spring is used to provide a modest preload of the graphite insert against the wear plate. The sealing geometry is configured to give an approximate hydraulic force balance on the seal elements, thus reducing friction losses.

Shafts and Bearings

The shafting arrangement used in the recommended configuration consists of a separate shaft for each of the four pulleys. These shafts are each supported by a pair of deep groove ball bearings. Two of the shafts are mechanically coupled by means of a spline coupling to form the countershaft system.

As discussed earlier, the pulley shifting arrangement is such that each of the four shafts must move axially to accomplish the shifting function. This necessitates the use of bronze sleeve type inserts to accommodate axial motion between the shafts and the bearing inner races. The bronze and steel composite inserts are pressed into the inner races of the rolling element bearings. On the fixed pulley ends of the shafts the inserts are keyed to the pulley hubs by a pin sliding in a slot. On the other end of the shafts, the synchronizing linkage components prevent rotation where it is not desired.

The splined countershaft coupling is used to couple the two sections of the countershaft, while permitting relative axial shaft motion. The splined ends are crowned so that both angular and parallel misalignment

between the sections can be accommodated. This feature compensates for any misalignment due to installation tolerances or due to transverse pulley loading on the shafts.

The shaft for the large low-speed pulley is splined on one end to accept torque input from the modulating clutch while permitting relative axial motion between the two. The small high-speed pulley shaft is extended and machined to accommodate the gear from the fixed ratio speed increaser. The gear is coupled to the shaft by a key and a snap ring.

All four of the shafts are of steel tubular construction, and the inner bore contains hydraulic fluid transfer elements and seals as discussed in an earlier section. The shaft material should be a high quality, heat treatable steel suitable for the drive splines and seal and bearing surfaces.

The shafts must be strong enough to transmit the required axial pulley forces as well as to withstand the transverse bending loads applied by belt tension forces.

The worst case axial tension force is approximately 8618 kg (19,000 lb.) in the large low-speed pulley shaft. For a nominal shaft cross-sectional area of 10.7 cm^2 (1.66 in^2) this corresponds to a nominal tensile stress of about $7.93 \times 10^7 \text{ N/m}^2$ (11,500 psi). Thus, even with the stress concentration factors arising from the snap ring grooves, etc., the shaft is adequately strong in tension. Similarly, for the small low-speed pulley shaft the maximum axial load is about 6123 kg (13,500 lb.), resulting in a nominal stress of about $9.48 \times 10^7 \text{ N/m}^2$ (13,750 psi), which should also be acceptable.

The most severe shaft bending loading occurs at the small low-speed pulley shaft. Here a maximum transverse load of about 1270 kg (2800 lb.) is applied at the belt centerline. For the shaft dimensions and bearing arrangement shown in Figure 17, this results in a maximum nominal shaft bending stress of about $8.96 \times 10^7 \text{ N/m}^2$ (13,000 psi). This should represent an acceptable level of loading even allowing for stress concentrations and the fully reversed bending nature of the loading. The other shaft segments are less highly stressed than this one, and therefore should be acceptable.

The shaft bearings selected for the preliminary design are conventional single row ball bearings, Numbers FAG 6012, 6016, 6019, and 6204. They were selected based on catalog ratings and dimensions. They have sufficient load capacity for brief periods of full torque operation and they have B_{10} life ratings of greater than 2600 hours at the design condition of 16.4 kW (22 hp).

Rolling element bearings were selected over journal bearing types because of their higher efficiency at the relatively high speeds involved. It should be noted, however, that the high-speed bearings, particularly those on the flywheel drive shaft, are running at speeds sufficient to warrant the use of good lubrication techniques. Light spray or mist type lubrication is recommended to maintain high efficiency and prevent overheating.

Speed Reducer

A fixed 2.8:1 ratio speed reducer is used to couple the flywheel speed range of 14,000 to 28,000 rpm to the CVT. The spur gearing was sized by a design method from Dudley⁽³⁾. The equation is of the form (U.S. units)

$$P_{at} = \frac{n_p d k_v}{126,000 k_o} \left(\frac{F}{K_m} \right) \left(\frac{J}{K_s P_d} \right) \left(\frac{S_{at} K_L}{K_R K_T} \right) \quad (5)$$

where

P_{at} is the allowable horsepower

P_d is the diametral pitch

n_p is the pinion rpm

d is the pinion pitch diameter

F is the face width

S_{at} is the allowable material stress

k_v , k_o , K_m , K_s , K_L , K_R , K_T and J are constants determined from figures and tables in Dudley according to the application and the geometry.

For our application, one gearing combination that meets the requirements is as follows.

Pinion pitch diameter = 1.216 in.
 Pinion face width = 1.216 in.
 Number of pinion teeth = 20
 Gear pitch diameter = 3.405 in.
 Center distance = 2.3104 in.

This combination was illustrated in the layout of Figure 17. Straight spur gears are shown because of their simplicity. Since the high-speed transmission shaft must be free to shift axially, the gear is wider than the pinion by an amount sufficient to maintain gear contact over the full width of the pinion regardless of the high-speed shaft position. This should prevent the formation of damaging wear patterns in the more highly loaded pinion.

The principal drawback to the use of straight spur gears is their potential for noise generation. Helical or double helical gears are often quieter than spur gears. Either of these gear types could be substituted for the spur gears in later designs should it prove necessary. With single helical gearing, the shaft bearings would have to be redesigned to accommodate the axial thrust generated by such gearing. Double helical (herringbone) gearing would eliminate the axial thrust, but would require an additional spline or other element to accommodate the axial shaft motion.

Modulating Clutch

The modulating clutch as shown at the input to the low-speed transmission shaft must be capable of handling the torque and energy required to

couple the drive motor with the transmission during start-up, shutdown, and at other operating conditions when the drive motor is below 850 rpm and the flywheel speed is above that at which the transmission ratios permit direct operation. The clutch must provide the additional function of a torque limiter to limit transient or unplanned torque inputs and prevent damaging belt slippage.

The clutch is of the single disc, twin plate, wet type, and is hydraulically actuated. The actuation pressure is modulated by one of the pressure control valves in the hydraulic portion of the control system. During start-up operations, the torque is modulated according to commands from the vehicle control system. Torques up to 450 N-m (330 lb-ft) are available. In the normal operating mode, with the clutch fully engaged, the clutch actuation pressure is controlled by the transmission control system so that clutch slippage would occur at torque levels slightly above the programmed torque value.

The clutch was designed for operation at hydraulic pressures similar to the pressures used in the large low-speed pulley, i.e., at pressures up to about $8.274 \times 10^6 \text{ N/m}^2$ (1200 psi) maximum. The clutch plates would then be operating at a maximum contact pressure of about $3.24 \times 10^6 \text{ N/m}^2$ (470 psi). Clutch performance was based on a friction coefficient of 0.10, which represents a typical value for applications of this type. A light wave spring is installed between the plates near the plate outside diameter for the purpose of separating the plates while the clutch is disengaged to reduce clutch drag.

The energy dissipation capacity of the clutch should be adequate. The capacity was investigated by estimating the energy that has to be dissipated and the rate of energy dissipation. It requires about 0.00575 kWh to bring a 1700 kg (3750 lb) vehicle from rest to a speed of about 18 kmh (11 mph), which corresponds to an 850 rpm drive motor speed. If the flywheel is to provide this starting energy, the clutch must slip during this period. Since a slipping clutch would dissipate an amount of energy equal to that which it transmits, this means that the clutch would have to dissipate 0.0207 MJ (0.00575 kWh) per vehicle start, and the flywheel would have to provide twice this amount, or 0.0414 MJ (0.0115 kWh).

Another mode in which the clutch might have to dissipate energy is to bring the flywheel from rest to the minimum (14,000 rpm) operating condition while the drive motor is running at high speed. In this case, the energy required at the flywheel is about 0.601 MJ (0.167 kWh). (This assumes a maximum flywheel energy of 2.401 MJ, or 0.667 kWh is available at 28,000 rpm, and a minimum energy of 0.601 MJ, or 0.167 kWh at 14,000 rpm.) The clutch would also have to be able to dissipate 0.601 MJ (0.167 kWh) of energy during this flywheel startup mode, and this dissipation requirement would be much more severe than the vehicle start-up mode. For this reason, it seems advisable to design the control system logic so that this flywheel start-up mode is not encountered. If, for example, flywheel start-up was only permitted at motor speeds up to 2500 rpm, the clutch could be fully engaged when the flywheel is at 7000 rpm rather than 14,000 rpm, and only one-fourth the energy would have to be dissipated.

Assuming then that the maximum short-term energy dissipation requirement for the clutch is about 0.14 MJ (0.04 kWh), and that this occurs over a 1-minute interval, the temperature rise that would occur in the clutch was estimated. An oil cooling flow of about .8 liters per minute (0.2 gpm) was assumed. If all the energy went into the oil, this would result in an oil temperature rise of about

$$\Delta T \approx \frac{Q}{mC_p} = \frac{(.04 \text{ kWh}) \left(\frac{3414 \text{ Btu}}{\text{kWh}} \right)}{(1.74 \text{ lbm}) \left(.48 \frac{\text{Btu}}{\text{lbm F}} \right)} \quad (6)$$

$$\Delta T \approx 164 \text{ F or } 73 \text{ C}$$

Obviously, not all the energy goes into the cooling oil, and the clutch parts also increase in temperature. It would appear, however, that the clutch should be adequate to dissipate the energy without difficulty, since the vehicle start-up mode, which occurs more frequently than flywheel start-up, requires even less energy dissipation in the clutch.

Torque and Speed Sensors

The torque and speed sensing devices in the transmission are all similar units. The sensors are "Hall Effect" digital sensors located adjacent to the transmission shaft ends. These are magnetically-activated electronic switches utilizing the Hall Effect for sensing a magnetic field. The sensors are mounted in close proximity to the rotating shaft ends. Small permanent magnets are mounted in the shaft ends to provide the magnetic field.

The sensors switch on and off according to the strength of the magnetic field and hence provide a digital signal which can be used directly to calculate shaft speed. On the high-speed output shaft, two sensors are used, one on either end of the shaft. By sensing the change in phase between the digital signals from the two transducers, the torque in the shaft can be determined. Shaft windup due to torque will generate phase shift in the two signals that should be proportional to torque.

The power supply and signal conditioning for the Hall Effect sensors is provided by the TCS. The sensors themselves are quite small and have no moving parts and no wear.

Hydraulic System Components

The hydraulic system, as illustrated in the schematic of Figure 23, incorporates a number of components that are not presently available "off-the-shelf". Although in each case components of the same generic type and function are commercially available, it was thought that for this high production application new models should be developed to reduce size, weight, and/or cost.

Pressure Control Valves

Perhaps the most difficult and critical components in the transmission hydraulic system are the electrohydraulic pressure control valves. A total of six of these valves is required and therefore size and cost are important considerations. The valves should be capable of peak flow rates of 4 to 8 liters per minute (1 to 2 gpm) and operating pressures of up to $9.653 \times 10^6 \text{ N/m}^2$ (1400 psi). Leakage and quiescent flow should be less than about 0.8 liters per minute (0.2 gpm) for each valve.

A substantial search to locate suitable valves was undertaken. Many small electrohydraulic servo valves are available and a number of these were small enough to do the job. The problem with these standard servo valves is their cost and to a lesser extent their size. These are high-precision devices made in relatively small quantities. In general they are two-stage devices with a spool-type main stage and smaller pilot stage of another type, such as a nozzle flapper.

Another pressure control valve type that is generally available uses an electrically controlled single-stage poppet, or variable orifice type approach. These valves are simpler and less expensive but they have the drawback that the quiescent flow through the valve is essentially as great as the full rated flow. This would result in an excessive efficiency loss and therefore this valve type was ruled out.

A number of pressure control concepts were considered as alternatives to the commercially available valves. The concept illustrated in Figures 19 and 23 was eventually selected as the leading candidate. This concept consists of a single-stage, spool type, three-port valve with electrical solenoid actuation. The control pressure port is connected alternatively to either the high pressure supply port or to the drain port. The spool position is determined by a force balance between the solenoid actuating force and the counterbalancing pressure force applied to the opposite end of the spool. Thus, if the valve is at an equilibrium condition and the control system commands a new higher pressure, this pressure is achieved in the following manner. The control system increases the electrical current to the solenoid which therefore generates a higher actuating force on the spool. The spool shifts in the direction that permits flow from the supply port to the control port thus increasing the control pressure. The control pressure is applied to a counterbalance pin on the other end of the spool and when the pressure has increased sufficiently, a new equilibrium condition is established. Hence, control pressure is proportional to the current applied to the solenoid. The system works to reduce control pressure when the solenoid current is reduced by directing flow from the control port to the drain port.

The pressure control valve concept described above was selected because it lends itself to a relatively compact and inexpensive design. The parts could be mass produced and all the valves would be identical. The spools could be either powdered metal or die cast parts with a minimum of final machining. The "critical center" porting geometry can be controlled by pressing a sleeve with slot type ports into the manifold body. The counterbalance pin and the solenoid actuating pin can be separate parts, thus eliminating the need for critical bore concentricities.

The valve spools can be quite small due to the low flow rates required. A .32 cm (.125-in.) spool diameter is suggested as a good starting point. One advantage of the small flow rates and component size is that the valve flow forces are small. These flow forces are a principal reason for the use of more complicated two-stage valves in many applications. An estimate of the worst case flow force was obtained using a general method found in the literature⁽⁴⁾.

$$F = 2 C_d C_v A_o (P_1 - P_2) \cos \theta \quad (7)$$

where F is the steady-state flow force in the direction to close the orifice, C_d and C_v are orifice flow constants, A_o is the orifice area, and θ is the jet angle which the spouting fluid makes. For normal spool valve geometry, this equation reduces to

$$F = .43 A_o \sqrt{\Delta P} \quad (8)$$

For a 4 liters per minute (1 gpm) flow rate and an 8.274×10^6 N/m² (1200 psi) pressure drop (worst case) this gives a flow force of about .26 kg (.57 lb). Although significant, this force should be acceptable if a sufficiently powerful solenoid is used.

DC solenoids or force motors of sufficient strength and acceptable size are commercially available. However, it is expected that a custom unit would be designed for this special, high-volume application to minimize size and cost.

Control Pump

A variable displacement, pressure compensated vane pump was chosen to supply the system control hydraulic pressures. This pump, in addition to being pressure compensated, utilized a variable pressure compensation setting. This was accomplished by a simple electrohydraulic control valve working in conjunction with the pump's pressure compensation design. This system allowed both the flow and pressure to be reduced to match the demands of the CVT under any operating condition. This approach reduced the parasitic hydraulic loss to a bare minimum. It also extended the life of the pump and reduced the heating of the system hydraulic fluid.

A vane pump was chosen in preference to a variable piston pump for the following reasons

- Lower manufacturing cost
- Better filling characteristics at high operating speeds
- Better efficiency at high speeds and modest flows and pressures
- Higher operating speeds allow a lighter weight and lower cost electric drive motor

- Higher operating speeds also allows the inertia of the pump and drive motor to be more effectively used for short-term shifting transients
- Small size and ease of packaging in the CVT design
- Proven BCL experience in the design and fabrication of high speed, variable volume vane pumps.

A pump displacement of $.757 \text{ cm}^3/\text{rev}$ ($.046 \text{ in.}^3/\text{rev}$) gives a maximum flow rate of 8 liters per minute (2 gpm) under full displacement conditions at the design speed of 10,000 rpm. A potential configuration, as shown in Figures 18 and 19, has the following basic dimensions:

Cam diameter	=	1.887 cm (.743 in.)
Cam length	=	1.130 cm (.445 in.)
Vane stroke	=	.113 cm (.0445 in.)
Rotor diameter	=	1.711 cm (.674 in.)
Number of vanes	=	10.

The cam ring is lightly spring loaded toward full displacement, to aid in developing startup flow and pressure. During normal operation, a control piston positions the cam ring for the displacement required to maintain the desired pressure. This pressure is varied according to system demand by the output pressure of a servo valve which receives its electrical inputs from the transmission control system.

Lubrication Pump

The lubrication pump is required to provide a continuous source of low-pressure lubricating and cooling flow, independent of the flow from the high-pressure pump. This minimizes power losses by not requiring the use of high-pressure oil for lubrication and cooling.

The exact lubrication and cooling flow requirements will have to be determined experimentally during hardware development. For preliminary purposes it has been estimated that a total of 4 liters per minute (1 gpm) should be more than adequate.

The pump selected is a standard Gerotor® cartridge. Inexpensive pumping cartridges of this type are available for OEM use. One example is a Nichols Model 6020 which is rated at about 4 liters per minute (1 gpm) delivery at 10,000 rpm operation. This unit is driven from the same shaft as the high-pressure pump and operates from a common sump. The Gerotor® output pressure is limited by a poppet type relief valve to prevent excessive pressure buildup and reduce power losses.

Pump Drive Motor

The pump drive motor should be capable of driving both pumps at their design speed of approximately 10,000 rpm. This relatively high

speed was chosen to reduce the size and weight of the pump and motor components.

During normal transmission operation the hydraulic pump input power requirements are well within the electric motor rating. However, during brief periods in which the pulleys must be shifted rapidly while at high pressures (corresponding to full power operation at high transmission ratios), the hydraulic power requirements could be as great as about 1.1kW (1.5 hp). This would occur only during momentary situations in which the high-pressure pump is at nearly full stroke and maximum pressure.

The motor shown schematically in Figure 18 is about the size of typical DC electric motors rated at 10,000 rpm and about .7kW (1.0 hp) intermittent duty. This size is expected to be adequate for the application. The brief (1 to 2 second) occasional requirements for higher power levels can be provided by the rotational inertia of the high-speed motor and if necessary, by the addition of a modest mass to provide additional inertia. During normal operation only a small fraction of the motor's rated power will be required, and therefore motor overheating should not be a problem.

The DC motor would probably be of the shunt-wound type, to minimize the variation of speed as the load changes. While precise speed control is not required for this application, some speed control components may be required, depending on the electric motor selected. An AC motor could also be used, but this would probably only be practical if an AC power source was already available in the vehicle for other purposes.

Hydraulic System Packaging

Figure 19 illustrates the packaging arrangement for the hydraulic system. A hydraulic reservoir is located beneath the transmission and is connected with the transmission housing by several flow passages which permit the lubrication, cooling, and leakage flows to drain back into the reservoir. This is essential because excess oil buildup in the main transmission housing would contribute to windage losses and heat generation.

The oil reservoir should be of sufficient volume to contain about 1 liter (1 quart) of fluid during normal operation. The entire system would then contain greater than 1 liter (1 quart) of oil, since the pulley actuating cylinders will contain significant oil quantities, as will the hydraulic lines, valves, and fittings. Due to the overall efficiency for the steel V-belt transmission system, special provisions for transmission or transmission oil cooling should not be required.

The major hydraulic system components are located in or on the reservoir. The only filter that is shown in the system is an inlet strainer located at the inlet to the hydraulic pumps. It is anticipated that this will provide adequate protection for the system. Should it later prove desirable, an inline filter could be installed in the high-pressure pump discharge line. This would provide additional protection to the pressure control valves and would prevent the buildup of extremely small particles (fines) in the system.

Transmission Control System

The drive ratio of the transmission is varied in a continuous manner by two sets of variable pulleys. Varying the drive ratio matches the vehicle speed to the flywheel speed and transmits the required amount of power between the vehicle and the flywheel. A Transmission Control System (TCS) has been functionally defined to monitor the transmission's operation and provide the necessary control function to optimize efficiency and life while providing safeguards against transmission damage.

The control system is modular in structure to allow small changes to individual modules without changing the entire system. This aspect will allow quick adaptation to new transmission applications and various control environments. The modular feature will permit rapid debugging and inexpensive component replacement. The modular design will also facilitate component selection. Since one of the aims of the system is to investigate economic feasibility, components may be chosen with cost and specifications in mind.

Modes of Operation

The TCS will run in any one of the following conditions during its operation:

- (1) Startup
- (2) Shutdown
- (3) Continuous ; or Normal
- (4) Failure Conditions

The startup sequence will be initiated by either a command from the Vehicle Control System (VCS) or from the initial introduction of power to the TCS. Because the current TCS does not include any position or proximity sensors for finding pulley radii, the TCS will assume that the transmission was shifted to its lowest drive ratio during shutdown. The TCS will issue the proper analog control signal to the servo-controlled hydraulic pump and the lubrication pump to pressurize the hydraulic control lines. The minimum hydraulic fluid pressure threshold will be sensed by a pressure switch. Until the pressure switch has indicated that the hydraulic system has been pressurized, the modulating clutch will remain disengaged. After all systems have been initialized, sequence status information will be transmitted to the VCS to signal that the transmission is ready for operation. After the successful completion of this sequence, the process schedule will be diverted to the normal or continuous mode of operation.

The normal mode sequence is the mode that the TCS will be executing during normal vehicle operation. Commands and data from the VCS will be accepted, stored, and interpreted. The information received from the VCS will be:

- (1) The amount of torque transfer desired to or from the flywheel,
- (2) The flywheel setpoint speed (an indication of the desired nominal flywheel energy level), and,

(3) The speed of the electric drive motor.

Critical data values will be sent to the VCS that reflect the condition of the transmission and flywheel. This information will include the flywheel speed and status information such as condition normal, disengaged, or failure.

If the flywheel has been engaged by the vehicle operator, the VCS will transmit a desired torque set point value to the TCS. This torque set point value is a function of the amount of braking or acceleration that the operator desires as well as the flywheel set point speed. The flywheel set point speed is an operator-selected value that reflects how much energy should be diverted to the flywheel under normal cruising conditions.

Given the torque set point, each of the shaft speeds, and the flywheel speed, the TCS will make control decisions as to what course of action to be pursued. The TCS will attempt to deliver the desired torque; however, if an alarm condition should prevail, such as over-torque, or flywheel not up to speed, the torque set point is flagged as an error and the TCS will await a new set point or command. The transmission will be stabilized by the TCS to a safe condition given this sequence of events.

The shutdown mode is initialized by the operator when he turns the car ignition to the off position. The VCS senses this condition and communicates the shutdown mode command to the TCS. The TCS follows the shutdown sequence which disengages the modulating clutch, alters the transmission drive ratio to its lowest condition, and turns off the hydraulic pumps. The TCS status message then informs the VCS whether the shutdown sequence was successful or not.

The failure mode is initiated by some emergency condition that exists either in or outside of the transmission. Faults that could cause the execution of the failure mode include loss of hydraulic pressure, excessive belt slippage, or some external event that the VCS has sensed. In this mode the transmission is brought to a stable condition as quickly as possible in order to protect the automobile's hardware and the passenger's safety. During the failure mode the failure mode status information is sent to the VCS, the modulating clutch is disengaged, and the drive ratio is decreased to its minimum value.

Functional Hardware Blocks

The heart of the transmission control lies within the processor system. The processor and its associated control program will contain the proper logic to monitor each of the transmission shaft speeds, sense the amount of torque that is transferred through the system, compute each of the pulley radii, compute the required hydraulic pulley loading pressures, and to engage or disengage the modulating clutch according to the conditions that prevail.

Associated with the processor will be a programmable read-only memory that will contain the process schedule of the system, system control

constraints such as transmission maximum ratings, and the logic necessary to communicate with the control devices as well as with the vehicle control system. If a new transmission is implemented that has different operating characteristics or a different process schedule is desired, the control program need only be altered to suit the new specifications. This module design could save much time and effort over changing a hardware-only design.

A random access, read/write memory will also be included with the controlling unit for the purpose of variable data storage. As data are sensed and collected from the transmission, they will be stored in the data table for later reference or transmission to the Vehicle Control System.

A communications link will be established between the transmission control and the vehicle control systems. The link is needed in order to establish a two-way communication between the two control systems. The VCS will issue commands and transmit data to the TCS. The vocabulary of commands will consist of startup, shutdown, normal/cruise, and failure condition modes. The transmission system acts as a slave controller to the vehicle control processor as it only transmits status indication codes and necessary data values to the vehicle processor.

Transmission data values will be sensed by transducers that send analog signals to the transmission control processor. The analog signals will be converted to digital values that can be manipulated arithmetically by the controlling unit. These sensed values reflect the state of the transmission and will be used in calculations to further control the drive mechanism.

The transducers selected to measure shaft rotation speeds and transmitted torque are Hall Effect sensors, combined with magnets imbedded in the shaft itself. The Hall sensor measures magnetic flux density--unlike a magnetic coil pickup that senses the change in magnetic flux over time. If the Hall sensor is placed in a magnetic field whose flux density is greater than the threshold, the sensor turns on. If the sensor is positioned close to the shaft surface such that the magnet passes beneath it once per shaft revolution, the result is a digital pulse. The speed of the shaft can be measured in any one of three ways given this train of digital pulses.

The amount of time between rising and falling edges of the pulse can be measured. Given the arc length of the shaft that passed beneath the sensor during the pulse, the angular velocity may be calculated by:

$$w = d\theta/dt \approx \Delta\theta/\Delta t \quad (9)$$

where θ is the arc length, t is the time between the rising and falling pulse edges, and w is the angular velocity.

The second method is much like the first with the exception that the arc length is equal to one full revolution or 2π radians. The time between rising edges of the pulse may be measured and the angular velocity is calculated by:

$$\omega = 2\pi/\Delta t \quad (10)$$

The third method is useful for finding average speeds over longer amounts of time. Over a specified time interval, the digital pulses that are sensed are counted. The angular velocity of the shaft is then calculated by:

$$\omega = N (2\pi/\Delta t) \quad (11)$$

where N is the number of recorded pulses inside the time interval Δt .

The torque measurement uses the same type of sensing method; however, the digital signals are treated differently. Since the torsion modulus is well known for the shaft material, the amount of shaft twist is a very accurate measure of the transmitted torques. In order to measure the shaft twist, two Hall sensors along with their magnetic excitors are placed on either end of the high-speed shaft. As the shaft begins to twist while a torque is presented to the system, the signals from the two Hall sensors show a phase shift which reflects the angular deflection of the shaft. This phase difference, or time difference between the leading edges of the digital pulses, can be measured with conventional synchro-to-digital convertors. According to recent calculations, the angular twist of the high-speed shaft at maximum load will be about 0.07 radians. Synchro-to-digital measurement packages do exist that can measure the angular twist of the shaft to 0.001 radians with an accuracy to ± 0.001 radians.

The hydraulic fluid pressure is monitored by a pressure switch. If the fluid pressure falls below a certain threshold value, due to pump failure or hydraulic line rupture, the control system will sense this change and will be able to initiate the failure mode of operation.

Six analog control signals are used to control the various dynamic components of the transmission. One signal is used to control the motor hydraulic servo pump, four signals are used to control the hydraulic valves that regulate the pressure on the pulleys, and one signal is used to control the modulating clutch.

The analog signals are created by a team of one analog-to-digital convertor and six sample and hold circuits. The digital word representing the magnitude of the output current is presented to the analog-to-digital conversion unit (ADC) after which the sample and hold circuit for the desired channel is tripped. The voltage is then sampled by the unit and the voltage is maintained at its output. The final stage is the amplifier which provides the current necessary to drive the solenoid controlled hydraulic valves.

Figures 24 through 31 show block diagrams of the TCS and its primary process schedules.

Stability and Responsiveness

The control system must be developed during prototype testing so that stable operation with good driver feel is achieved. It is not possible to

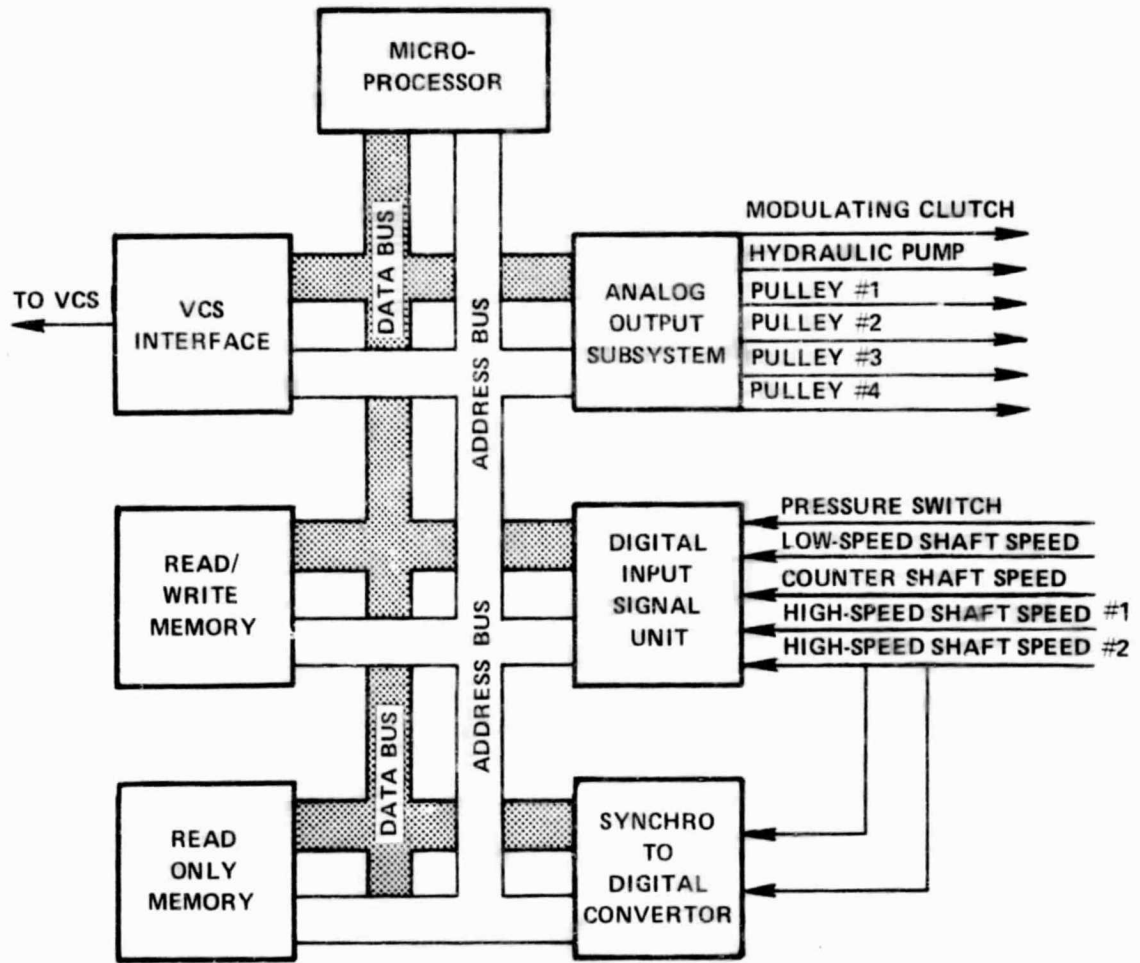


FIGURE 24. BLOCK DIAGRAM OF TRANSMISSION CONTROL SYSTEM

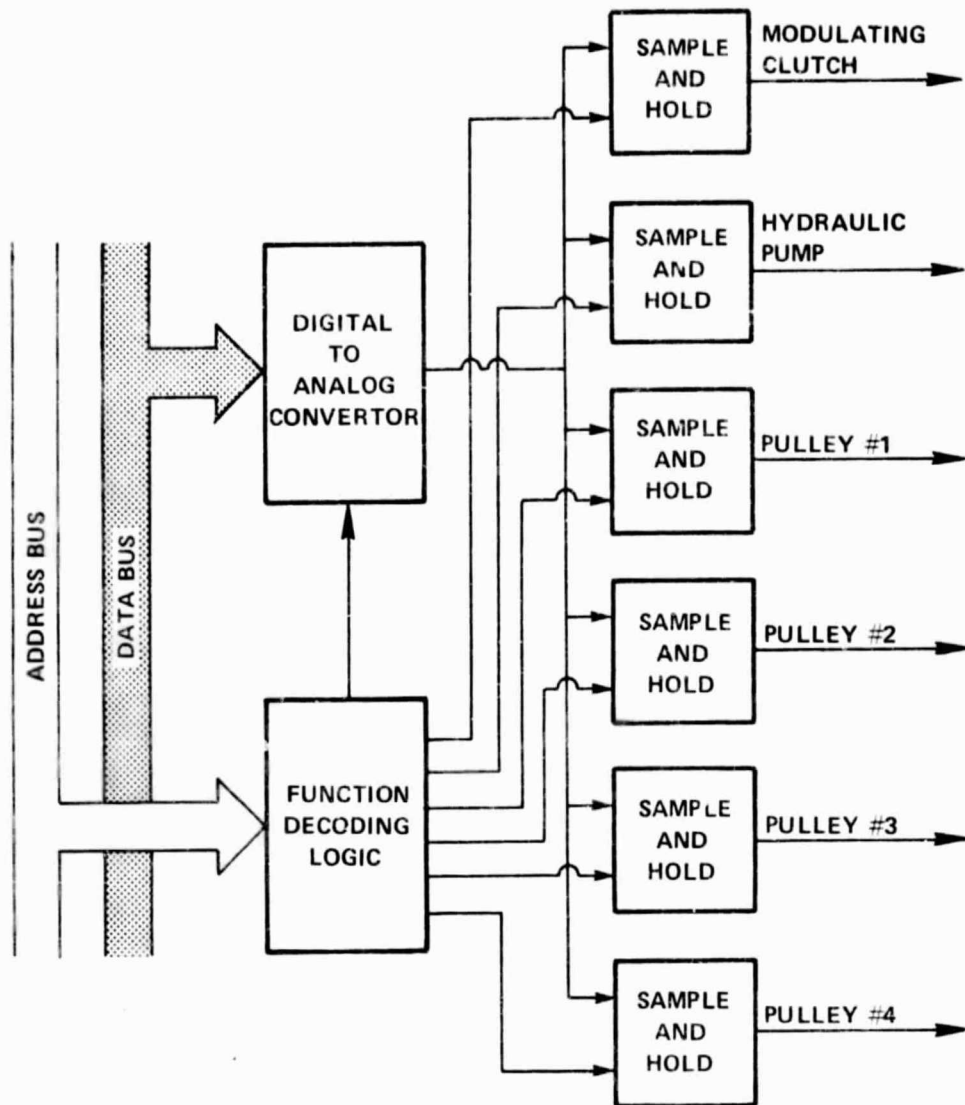


FIGURE 25. BLOCK DIAGRAM OF TCS ANALOG OUTPUT SUBSYSTEM

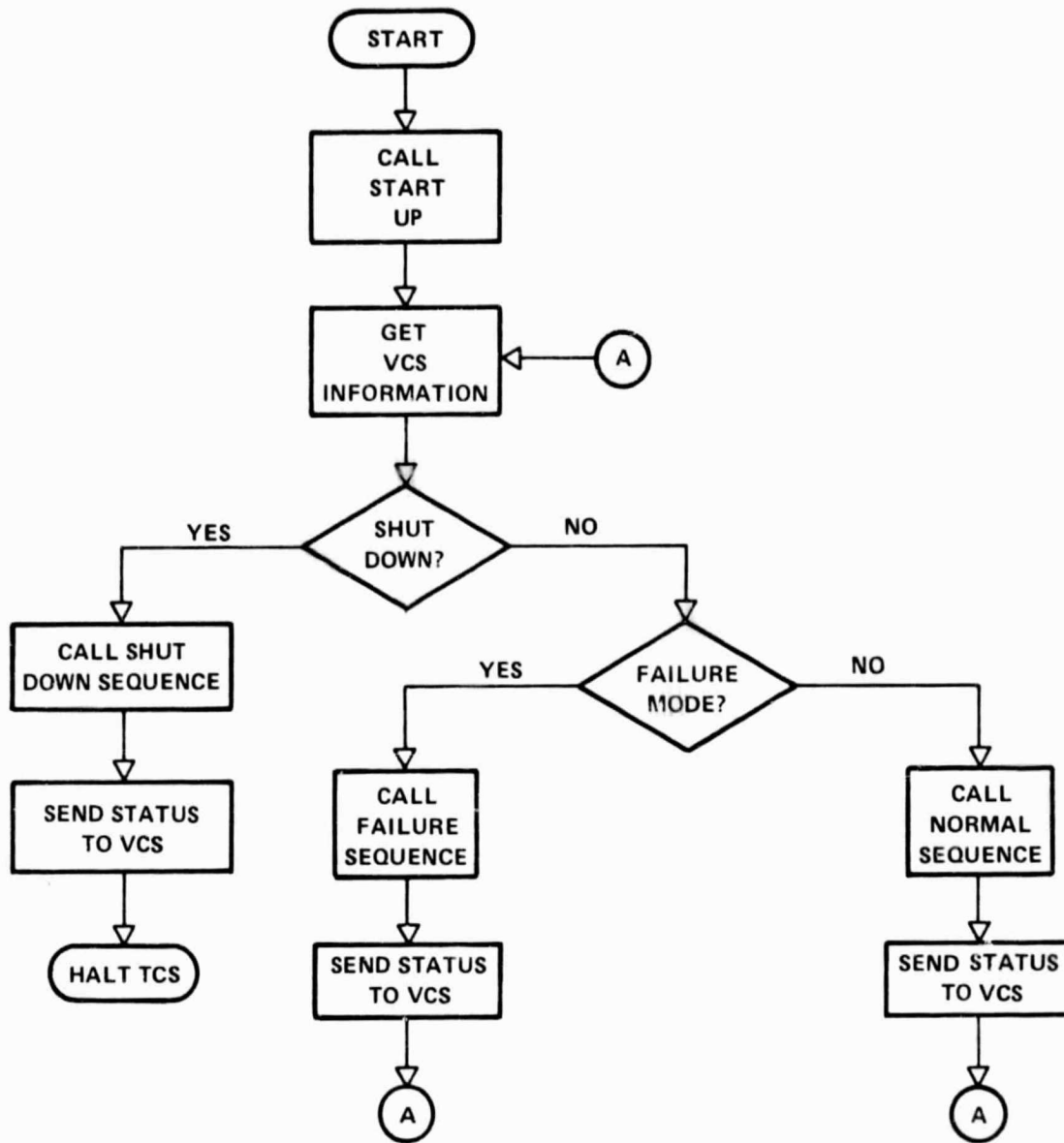


FIGURE 26. BLOCK DIAGRAM OF TCS MAIN PROCESS SCHEDULE

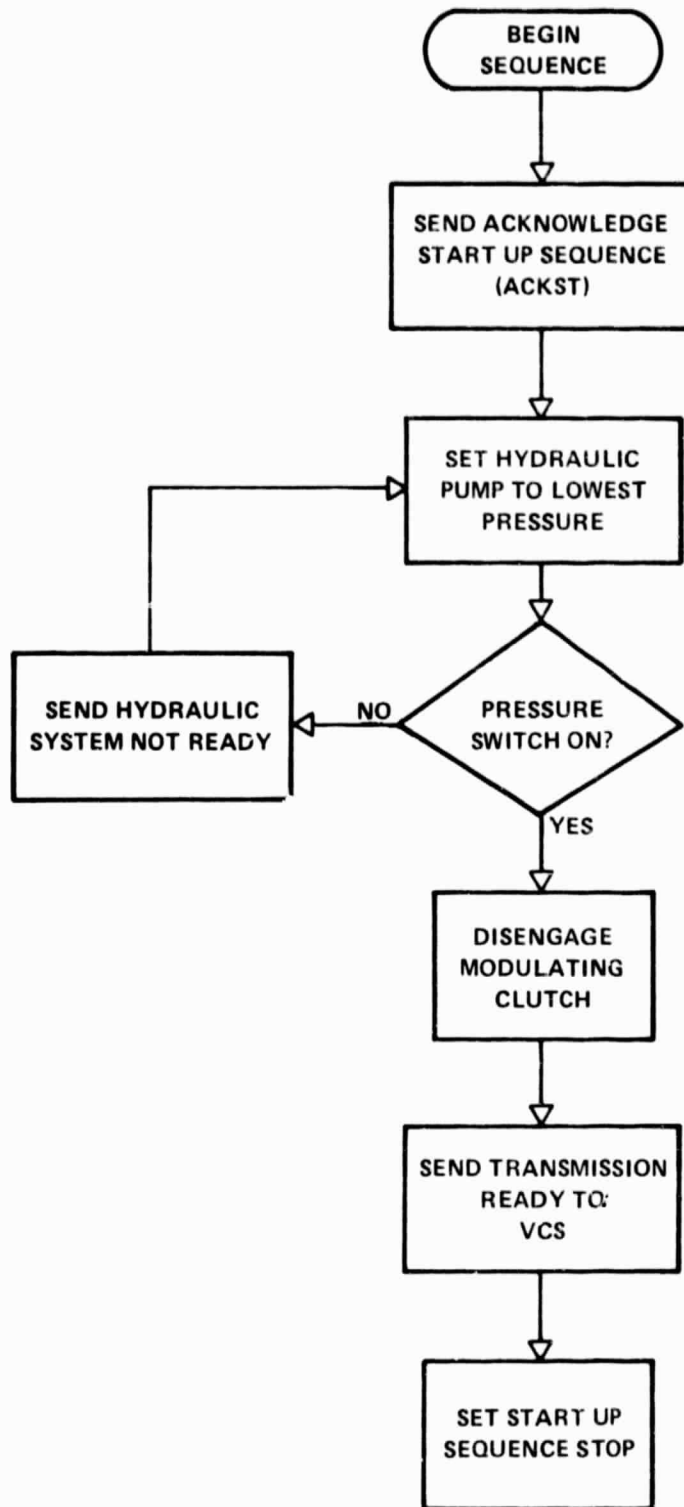


FIGURE 27. BLOCK DIAGRAM OF TCS STARTUP SEQUENCE

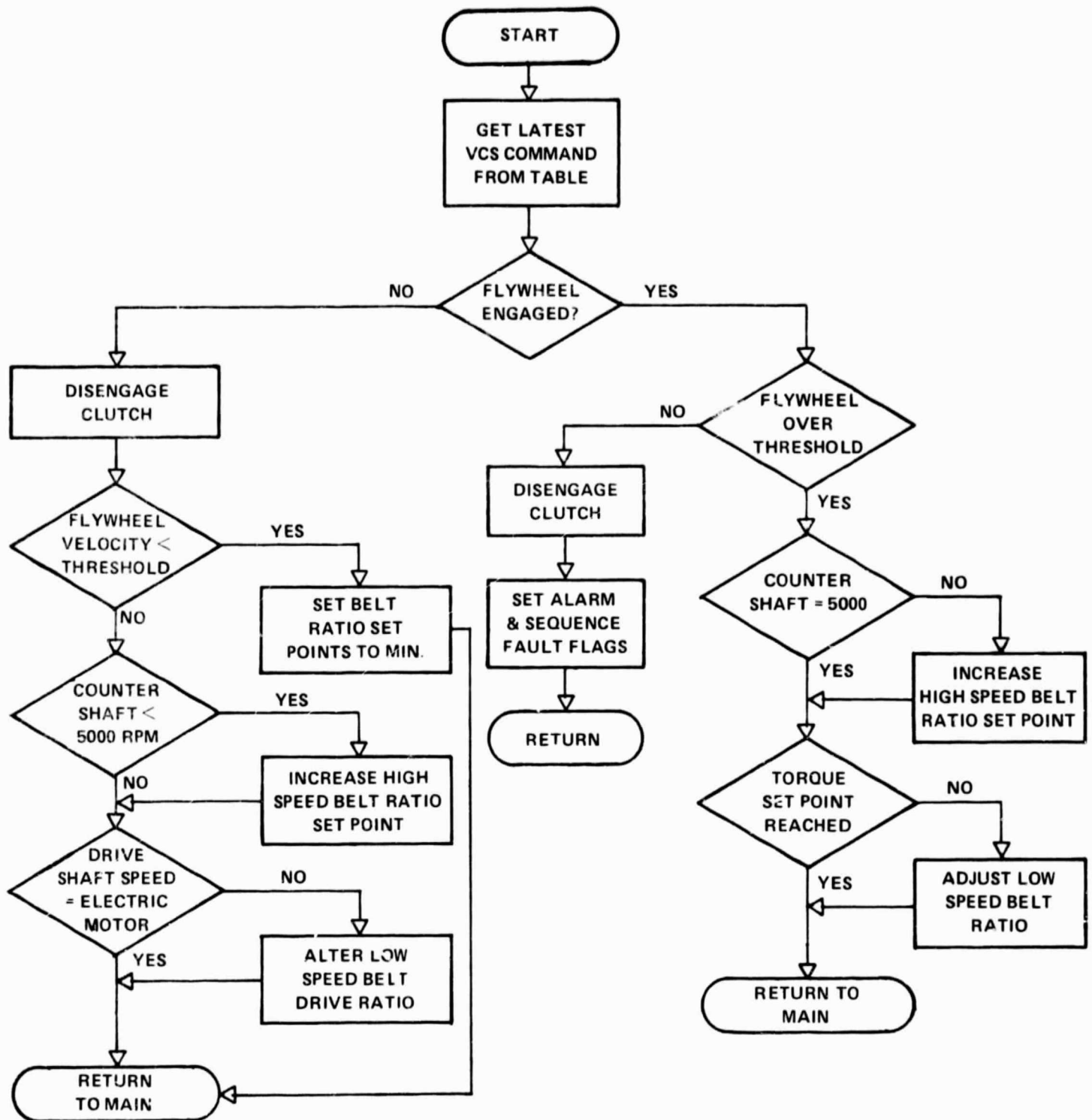


FIGURE 28. BLOCK DIAGRAM OF TCS NORMAL CONTROL SEQUENCE

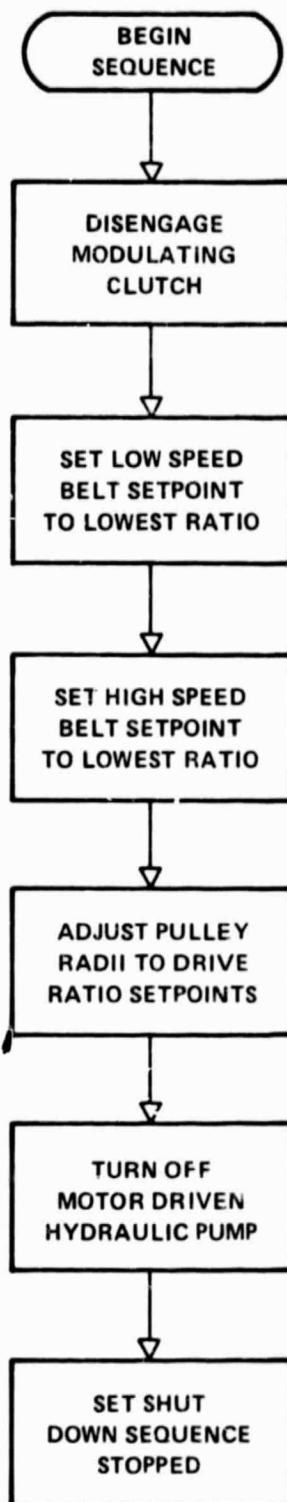


FIGURE 29. BLOCK DIAGRAM OF TCS SHUTDOWN SEQUENCE

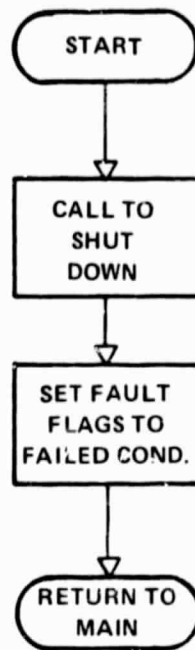


FIGURE 30. BLOCK DIAGRAM OF TCS FAILURE MODE

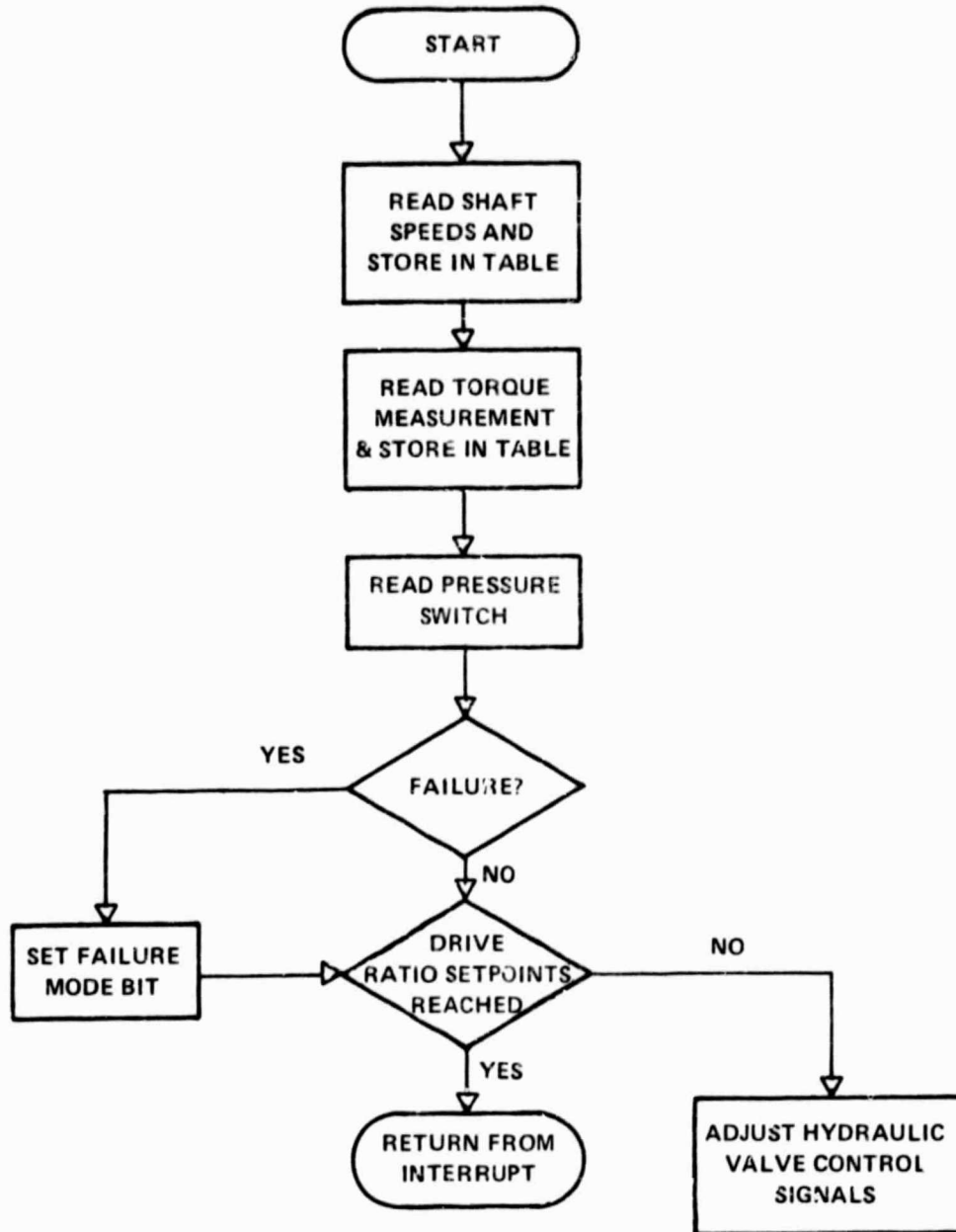


FIGURE 31. BLOCK DIAGRAM OF TCS INTERRUPT ROUTINE TO SERVICE I/O

perform a detailed stability analysis at this point, because the overall vehicle control system and the vehicle components have not been sufficiently well defined. The control system suggested above, however, should offer sufficient flexibility to meet the objectives.

Stability of the proposed transmission system is enhanced by using transmitted torque as the feedback signal rather than pulley ratios or speeds. Torque is used as the feedback parameter because it is the variable actually being commanded by the driver. Also, small changes in pulley ratio can result in substantial torque changes and hence make pulley ratios undesirable feedback parameters. In the event of the loss of the microprocessor the control system will reduce the pressure to the modulating clutch and to the flywheel clutch (if such is employed), thus disengaging both and preventing any torque delivery to or from the flywheel.

Efficiency Estimates

Belt and Bearing Losses

Calculated belt and bearing losses at full torque are shown in Figure 32 for the low-speed belt and at full power in Figure 33 for the high-speed belt. Losses at lower power levels may be calculated from the fixed and variable components shown. These curves are based on operation at the design tension ratio, not the lower tension ratio used for stress calculations. These calculated losses were lower than the measured losses in the earlier Battelle experimental belts (Table 1). It is felt that the primary reasons for this difference were (1) that the experimental belts had unnecessarily high losses due to vibration of the test apparatus which allowed the pulley-to-pulley center distance to vary cyclically and (2) that the experimental belts had excessive losses due to the substantial radial offset between the strut pitch diameter and the inside of the band stack. It should also be noted that the lowest efficiencies shown in Table 1 were for belts in which the pulley cone angle was the smallest. Perhaps some strut-to-pulley locking was occurring.

Friction losses occur within the belt at the band-to-strut contact and, to a lesser extent, at the band-to-band contacts. If the axial pulley forces are properly modulated to maintain the same tension ratio as power is reduced, band bearing losses also go down so that they remain a fixed percentage of the power transmitted. Band loss calculations were based on a coefficient of friction of 0.10.

The creep loss due to compression of the strut stack in the driver is small because of the rigidity of the steel parts. This component will never substantially exceed 0.2 percent of the transmitted power.

Losses at the pulley faces may be interpreted as friction or as creep, but ultimately all of this energy is dissipated by scrubbing of the strut ends against the pulleys. On the driver, the belt enters at maximum net tension and the struts are immediately pulled deep into the pulley. Friction

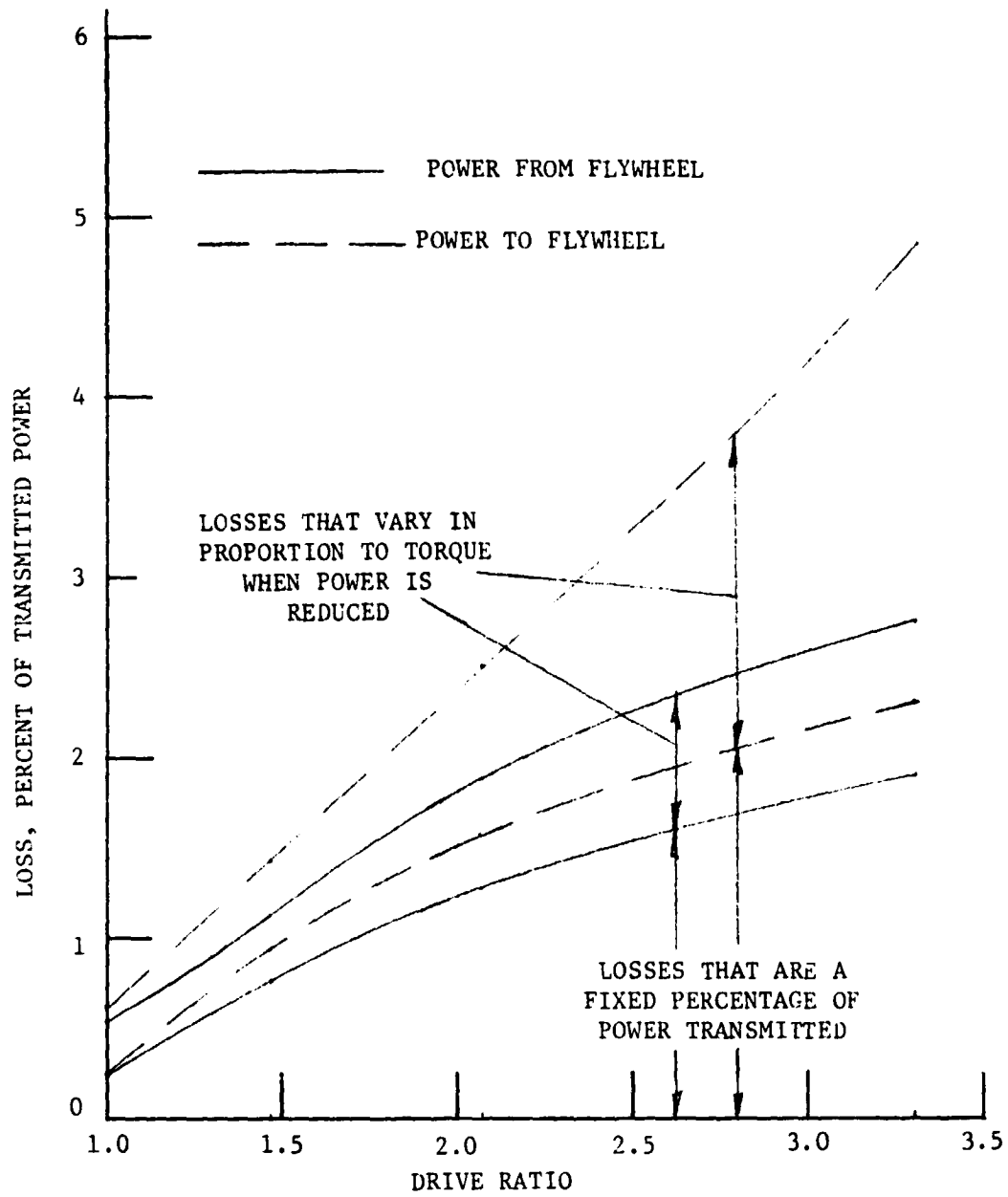


FIGURE 32. FULL TORQUE LOSSES IN LOW-SPEED BELT
 Small Pulley Torque Constant Over Ratio
 Spread. Bearing Drag Included.

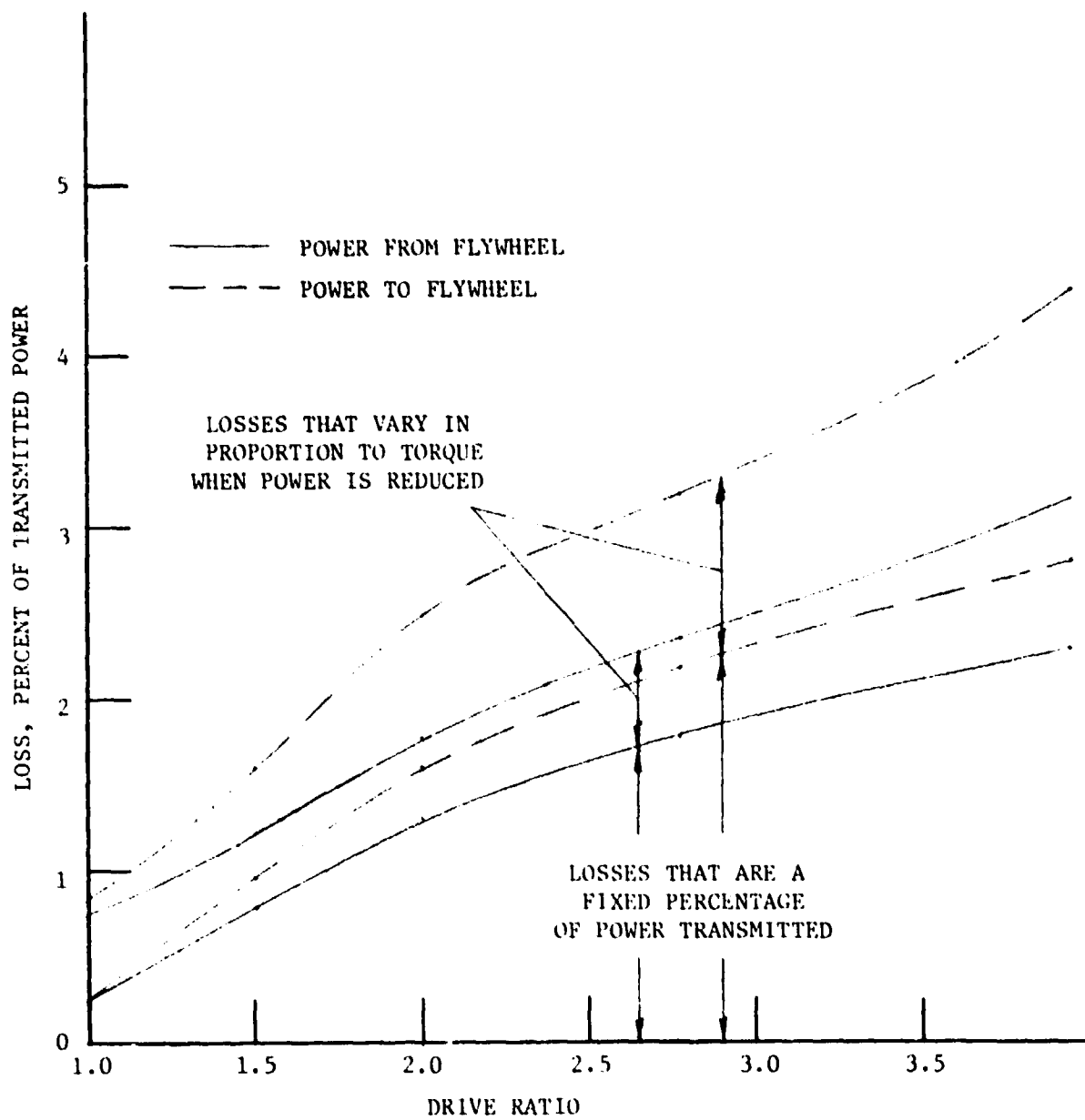


FIGURE 33. CALCULATED LOSSES IN HIGH-SPEED BELT AT FULL POWER

Large Pulley Torque Constant Over Ratio Spread.
Bearing Drag Included.

tends to keep them more or less in the same position as they round the pulley", and the relative motions are primarily radial. On the driven pulley, the struts are pulled continuously deeper as they round the pulley, and since less belt length is required at the smaller radius, the struts near the exit point have a tangential component of relative motion that is generally larger than their radial motion. This "spiral run" of the belt is difficult to treat analytically because rigidity of the pulley face support structure must be considered as well as local deformations of the belt parts and pulley surface. However, a rough estimate of the efficiency loss may be made if the total depth of strut wedging is known.

Calculations indicate that the axial compression of the struts and the local surface of the pulley faces will be about .005cm (.002 in.) under the highest load, resulting in a radial motion of .023cm (.009 in.). It was assumed that gross deflections of the pulley would allow an additional radial motion of the same amount. This is not to say that the pulley faces must be rigid within .005cm (.002 in.), but rather that additional deflection once the struts are seated should be of this order.

Pulley friction losses vary approximately with the square of the belt tension, so that they represent a greater percentage loss at higher power levels. No significant losses were identified that become greater, percentage-wise, as power is decreased. For very low powers, of course, it will become impractical to maintain the design tension ratio, and this will no longer be true.

Losses in the ball bearings that support the pulleys are included with the belt losses, but these are less than 0.5 percent. They were calculated as follows:

$$T = \frac{FBu}{2} \quad (12)$$

where

T = bearing torque drag
 F = bearing radial load
 B = bore of bearing inner race
 u = coefficient = .001.

The bearing radial loads were calculated from belt tensions for each operating condition and the total bearing drag was added to the losses calculated for the belts and belt-to-pulley interfaces.

Hydraulic System and Other Losses

In addition to the belt and shaft bearing losses, the following loss components were computed:

- Hydraulic control pressure
- Lubrication and cooling flow

- Rotary seals
- Spur reduction gear and its bearings.

In order to calculate the hydraulic control pressure losses, the various hydraulic pressures within the system had to be estimated for each operating condition of interest. This was done by referring to the axial force requirement curves discussed earlier in this report. The system supply pressure, provided by the high-pressure pump, was then set at 1,378,950 N/m² (200 psi) above the highest pressure required by any control valve at a given operating condition. This pressure is listed in Table 8. Based on this system pressure, the leakage flows of the pulley and clutch valves were estimated. (Only orifice-type leakage paths were considered, since the laminar flow paths represented negligible leakage components.) The sum of the pulley and clutch valve leakages was then increased by 25 percent to account for the pump's servo control valve system. A leakage value for the pump itself was then added. This value was proportional to the pump pressure and was based on pertinent Battelle experience on small vane pumps. The viscosity assumed was that of ATF at 99 C (210 F), 7 centistokes. The hydraulic control system horsepower was then calculated as follows (U.S. units):

$$HP = \frac{Q \times P \times 583 \times 10^{-6}}{E_p E_m} \quad (13)$$

where

- Q = pump flow, gpm
- P = pump pressure, psi
- E_p = pump mechanical efficiency = .75
- E_m = motor overall efficiency = .75.

These losses are small compared to the belt losses.

The loss for the lubrication/cooling pump was estimated by assuming a 4 liters per minute (1 gpm) displacement at 1.4 x 10⁵ N/m² (20 psi), a pump mechanical efficiency of 50 percent (due to the high speed, low pressure operating condition), and a motor efficiency of 75 percent. The resulting .02kW (.03 hp) was applied as a constant loss.

The seal losses were estimated assuming them to be independent of torque and speed. An average shaft speed of 5125 rpm was used. A spring-loading force of 2kg (5 lb) was used for each of the internal pulley feeding shaft seals. An average system pressure of 5.17 x 10⁶ N/m² (750 psi) was used. A coefficient of friction of .05 was assumed for the seal faces and there were assumed to be six seals rather than four to provide an allowance for the CVT input and output shaft seals. The resulting .04 kW (.06 hp) was applied as a constant loss.

A loss of 1 percent of the transmitted power was assigned to the spur gear mesh and its bearings based on qualitative projections from Chapter 14 of Reference (3). No attempt was made to calculate the windage and churning loss

TABLE 8. HYDRAULIC CONTROL SYSTEM POWER

kW	(hp)	CVT Operating Condition		Control System Pressure, psi	Pump Output Flow, gpm	Pump Leakage, gpm	Pump Displacement, gpm	System hp	
		Flywheel Speed, rpm	Driveline Speed, rpm						
7	(10)	14,000	1550	318	.125	.093	.218	.069	
			3000	268	.120	.078	.198	.053	
			500	268	.122	.078	.200	.054	
		21,000		1550	318	.126	.093	.219	.070
				3000	262	.119	.076	.195	.051
				500	257	.121	.075	.196	.050
		28,000		1550	318	.122	.093	.215	.068
				3000	262	.120	.077	.197	.052
				5000	250	.114	.073	.187	.047
	16	(22)	14,000	1550	459	.141	.134	.275	.126
				3000	350	.127	.103	.230	.081
				5000	350	.132	.103	.235	.082
		21,000		1550	459	.142	.134	.276	.127
				3000	336	.125	.098	.223	.075
				5000	325	.128	.095	.223	.072
		28,000		1550	457	.147	.134	.281	.128
				3000	336	.125	.098	.223	.075
				5000	310	.124	.091	.215	.067
30		(40)	14,000	1550	670	.171	.196	.367	.246
				3000	472	.137	.138	.275	.130
				5000	472	.145	.138	.283	.134
		21,000		1550	670	.173	.196	.369	.247
				3000	448	.135	.131	.266	.119
				5000	427	.138	.125	.263	.112
		28,000		1550	670	.173	.196	.369	.247
				3000	448	.136	.131	.267	.120
				5000	399	.131	.117	.248	.099
	52	(70)	14,000	1550	1024	.212	.300	.512	.524
				3000	677	.172	.198	.370	.250
				5000	677	.175	.198	.373	.252

TABLE 8. HYDRAULIC CONTROL SYSTEM POWER (CONTINUED)

CVT Operating Condition		Flywheel Speed, rpm	Driveline Speed, rpm	Control System Pressure, psi	Pump Output Flow, gpm	Pump Leakage, gpm	Pump Displace- ment, gpm	System hp
kW	(hp)							
	21,000		1550	1024	.215	.300	.515	.257
			3000	633	.166	.185	.351	.222
			5000	597	.163	.175	.338	.202
	28,000		1550	1024	.220	.300	.520	.532
			3000	633	.165	.185	.350	.221
			5000	531	.149	.156	.305	.162
75 (100)	14,000		1550	1377	.249	.403	.652	.898
			3000	882	.210	.258	.458	.404
			5000	882	.199	.258	.457	.403
	21,000		1550	1377	.254	.403	.657	.905
			3000	819	.193	.240	.433	.355
			5000	762	.187	.233	.410	.312
	28,000		1550	1377	.254	.403	.657	.905
			3000	819	.189	.240	.429	.351
			5000	699	.176	.205	.381	.266

of this gear mesh. However, a constant windage and churning loss of .19 kW (.25 hp) was assigned to the overall CVT.

Table 9 shows the combined calculated losses for the high and low speed belts in the CVT. The losses are expressed as a percent of the power and are displayed as a function of flywheel speed, driveshaft speed, direction of power flow (to or from the flywheel), and power level. They include a loss component for the pulley bearings. This table was included so that the reader can conveniently determine the belt losses independent of the total losses in the CVT.

Figures 34 through 39 show the combined total loss for the CVT expressed as a percent of power. Belts, pulley bearings, hydraulic control pump, lubrication/cooling oil pump, spur reduction gear, seals, and a windage loss were included. Figures 40 through 42 show overall CVT efficiency for the same conditions as the losses above. These calculated curves illustrate that the transmission should be efficient under all intended operating conditions, and that the transmission is somewhat more efficient when transmitting power from the flywheel to the driveline than vice versa. Actual power losses in a working transmission are typically somewhat higher than calculated values. Losses 20 percent greater than the calculated values would not be unusual. The overall efficiency will still be quite attractive.

Maximum Transient Power Output

The CVT was required to transmit a 75 kW (100 hp) power transient in either direction for 5 seconds. The maximum torque requirement was also specified as 450 N-m (330 lb-ft). This means that the 75 kW (100 hp) requirement applies above that driveline speed at which 447 N-m (330 lb-ft) of torque equals 75 kW (100 hp) [1590 rpm]. The steel V-belt CVT was designed to handle 450 N-m (330 lb-ft) of torque from zero to 1590 driveline rpm and 75 kW (100 hp) from 1590 to 5000 rpm.

The thermal input to the CVT during the 5-second transient was estimated to be .018MJ (.005 kWh) based on a 95 percent overall efficiency during the transient. This is essentially the same energy that the clutch receives during each vehicle startup and was considered benign. The 75 kW (100 hp), 5 second transient should pose no problems.

Reliability and Maintainability

The CVT was designed with the intent of exceeding the 90 percent 2600-hour minimum requirements of the work statement. The only periodic maintenance anticipated would be the maintenance of the required lubricant level in the sump. Loss of lubrication pressure in the hydraulic system would be displayed by the transmission control system and would result in automatic transmission shutdown. It is not intended that any of the internal components will require periodic replacement.

TABLE 9. BELT LOSSES - PERCENT OF POWER TO OR FROM THE FLYWHEEL

Operating Condition			Losses						
Flywheel Speed, rpm	Power Direction	Power Level, kW (hp)	Driveshaft Speed, rpm						
			850	1250	1590	2500	3750	5000	
28,000	To flywheel	7 (10)	5.4	4.7	4.2	3.4	2.6	2.1	
		15 (20)	5.8	5.1	4.6	3.5	2.7	2.2	
		30 (40)	6.6	5.8	5.2	3.9	3.0	2.4	
		52 (70)	7.7	6.8	6.2	4.5	3.4	2.8	
		75 (100)	8.9	7.9	7.2	5.0	3.8	3.2	
	From flywheel	7 (10)	4.3	3.7	3.3	2.7	2.0	1.7	
		15 (20)	4.4	3.8	3.5	2.8	2.1	1.7	
		36 (40)	4.8	4.1	3.7	3.0	2.3	1.9	
		52 (70)	5.3	4.6	4.1	3.3	2.5	2.1	
		75 (100)	5.8	5.0	4.5	3.7	2.8	2.4	
21,000	To flywheel	7 (10)	4.9	4.1	3.6	2.7	1.9	1.4	
		15 (20)	5.2	4.5	3.9	2.9	2.0	1.5	
		36 (40)	5.9	5.1	4.5	3.0	2.3	1.7	
		52 (70)	6.9	6.1	5.4	3.7	2.6	2.0	
		75 (100)	7.9	7.1	6.3	4.1	2.9	2.3	
	From flywheel	7 (10)	3.9	3.3	2.8	2.2	1.5	1.2	
		15 (20)	4.0	3.4	3.0	2.3	1.6	1.2	
		36 (40)	4.3	3.6	3.2	2.5	1.8	1.4	
		52 (70)	4.7	4.0	3.6	2.8	2.0	1.6	
		75 (100)	5.1	4.4	4.0	3.1	2.2	1.8	
41,000	To flywheel	7 (10)	4.1	3.3	2.9	2.0	1.2	0.7	
		30 (40)	5.1	4.2	3.8	2.4	1.5	1.0	
		52 (70)	6.1	5.0	4.6	2.9	1.8	1.2	
		75 (100)	7.0	5.9	5.5	3.3	2.1	1.5	
	From flywheel	7 (10)	3.2	2.6	2.3	1.6	1.0	0.6	
		30 (40)	3.6	3.0	2.7	2.0	1.2	0.8	
		52 (70)	4.0	3.4	3.1	2.3	1.5	1.1	
		75 (100)	4.4	3.7	3.5	2.6	1.7	1.3	

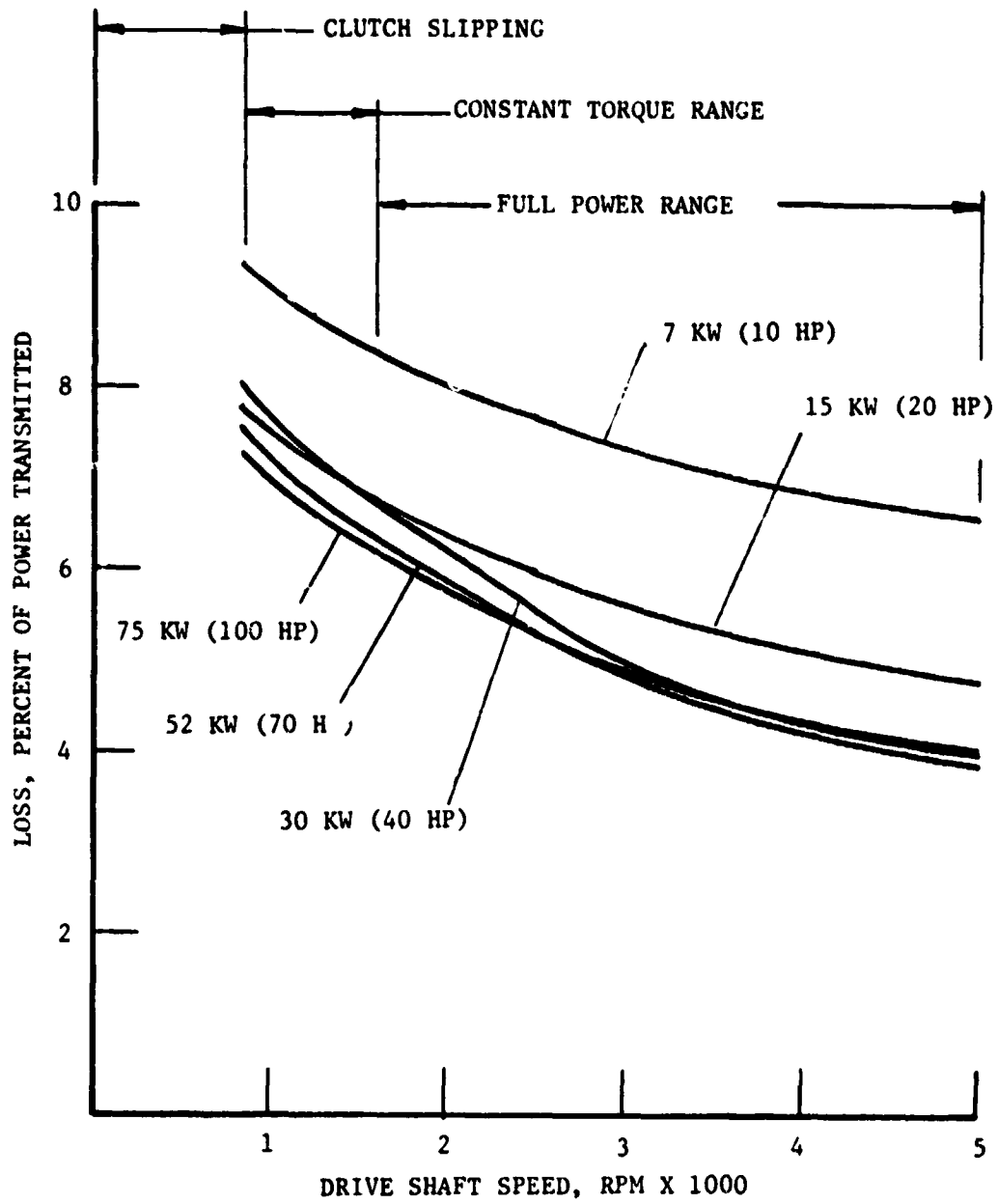


FIGURE 34. TOTAL LOSSES IN CVT AT 28,000 RPM OF FLYWHEEL
(Power from Flywheel)

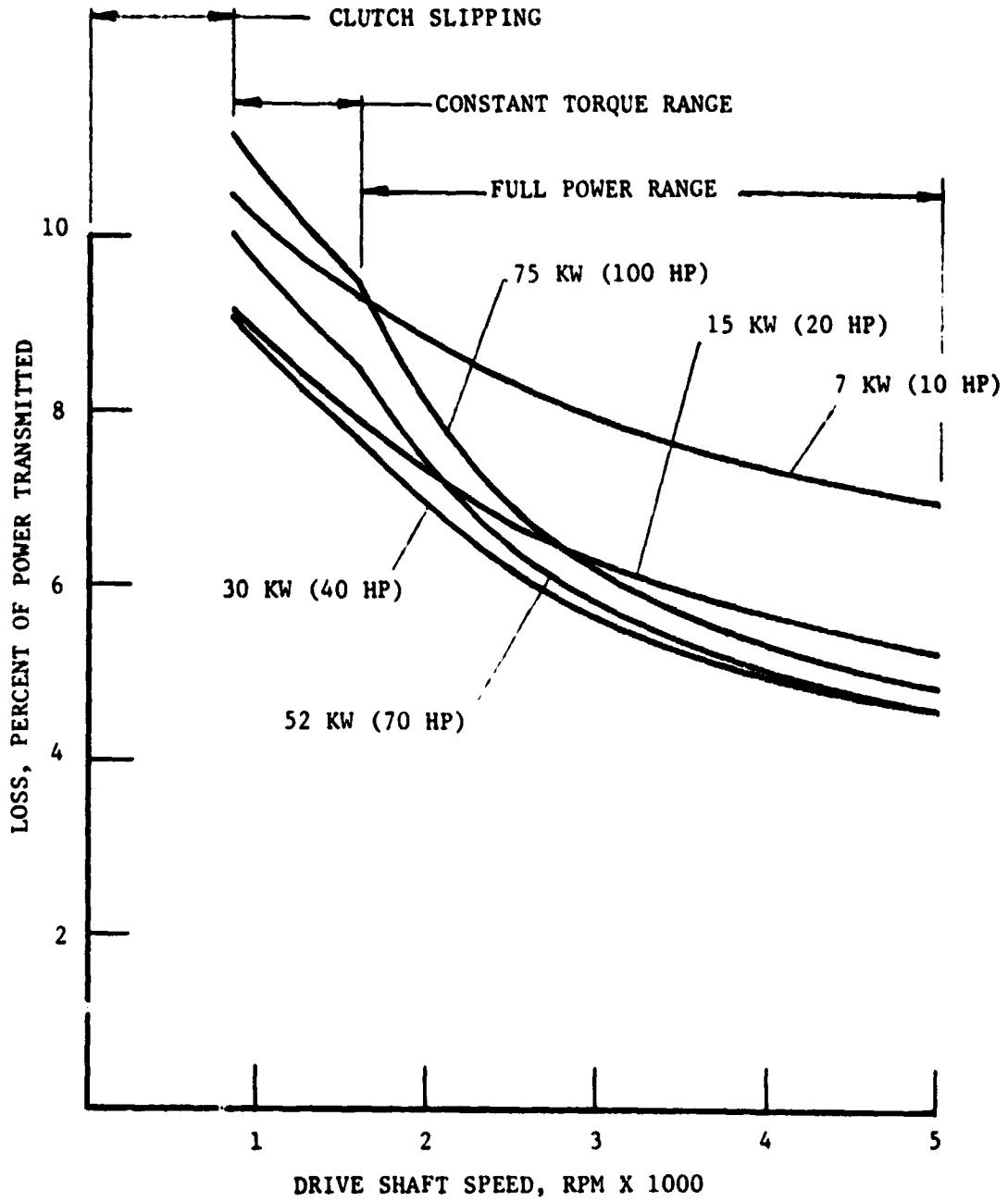


FIGURE 35. TOTAL LOSSES IN CVT AT 28,000 RPM OF FLYWHEEL
(Power to Flywheel)

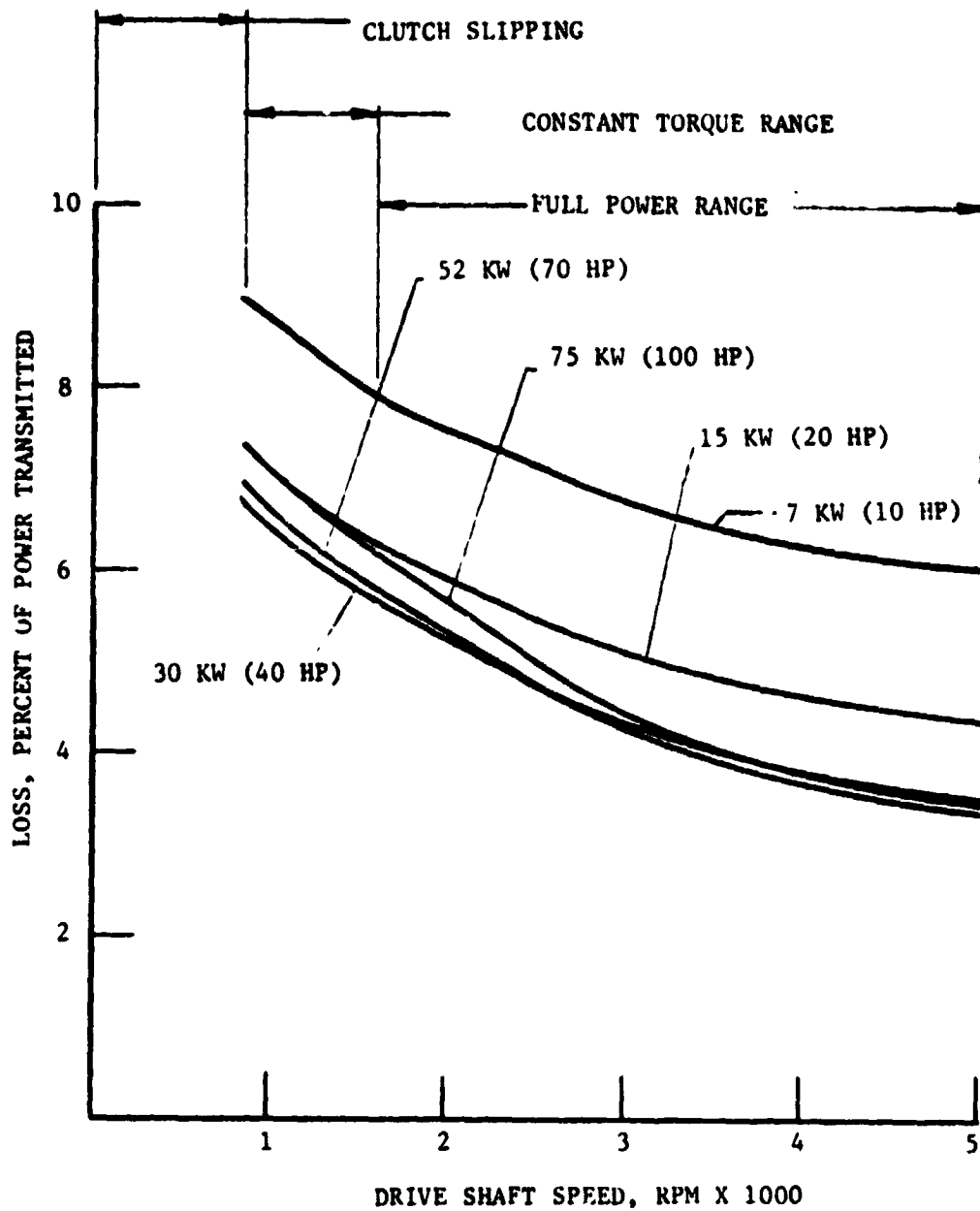


FIGURE 36. TOTAL LOSSES IN CVT AT 21,000 RPM OF FLYWHEEL
(Power from Flywheel)

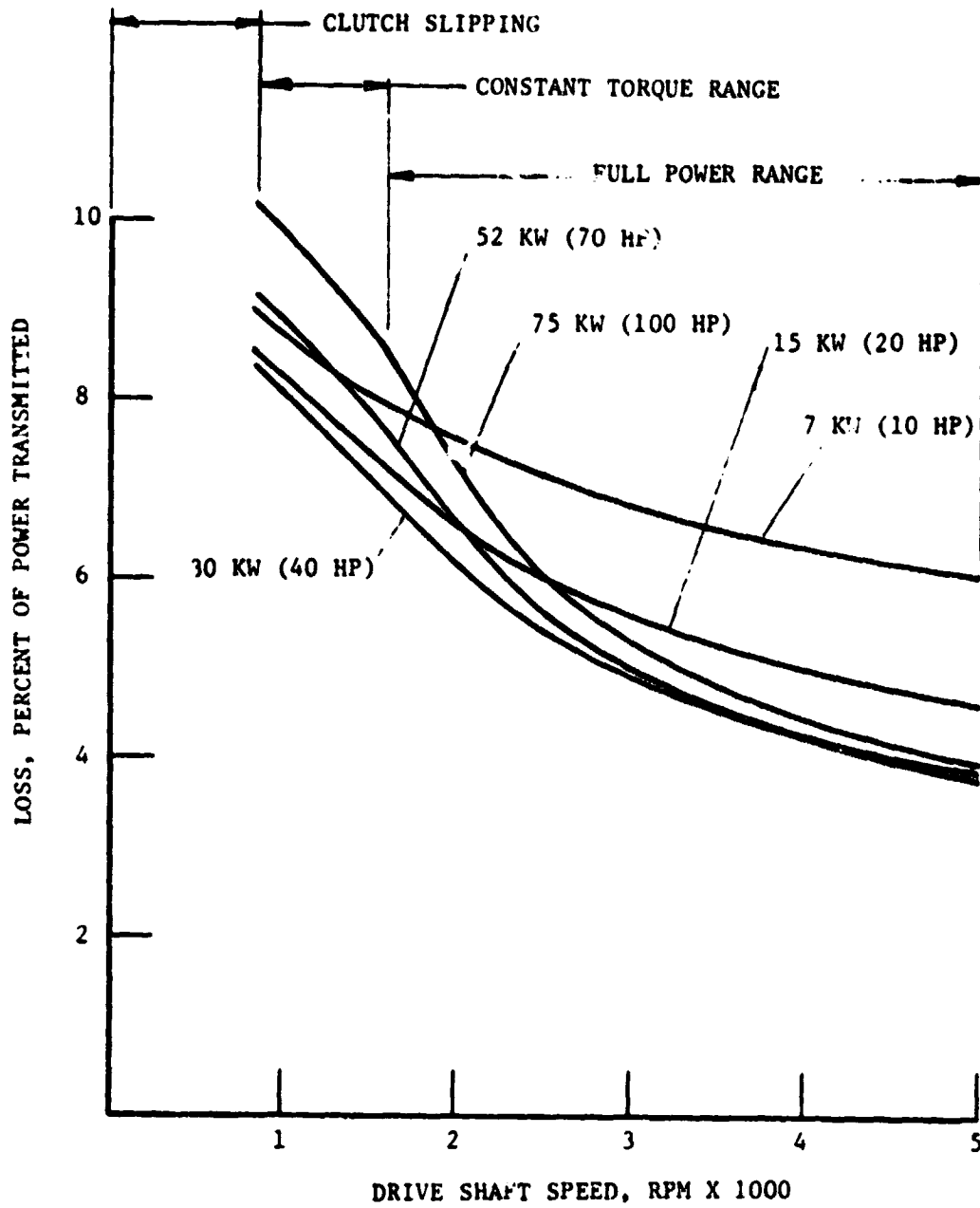


FIGURE 37. TOTAL LOSSES IN CVT AT 21,000 RPM OF FLYWHEEL
(Power to Flywheel)

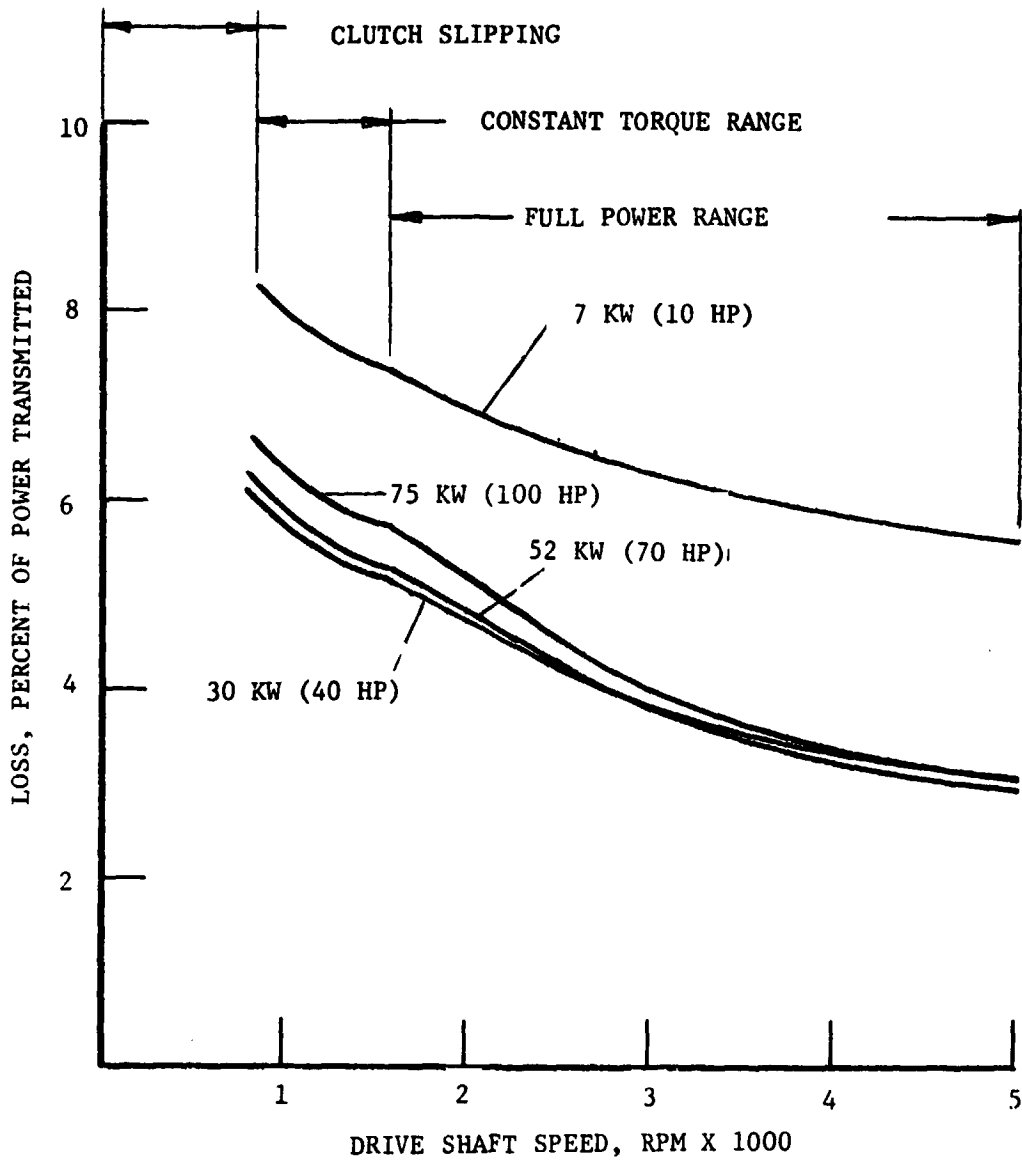


FIGURE 38. TOTAL LOSSES IN CVT AT 14,000 RPM OF FLYWHEEL
(Power from Flywheel)

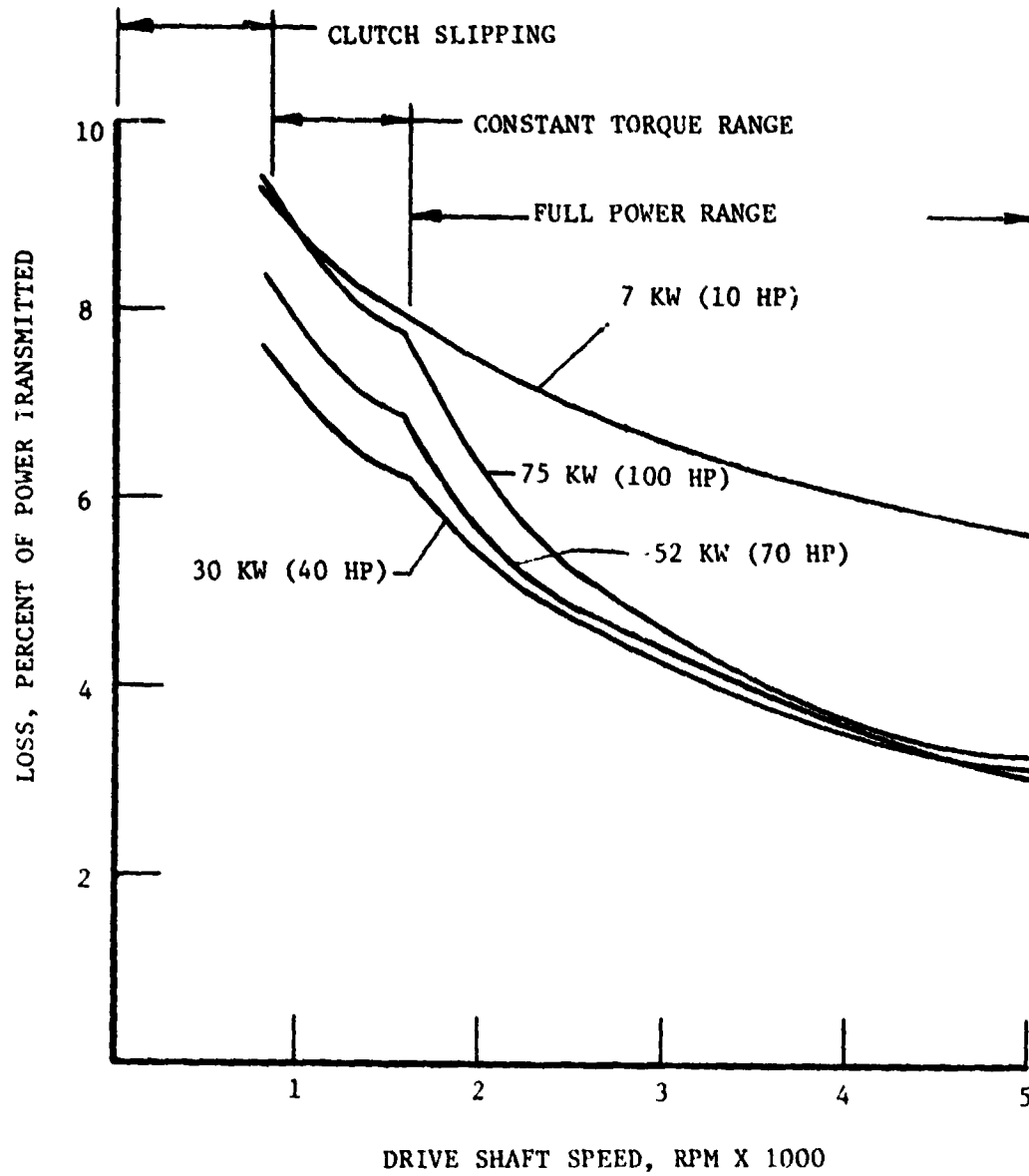


FIGURE 39. TOTAL LOSSES IN CVT AT 14,000 RPM OF FLYWHEEL
(Power to Flywheel)

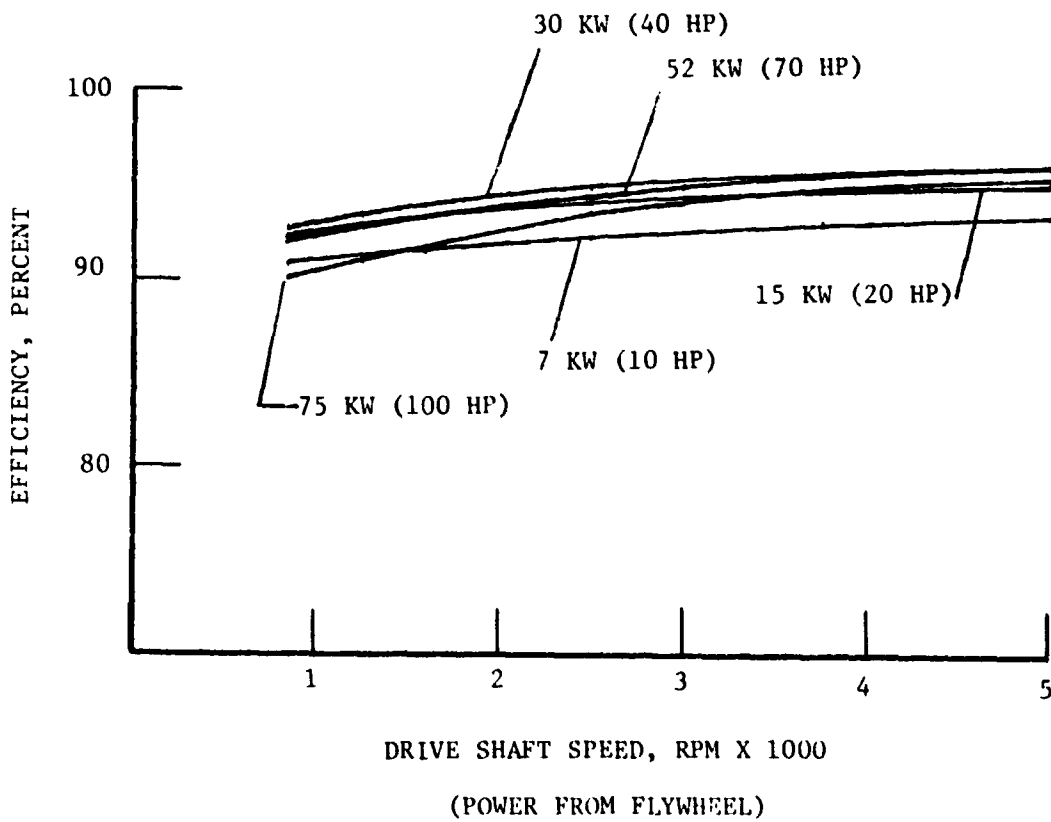
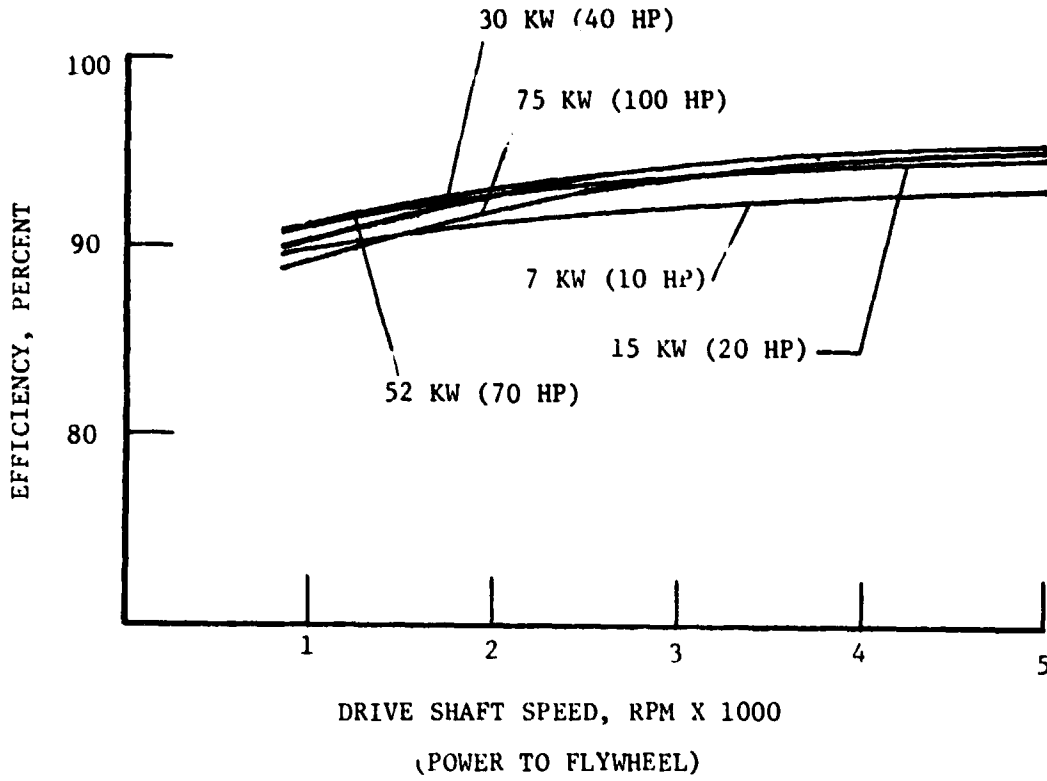


FIGURE 40. OVERALL CVT EFFICIENCY AT 28,000 RPM OF FLYWHEEL

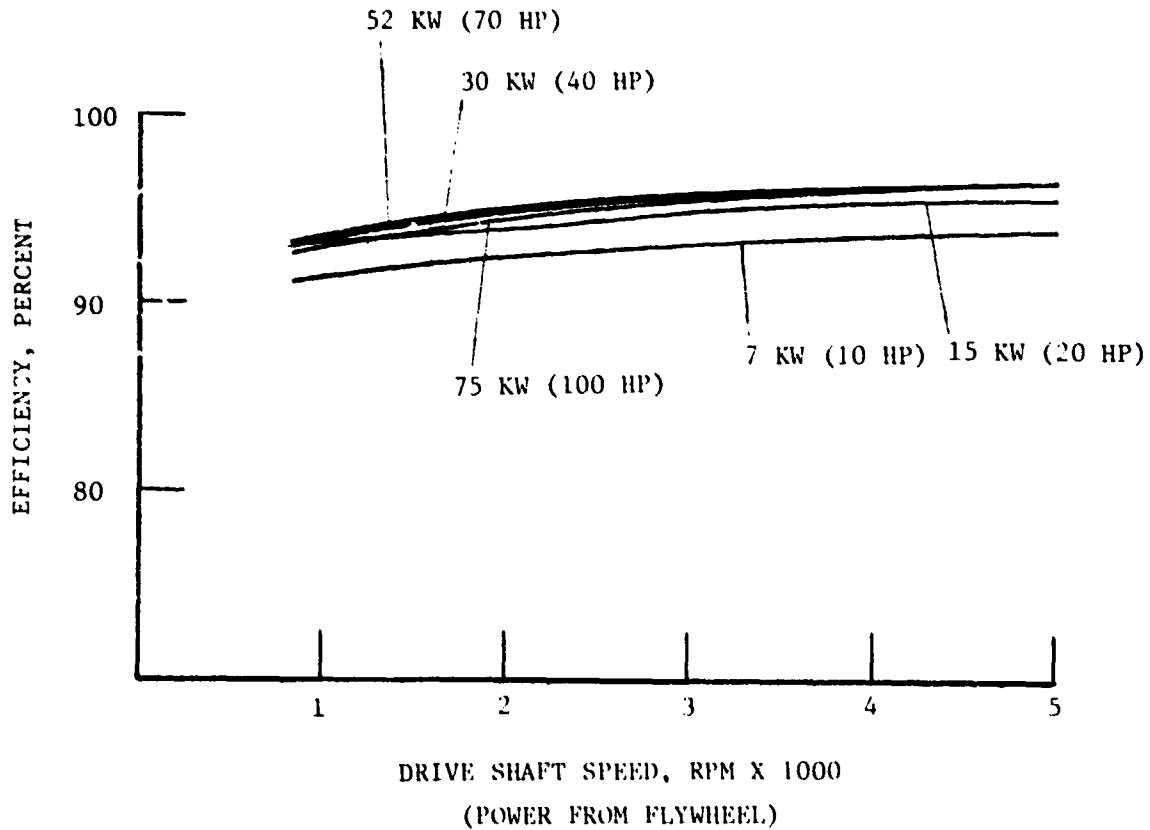
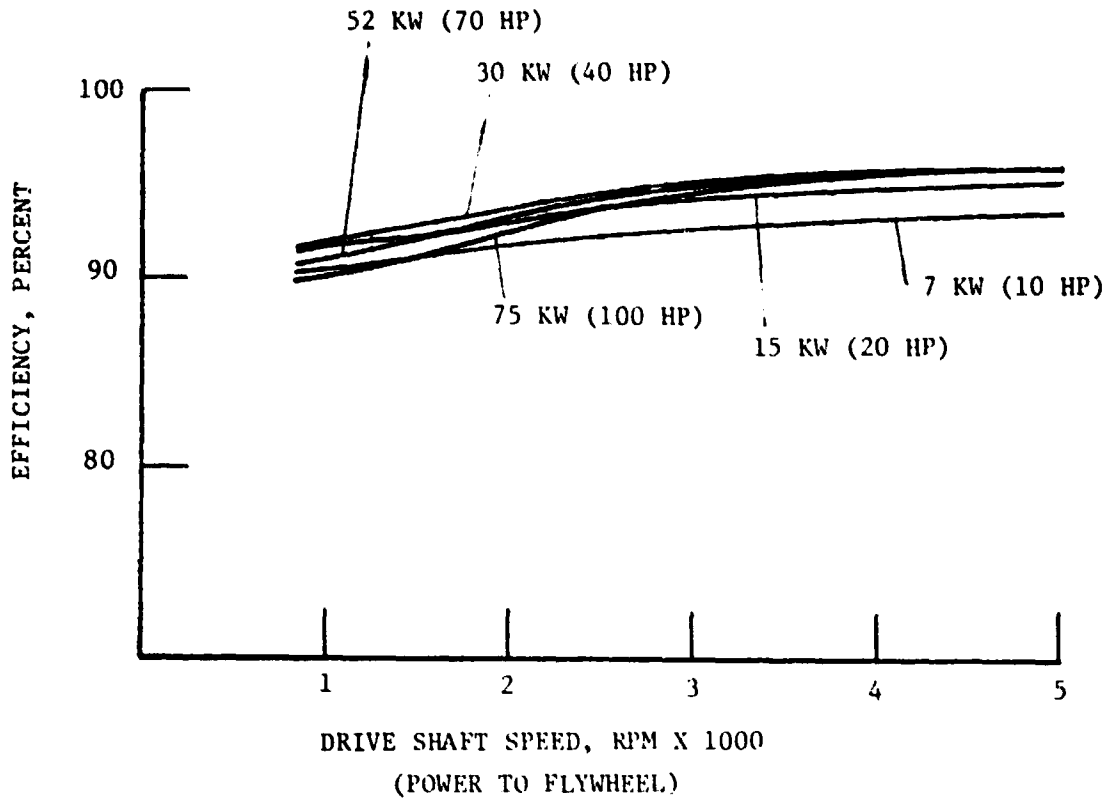


FIGURE 41. OVERALL CVT EFFICIENCY AT 21,000 RPM OF FLYWHEEL

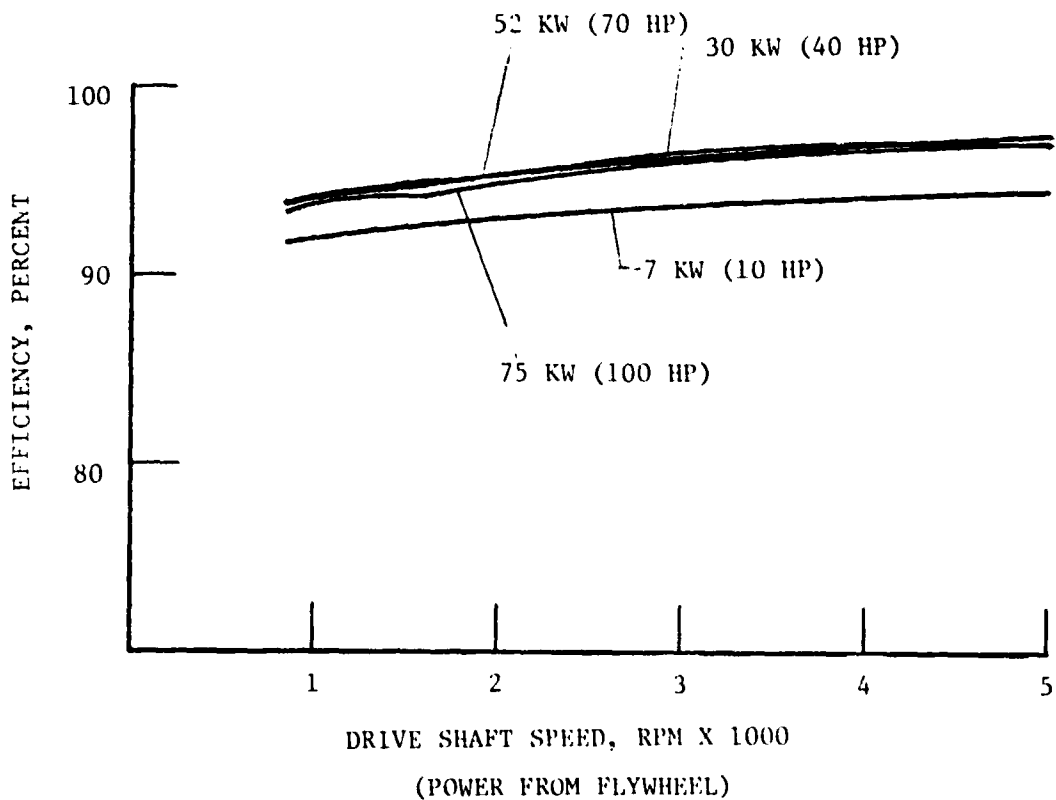
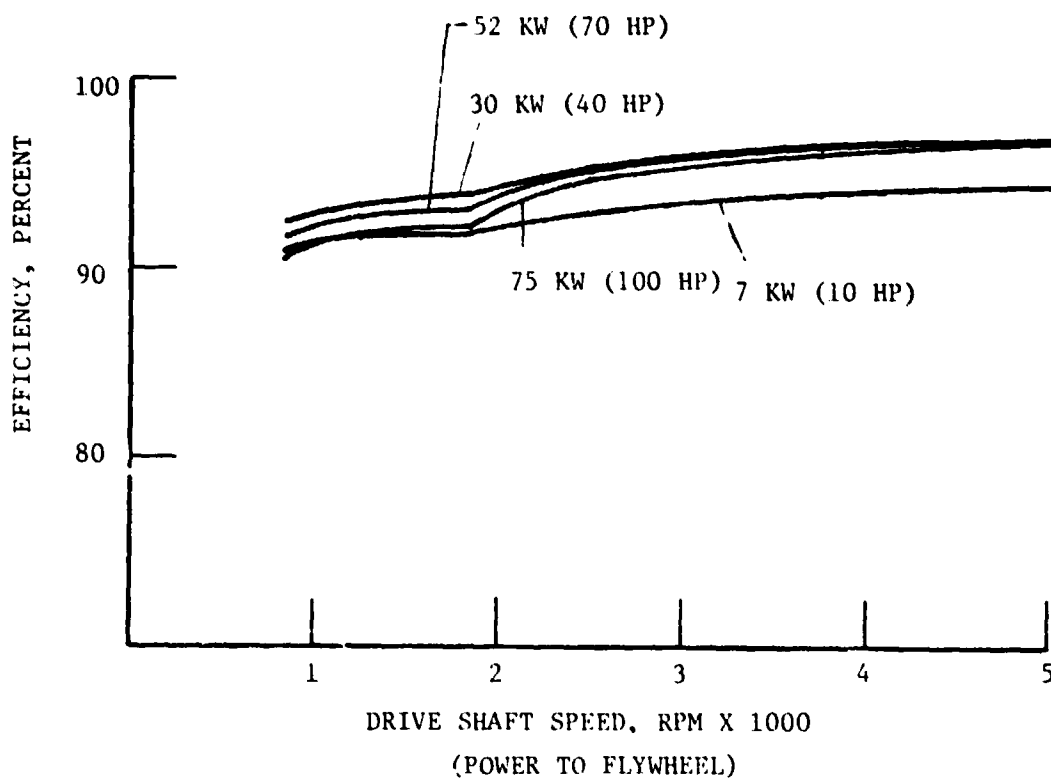


FIGURE 42. OVERALL CVT EFFICIENCY AT 14,000 RPM OF FLYWHEEL

Calculated stresses and friction levels in the belt and pulley systems are sufficiently low that the life of these components should exceed the 2600-hour service life. The rolling element bearings all have B₁₀ levels greater than 2600 hours at the average power condition. They all have adequate short-term load capacity at the maximum torque (hence maximum bearing load) conditions. The spur gear speed reducer was sized to provide more than adequate calculated life. The shaft splines are subject to wear due to the nature of the V-belt drive loading. Forced lubrication provided in these areas should result in adequate life.

As in any sophisticated and complex mechanical device (current passenger car automatic transmissions are a good example), a substantial period of development will probably be required to achieve the desired durability. The steel V-belt transmission appears to offer a practical approach to a reliable, high-efficiency CVT.

Noise and Critical Speeds

The noise level is a significant concern in the application of any type of mechanical transmission in a passenger car. Past experimental work at Battelle has indicated that compression, steel V-belt drives are relatively quiet for the amount of power transmitted. It is anticipated that the belt and pulley configuration recommended in this report will be satisfactorily quiet for the intended application. Should the strut passage frequency prove to be a problem (i.e., if resonances in the system are excited), the strut thickness could be varied in a random manner to avoid resonances and pure tone components, as was discussed in an earlier report section.

The straight spur gears shown in the fixed ratio speed increaser could be replaced by helical or herringbone-type gearing if the spur gear noise should prove objectionable. This would require minor revisions to the shafting and bearings, however, and the change is not recommended unless prototype testing shows it is warranted.

Preliminary analyses of shaft critical speeds indicate that in the recommended design, critical speeds should not be a problem. A check of the first critical speed of the shaft and large pulley for the low-speed belt was made by applying standard equations.

$$\delta_{ST} = [W' + \left(\frac{l^2 + CC_1}{8 CC_1}\right) W] \frac{C^2 C_1^2}{3 EI l}, \quad (14)$$

where W' is the weight of the pulley, and W is the weight of the shaft. Then, assuming the pulley is a point mass,

$$N_c \text{ (rpm)} = \frac{60}{\pi} \sqrt{\frac{g}{\delta_{ST}}} \quad (15)$$

The first critical speed (N_c) was calculated to be about 230,000 rpm. The short distance between bearings, combined with the relatively stiff shaft results in a very high critical speed. Critical speeds are therefore not expected to be a problem in any of the transmission shafts.

Weight Estimates

The transmission configuration described in this report should be competitive in weight with conventional automatic transmissions of similar power. Table 10 shows estimated weights for the major components in the transmission system. The total estimated weight is about 70 kg (155 lb). This weight is exclusive of the microprocessor control components. The components influencing the total package weight most significantly are the steel pulleys and the aluminum housing, in that order.

TABLE 10. STEEL V-BELT CVT WEIGHT ESTIMATE

	kg	(lb)
Housing (Aluminum Casting)	9.9	(22.0)
Clutch Fittings (Aluminum and Steel)	3.4	(7.6)
Pulley Support Fittings (Steel)	6.7	(14.7)
Pulleys (Steel)	17.2	(38.0)
Shafts (Steel)	4.9	(10.8)
Spur Gears (Steel)	1.5	(3.4)
DC Motor (Pesco 224388-020)	1.9	(4.4)
Bearings	7.3	(16.2)
Sleeves (Steel)	2.0	(4.5)
Belts	2.6	(5.8)
Oil	1.7	(3.7)
Control Valve Package	3.1	(6.8)
Hydraulic Pump Package	.8	(1.8)
Miscellaneous	<u>6.8</u>	<u>(15.0)</u>
Total	69.8	(154.7)

CVT Cost Estimate

It was difficult to prepare a cost estimate for the eventual high volume manufacture of 100,000 units a year during this project. Detail drawings did not exist so conventional industrial engineering approaches to cost estimating could not be used. The approach that was used was to group the CVT parts into major categories and apply either a factor by weight or a specific discrete estimate to them. Table 11 summarizes the results.

TABLE 11. MANUFACTURING COST ESTIMATES FOR
STEEL V-BELT CVT

Type of Part	Factor	Cost
Electrical Portions of Electrohydraulic Valves	6 valves @ \$2.50	\$15.00
Electric Motor		12.00
Steel V-Belts	2 belts @ \$25.00	50.00
Electronics (Sensors, Microprocessor, etc.)		15.00
Mechanical Parts (Similar to current automatic transmissions)	110 lb @ \$2.00	220.00
	Total -	<u>\$312.00*</u>

*1980 Dollars

Identification of Required Technical Advancements

Task II of the contract called for an identification of critical path technologies that need to be developed to assure the commercial development of steel V-belt CVT's. Only a modest effort was applied to this during the project. However, the feasibility engineering design and analyses deals with this question as a natural consequence.

It was concluded that development work will be required on the manufacturing of the steel bands for the belts for the purpose of reducing costs. Functionally satisfactory bands obviously exist at this time. The same statements can be made with regard to the struts for the belts.

The approach taken to the control of the pulleys was based on interfacing with next generation vehicles with reasonably sophisticated overall vehicle control and information-handling systems. Electrohydraulic control valves were chosen for the interface between the vehicle control and pulley actuation. Six such valves are required, four for the pulleys, one for the modulating clutch, and one for the pressure compensated (variable pressure) pump. No off-the-shelf valves were found at a price compatible with the ultimate automotive application intended for this CVT. This area of technology and commercialization needs to be pursued parallel to the continued CVT development. There is, however, reason for optimism. The requirements are not unique to CVT's and there is evidence that other commercial transmission products will provide a parallel impetus for the development of these valves.

Suitability of a Steel V-Belt CVT for Electric
Vehicle Powered by Electric Motor Only

The use of a steel belt CVT in the driveline of an otherwise conventional all-electric vehicle might be advocated if it could be shown to substantially improve overall average efficiency, total weight, or life of the electric components. A substantial improvement in these areas would be needed to offset penalties in the areas of first cost, complexity of control, reliability, and maintenance.

Since the ratio range required of such a CVT would be much less than that required for the flywheel vehicle, a single belt would be adequate. In a typical front wheel drive configuration with cross-mounted motor, the belt would package attractively as a part of the power train from the motor axis to the axle axis, replacing gears or a chain that would otherwise be required, and needing little extra housing space. An additional final reduction gearset would be desirable, which could be a planetary similar to that used in GM X-body cars. Although all-electric vehicles generally deliver substantially less power than the flywheel CVT is designed for, the size of the belt would be similar to the low-speed belt of the flywheel CVT to provide adequate low-speed torque.

Typical efficiency curves for DC series motors⁽⁵⁾ are quite flat with respect to speed down to 30 percent of maximum speed. Below that speed efficiency could be improved substantially by a CVT that would allow the motor to run faster. However, since the motor does not operate at high power and low speed for very long in typical mission cycles, the effect on overall energy consumption would not be great. A slight efficiency improvement can also be realized when cruising at high speed by decreasing motor speed when full power is not required. At one-third power, for instance, motor efficiency could be increased from 67 percent to 72 percent by reducing the speed to one-half maximum. A steel belt CVT would have adequate efficiency to produce a net gain under this condition, but at the moderate speeds more typical of urban driving the belt's inefficiency might offset the gain in motor efficiency.

The size of a DC motor is proportional to the torque required of it, and in most electric vehicles is determined by the ability to start on a steep

grade. A CVT can reduce the weight of the motor by providing torque multiplication at low speed. The extent of the weight saving depends upon the torque required at maximum speed, where the CVT cannot provide multiplication. To climb a 5 percent grade at 80 kmph (50 mph), for instance, a typical vehicle requires 25 to 30 percent as much axle torque as to start on a 25 percent grade.⁽⁶⁾ If the base speed of the motor is reached at 40 kmph (25 mph) (and further speed achieved by field reduction), a twofold increase in torque is available without increase in motor size. By providing the remaining torque requirement, the CVT would reduce motor weight by 40 to 50 percent. The savings could be higher for a vehicle requiring less high-speed gradeability, or for a motor having a base speed closer to its maximum speed. Much the same armature current control circuitry would be required since the motor would still go to zero speed, but its duty cycle would be less demanding because the motor would be at low speed less of the time. An improvement in reliability and life of the electrical components would be expected, but whether the steel V-belt would have sufficient reliability to retain an overall advantage is impossible to assess at this time.

An interesting alternative arises when more radical departures from conventional electric vehicle design are contemplated. This alternative is to allow the CVT to take over the primary control function. It appears that the most troublesome components of the electrical system could be completely eliminated, resulting in a substantial improvement in efficiency, size and weight, and life of the electrical components.

The motor would be direct current with a compound winding. The armature would be continuously connected across full battery voltage. The field strength would be variable to provide an unloaded motor speed range of, say, 2500 to 5000 rpm. (A 2:1 speed range by field control was found practical by General Electric in the design of the ETV-1 vehicle.)⁽⁷⁾

A steel belt CVT with a 4:1 ratio spread would then provide a driveshaft speed range of 625 to 5000 rpm at full power. A clutch would be used for start-from-stop to bring the driveshaft to 625 rpm, and a simple forward-neutral-reverse gearshift would be incorporated in the final drive.

In operation, the motor would run continuously at or near the speed where its internally generated voltage balances the battery voltage, as determined by the field excitation. In response to an operator call for more torque, the belt would make a small ratio shift to pull down the motor speed, decreasing its internally generated voltage so that more armature current would flow. A belt shift in the other direction would cause the motor to speed up such that its voltage would exceed that of the battery, and the system would go smoothly into a regenerative mode. The 2:1 controlled speed range of the motor would augment the range of the belt and would help to mitigate noise or vibrations of fast-turning machinery under the hood when the vehicle is stopped or moving slowly.

The only high-amperage switchgear required would be that for starting the motor at the beginning of a mission against the inertia of its rotor and the pulleys of the CVT. This operation would be similar to starting the engine of an IC vehicle. The field control circuitry would be small and

inexpensive because only small amperage is involved, and its components would serve a dual purpose as the battery charger. Energy losses in the electrical control system would be very low.

The features of interest in such an arrangement would be the following:

- Substantial efficiency improvement over systems using choppers for armature current control
- Substantial improvement in smoothness and flexibility over systems using battery switching for armature current control
- Substantial weight and space savings by elimination of choppers or switchgear and reduction in motor weight and size
- Elimination of separate motor cooling blower since the motor could be cooled by an internal fan
- Improvement in motor and battery life by elimination of deleterious chopper effects and switching transients
- Efficient regenerative braking without additional complexity
- Natural "feel" of a clutch for low-speed maneuvering.

Suitability of a Steel V-Belt CVT for IC Engine/Battery Hybrid Vehicles

The design requirements of a CVT for an IC engine/battery application are essentially the same as those for 4-cylinder front wheel drive cars currently being engineered. Commercial versions of steel V-belt CVT's for these cars are reasonably mature and are undergoing tests on approximately 200 cars worldwide. This evidence speaks to the point well beyond the scope of any investigation that could be carried forward in this limited program. There seems to be a growing body of technical opinion, based on simulation studies on various driving cycles, that the continuously variable transmission can improve fuel consumption over torque converter automatics, provided the CVT is itself highly efficient and effectively controls its own parasitic losses at lower power levels. There may also be gains from an emissions standpoint.

A steel belt CVT for this application would use only one belt. It would be a slightly smaller belt than the low-speed belt of the current flywheel/electric vehicle project. The pulley sizes would be similar and therefore a transmission width, length, and height of 33, 30, and 23 cm (13, 12, and 9 in.), respectively, would result (including a modulated vehicle starting clutch). The weight of this CVT would be approximately 41 kg (90 lb).

The control approach would be similar but simpler because only two pulleys would need to be controlled. An electric motor to drive the control pump would not be required.

The efficiency of this CVT for IC engine/battery hybrid use could be estimated (for the belt and pulley bearing portions) by referring to Figure 32 for the low-speed belt in the current flywheel/electric vehicle project CVT. The curves for "power from flywheel" should be used. They can be extrapolated up to a speed ratio of 4.0/1 which should be adequate. Since these curves are calculated and are for the belt and pulley portions only, a multiplication factor of about 2.0 on the percent loss is suggested to arrive at an overall CVT efficiency. For example, when delivering power from the engine at cruising speeds, an overall efficiency of 93 to 94 percent might be expected.

Scalability of Steel Belt CVT

Steel belt drives respond well to the classical scaling technique of varying all dimensions by the same factor and varying shaft speed inversely with the dimension. If this is done, power capability is proportional to the square of dimension, and critical loadings such as bending stresses, bearing pressures, and rubbing velocities remain fixed. Centrifugal tension remains a fixed proportion of tensile capacity, and all major efficiency losses remain a fixed proportion of power transmitted.

There is no apparent limit to the extent to which the drive could be scaled up by classical means. In scaling down, the state of the art of fabricating thin bands may be reached rather quickly. Additional down-scaling could be accomplished without making the bands thinner if the ratio ranges of the belts were more nearly centered about unity ratio.

If shaft speed is not varied inversely with dimension in the classical manner, centrifugal tension becomes a limiting factor in drives that are both large and fast. Steel belts of the proportion recommended for the CVT should not be run above 4267 meters per minute (14,000 fpm) because centrifugal tension will then exceed the working tensile capacity of the bands and fatigue damage will result. In other words, at unity ratio the low speed belt could be run up to 11,700 rpm and the high-speed belt to 13,000 rpm. Additional tensile capacity can be added with virtually no additional weight by adding bands to the stack, provided the strut-to-band bearing surface is able to withstand the additional pressure. Since the durability of this bearing remains a point of question in the design of compression belts, the degree to which centrifugal tension is limiting to scaling cannot be adequately assessed at this time.

A drive for a 10,000 kg (22,000 lb) vehicle, if accomplished at the same driveshaft and flywheel speeds as those of the flywheel assisted battery car, represents a substantial departure from classical scaling. The torque required is 5.76 times greater, which would be achieved by increasing all dimensions by a factor of 1.79 if speed were not limiting. The low-speed belt would then operate up to 3353 meters per minute (11,000 fpm), which is acceptable and would not much decrease its capacity because it is not highly loaded by tractive forces when it is running fast. One or two additional bands would probably be sufficient. The high-speed belt would be more greatly affected because fairly high tractive force and speed occur simultaneously at the 2:1 ratio setting. Approximately 16 bands would be required in this belt, which

is thought to be too many. Consequently, it would be desirable to repropor-
tion the CVT for a greater gear reduction between the flywheel and the high-
speed pulley, and belt ranges more nearly centered about unity ratio. A
weight penalty is to be expected, because three of the four pulleys would then
operate at greater torque. Optimization of this drive has not been attempted
within the present program but the design of such a drive appears to be
practical.

APPENDIX A

STRUT-STRUT AND STRUT-PULLEY
LUBRICATION PROCESS

APPENDIX A

STRUT-STRUT AND STRUT-PULLEY
LUBRICATION PROCESS

The purpose of this analysis is to evaluate the layer of lubricant that exists between the strut and pulley or between struts during contact. This analysis is based on the cursory assumption that the strut is a rigid plate being squeezed against a flat pulley or strut (see Figure A-1) with some load, w . As the strut approaches the pulley, a thick layer of oil is assumed to be present. Under the strut-pulley or strut-strut loading, this oil is continuously squeezed outward until such time as the strut separates from the pulley.

The equilibrium equation for the trapped lubricant can be written (ignoring end leakage),

$$\frac{\partial}{\partial x} \left(\frac{h^3}{12\mu} \frac{\partial p}{\partial x} \right) = -v \quad (A-1)$$

The equation of state for the oil can be written,

$$\mu = \mu_0 e^{\gamma p} \quad (A-2)$$

where

- p = pressure (assumed to be independent of y)
- μ_0 = base oil viscosity
- γ = pressure-viscosity coefficient
- μ = viscosity of entrapped oil
- x, y = coordinate variables
- $v(x, y)$ = outward fluid velocity

Equation (A-1) can be integrated to show,

$$\frac{\partial p}{\partial x} = - \frac{12\mu v x}{h^3} \quad (A-3)$$

Using Equation (A-2), Equation (A-3) can be integrated on x to yield,

$$\frac{6 \mu_0 v \gamma}{h^3} (a^2 - x^2) = 1 - e^{-\gamma p} \quad (A-4)$$

In order for the pressure to remain finite at the center of contact ($x=0$), it can be seen that (ignoring end leakage),

$$\frac{6 \mu_0 v \gamma a^2}{h^3} \leq 1 \quad (A-5)$$

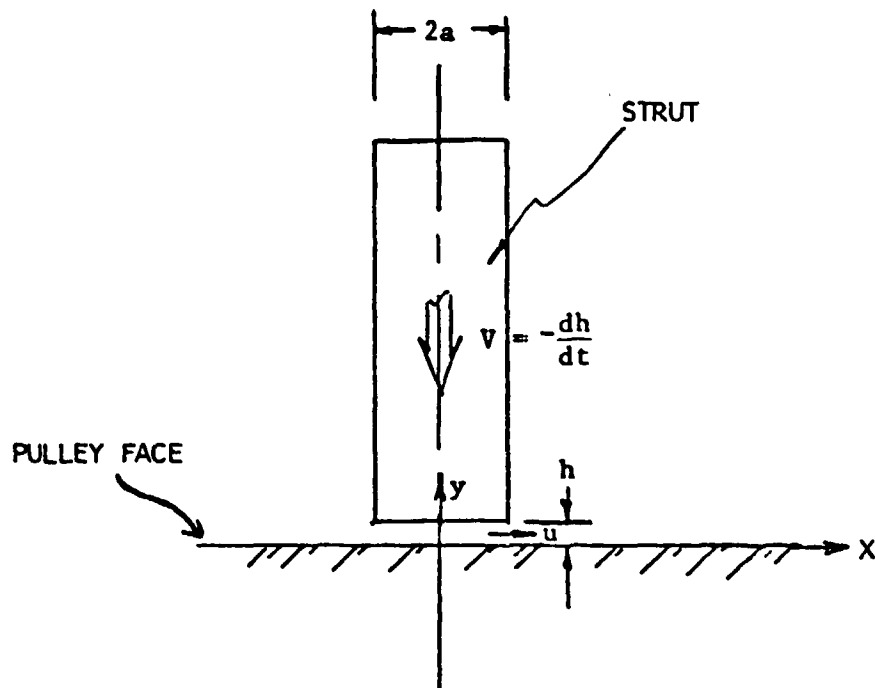


FIGURE A-1. COORDINATE SYSTEM FOR STRUT-PULLEY LUBRICANT ANALYSIS

Setting this parameter equal to 1 (which is the case for the limiting closure-velocity rate) shows,

$$-\frac{1}{h^3} \frac{dh}{dt} = \frac{1}{6 \mu_o \gamma a^2} \quad . \quad (A-6)$$

Integrating Equation (A-6) subject to the condition that $h(t=0) \rightarrow \infty$, we have finally,

$$h = \sqrt{\frac{3 \mu_o \gamma a^2}{t}} \quad , \quad (A-7)$$

where t is the time of contact between strut and pulley or between struts.

REFERENCES

- (1) Automotive Engineering, pp 136-140, Vol. 88, No. 2, February, 1980.
- (2) R. J. Roark, Formulas for Stress and Strain, McGraw-Hill Book Co., Fourth Edition, 1965.
- (3) Darle W. Dudley, Gear Handbook, McGraw-Hill Book Co., First Edition, 1962.
- (4) H. E. Merritt, Hydraulic Control System, John Wiley & Sons, Inc., New York, 1967, p 103.
- (5) U.S. Dept. of Energy, "State-of-the-Art Assessment of Electric and Hybrid Vehicles". Report No. HCP/1011-01, January, 1978.
- (6) A. B. Plunkett and G. B. Kliman, "Electric Vehicle AC Drive Development", SAE No. 800061, February, 1980.
- (7) E. A. Rowland and K. W. Schwarze, "System Design of the Electric Test Vehicle - One (ETV-1)". SAE No. 800057, February, 1980.
- (8) D. Dawson and G.R. Higgins, Elasto-Hydrodynamic Lubrication, Paragon Press, London, 1966.